

Prepared in Cooperation with the Virginia Department of Environmental Quality,
Office of Surface Water Investigations

Spatial and Temporal Trends in Runoff at Long-Term Streamgages within and near the Chesapeake Bay Watershed

Scientific Investigations Report 2012–5151

U.S. Department of the Interior
U.S. Geological Survey

Cover photo: Hughes River in the Shenandoah National Park within the Chesapeake Bay Watershed. Picture by Karen C. Rice, modified by James A. Tomberlin.

Spatial and Temporal Trends in Runoff at Long-Term Streamgages within and near the Chesapeake Bay Watershed

By Karen C. Rice and Robert M. Hirsch

Prepared in Cooperation with the Virginia Department of Environmental Quality,
Office of Surface Water Investigations

Scientific Investigations Report 2012–5151

U.S. Department of the Interior
U.S. Geological Survey

U.S. Department of the Interior
KEN SALAZAR, Secretary

U.S. Geological Survey
Marcia K. McNutt, Director

U.S. Geological Survey, Reston, Virginia: 2012

For more information on the USGS—the Federal source for science about the Earth, its natural and living resources, natural hazards, and the environment, visit <http://www.usgs.gov> or call 1–888–ASK–USGS.

For an overview of USGS information products, including maps, imagery, and publications, visit <http://www.usgs.gov/pubprod>

To order this and other USGS information products, visit <http://store.usgs.gov>

Any use of trade, firm, or product names is for descriptive purposes only and does not imply endorsement by the U.S. Government.

Although this information product, for the most part, is in the public domain, it also may contain copyrighted materials as noted in the text. Permission to reproduce copyrighted items must be secured from the copyright owner.

Suggested citation:

Rice, K.C., Hirsch, R.M., 2012, Spatial and temporal trends in runoff at long-term streamgages within and near the Chesapeake Bay Watershed: U.S. Geological Survey Scientific Investigations Report 2012–5151, 56 p.

Contents

Abstract.....	1
Introduction.....	1
Study Area.....	2
Methods.....	2
Time-Series Graphs.....	6
Flow Statistics.....	7
Spatial Trends In Runoff.....	7
Annual Flow Statistics.....	7
Annual 7-Day Minimum Runoff.....	7
Annual Mean Runoff.....	10
Annual 1-Day Maximum Runoff.....	10
Seasonal Flow Statistics.....	10
The 7-Day Minimum Runoff.....	11
Mean Runoff.....	12
The 1-Day Maximum Runoff.....	13
Discussion Of Annual And Seasonal Flow Statistics.....	14
Temporal Trends In Runoff.....	15
Summary.....	23
Acknowledgments.....	24
References Cited.....	24
Appendix.....	25

Figures

1. Map showing location of study area.....	3
2. Map showing locations of streamgages analyzed.....	4
3. Graph showing spatial trend in annual 7-day minimum runoff, 1930–2010.....	9
4. Graph showing spatial trend in annual mean runoff, 1930–2010.....	10
5. Graph showing spatial trend in annual 1-day maximum runoff, 1930–2010.....	11
6. Graph showing spatial trend in fall 7-day minimum runoff, 1930–2010.....	11
7. Graph showing spatial trend in winter 7-day minimum runoff, 1930–2010.....	11
8. Graph showing spatial trend in spring 7-day minimum runoff, 1930–2010.....	12
9. Graph showing spatial trend in summer 7-day minimum runoff, 1930–2010.....	12
10. Graph showing spatial trend in fall mean runoff, 1930–2010.....	12
11. Graph showing spatial trend in winter mean runoff, 1930–2010.....	12
12. Graph showing spatial trend in spring mean runoff, 1930–2010.....	13
13. Graph showing spatial trend in summer mean runoff, 1930–2010.....	13
14. Graph showing spatial trend in fall 1-day maximum runoff, 1930–2010.....	13
15. Graph showing spatial trend in winter 1-day maximum runoff, 1930–2010.....	14

16.	Graph showing spatial trend in spring 1-day maximum runoff, 1930–2010.....	14
17.	Graph showing spatial trend in summer 1-day maximum runoff, 1930–2010	14
18.	Graphs showing selected regression model for means of the 7-day minimum runoff...20	
19.	Graphs showing selected regression model for means of the mean runoff	21
20.	Graphs showing selected regression model for means of the 1-day maximum runoff..	21
1–1 to 1–30.	Graphs showing streamflow statistics, annual values and seasonal values, and locally weighted scatterplot smooth for selected streamgages within the Chesapeake Bay Watershed.....	26–55

Tables

1.	Attributes associated with streamgages and their location, Chesapeake Bay watershed	5
2.	Results of annual and seasonal trend slopes for 1930–2010.....	8
3.	Summary of results of annual and seasonal trends in data for 1930–2010.....	9
4.	Summary of results of annual and seasonal trends in data for 1930–2010 north and south of 40.25 degrees north latitude	10
5.	Results of annual and seasonal trend slopes for 1930–1969 and 1970–2010.....	15
6.	Summary of results of annual and seasonal trends in data for 1930–1969 and 1970–2010 north and south of 40.25 degrees north latitude.....	19
7.	Model form, selected model and model coefficients, standard errors of the model coefficients, and R^2 values for the six time series tested	23

Conversion Factors

Multiply	By	To obtain
	Area	
square kilometer (km ²)	0.3861	square mile (mi ²)
square mile (mi ²)	2.590	square kilometer (km ²)
	Flow rate	
millimeter per year (mm/yr)	0.3937	inch per year (in/yr)
inch per year (in/yr)	25.4	millimeter per year (mm/yr)

Abbreviations

ANCOVA	analysis of covariance
RSS	residual sum of squares
SSE	sum of squared errors
U.S.	United States
USGS	U.S. Geological Survey

Spatial and Temporal Trends in Runoff at Long-Term Streamgages within and near the Chesapeake Bay Watershed

By Karen C. Rice and Robert M. Hirsch

Abstract

Long-term streamflow data within the Chesapeake Bay watershed and surrounding area were analyzed in an attempt to identify trends in streamflow. Data from 30 streamgages near and within the Chesapeake Bay watershed were selected from 1930 through 2010 for analysis. Streamflow data were converted to runoff and trend slopes in percent change per decade were calculated. Trend slopes for three runoff statistics (the 7-day minimum, the mean, and the 1-day maximum) were analyzed annually and seasonally. The slopes also were analyzed both spatially and temporally. The spatial results indicated that trend slopes in the northern half of the watershed were generally greater than those in the southern half. The temporal analysis was done by splitting the 80-year flow record into two subsets; records for 28 streamgages were analyzed for 1930 through 1969 and records for 30 streamgages were analyzed for 1970 through 2010. The mean of the data for all sites for each year were plotted so that the following datasets were analyzed: the 7-day minimum runoff for the north, the 7-day minimum runoff for the south, the mean runoff for the north, the mean runoff for the south, the 1-day maximum runoff for the north, and the 1-day maximum runoff for the south. Results indicated that the period 1930 through 1969 was statistically different from the period 1970 through 2010. For the 7-day minimum runoff and the mean runoff, the latter period had significantly higher streamflow than did the earlier period, although within those two periods no significant linear trends were identified. For the 1-day maximum runoff, no step trend or linear trend could be shown to be statistically significant for the north, although the south showed a mixture of an upward step trend accompanied by linear downtrends within the periods. In no case was a change identified that indicated an increasing rate of change over time, and no general pattern was identified of hydrologic conditions becoming “more extreme” over time.

Introduction

The U.S. Geological Survey (USGS) has been measuring and recording streamflow throughout the United States (U.S.) since the late 1800s. Long-term records of streamflow are invaluable because of the information that they contain about temporal changes in the discharge of streams and rivers, a major component of the hydrologic cycle. Long-term records are necessary to detect and quantify natural and anthropogenic effects on streamflow. Analysis of long-term streamflow records can reveal information about the response of streamflow to climate and weather, to changes in land use in the watershed, and to changes in withdrawals of stream water for various human uses, because the records integrate those complex and interacting physical processes. Analysis of multiple streamflow records in a region is a particularly powerful tool for determining regional trends that may be related to climate.

The topic of climate change and variability is full of uncertainty, and any climatic changes are likely to result in changes to the hydrologic cycle at various scales. Some potential consequences of climate change and variability are changes in water availability for municipal and industrial use, changes in water demand for irrigation, changes in water quality, increased threats to stormwater and wastewater infrastructure, and a global rise in sea level. The longer the period of record of streamflow that is available, the better able hydrologists are to determine trends in streamflow, because shorter records can be dominated by the “noise” of natural variability, as well as long-term persistence (see, for example, Cohn and Lins, 2005). Evaluation of the trends that have taken place up to the present is important for the following reasons: (1) attaining an understanding of natural variability and the persistence of changing hydrologic conditions; (2) developing accurate representations of streamflow that can be useful in design and planning models for water quality, water supply, flood hazard mitigation, and ecosystem protection; and (3) forming a body of knowledge that can be used in the evaluation of models that are designed to forecast future changes in streamflow.

Eutrophication of coastal water bodies is a problem, both nationally (Bricker and others, 1999) and globally (Bricker and others, 2007). The water quality of Chesapeake Bay is threatened by excess nutrients (in particular, nitrogen and phosphorus) and sediments transported to the bay by runoff from the contributing watershed area. The amount and timing of streamflow to the bay are integral determinants of the amount of nutrients, sediments, and other dissolved constituents that are delivered to the bay. How, when, and where streamflow, and resulting water quality, might change in the future is of great interest to a wide variety of stakeholders. Understanding past and future changes in water quality is important but must be based on an understanding of past and future changes in streamflow.

A report by Karl and Knight (1998) documents an increase in precipitation across the U.S. during the 20th century, with winter precipitation only slightly increased but with more pronounced increases in the other seasons, in particular spring and fall. The report defines the six New England States, as well as New York, Pennsylvania, and Maryland, as being part of the Northeastern U.S.; Virginia is included as part of the Southeastern U.S. Karl and Knight (1998) document that precipitation has increased more in the Northeast than in the Southeast. Increased streamflow trends have been reported for the U.S. (Lins and Slack, 1999; McCabe and Wolock, 2002) and the New England States (Collins, 2009). Najjar and others (2009) report a summary of modeling studies that shows projections of streamflow in the Susquehanna River Basin and Mid-Atlantic area for the last quarter of the 21st century. These projections of annual streamflow change range from -25 to 33 percent (Najjar and others 2009). Another study for the Northeastern U.S. indicates that modeled streamflow will become more variable throughout the 21st century (Hayhoe and others, 2007). Finally, a state of the science review for Chesapeake Bay summarizes the wide range of projections for streamflow for the Chesapeake Bay watershed (Pyke and Najjar, 2008). On the basis of the uncertainties concerning projected streamflow in the region, a study of existing streamflow trends in the Chesapeake Bay watershed is needed.

The purposes of this study, conducted by the U.S. Geological Survey Environments Program and Hydrologic Network and Analysis Program in cooperation with the Virginia Department of Environmental Quality, were to: (1) compute and analyze long-term (80-year) trends in streamflow in 30 nontidal watersheds within and near the Chesapeake Bay watershed, (2) identify any spatial patterns in the trends, and (3) further explore major variations in the temporal trends over the 80-year record (1930–2010). The scope of this report is to present the results of the spatial and temporal analyses. Although this report does not address future changes to streamflow, the results should serve as a baseline that can be used to compare with hindcasts made by climate models to evaluate the capability of these models to accurately simulate the hydrologic changes that have taken place in the watershed over the last 80 years.

Study Area

The watershed that encompasses all streams that drain to Chesapeake Bay consists of 165,759 square kilometers (km²) and extends from New York to Virginia. The Chesapeake Bay watershed includes parts of New York, Pennsylvania, Delaware, Maryland, Virginia, and West Virginia, as well as Washington, D.C. (fig. 1). Parts of the physiographic provinces that lie within the bay watershed are the Appalachian Plateaus, the Valley and Ridge, the Blue Ridge, the Piedmont, and the Coastal Plain (Fenneman and Johnson, 1946). The major river basins that lie within the Chesapeake Bay watershed are the Susquehanna River, Western Shore, Patuxent River, Potomac River, Rappahannock River, York River, James River, and Eastern Shore (Phillips, 2007).

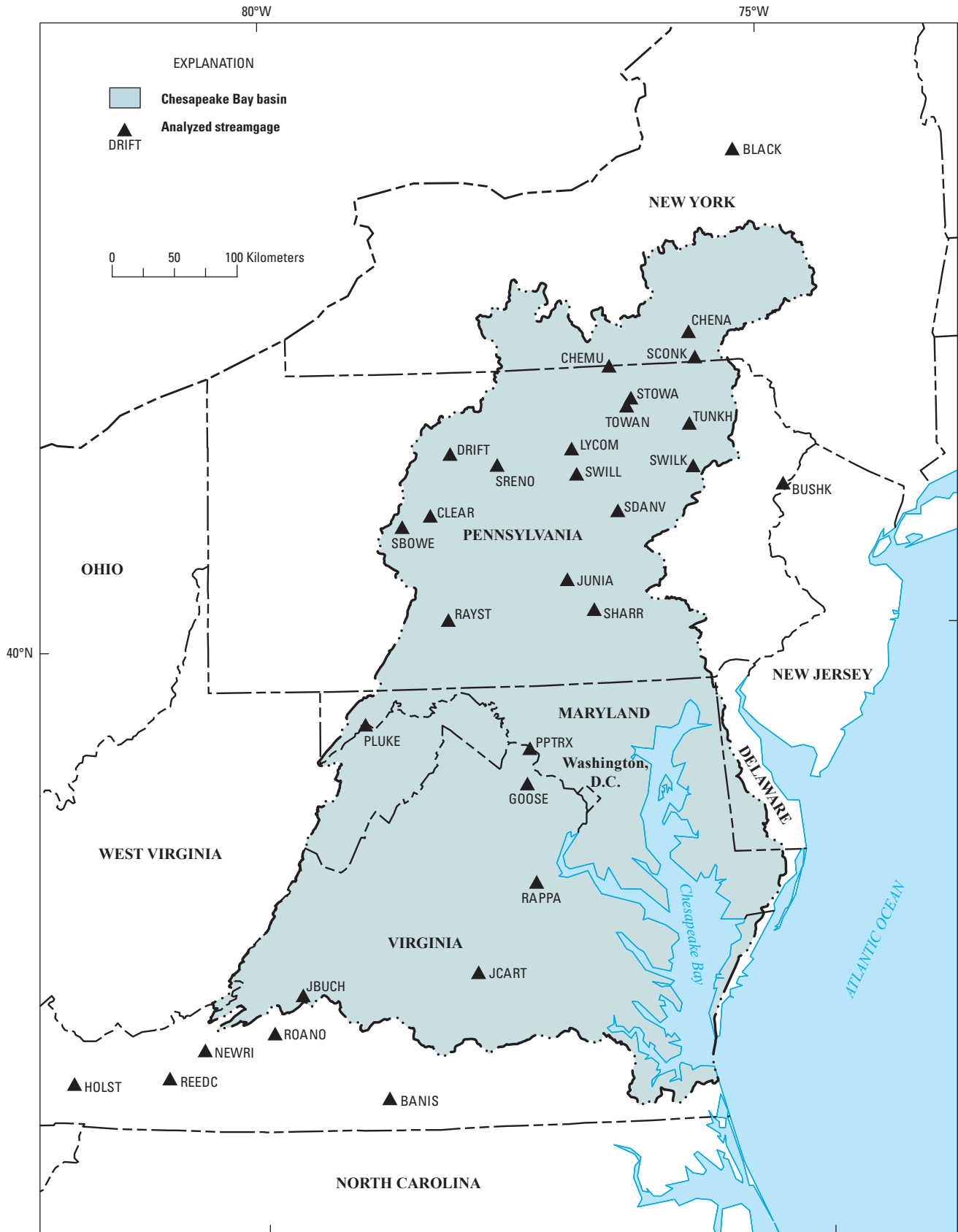
Data were analyzed from USGS streamgages located within and near the Chesapeake Bay watershed and having the longest continuous period of daily mean discharge record in common. A total of 23 nontidal streamgages within, and 7 nontidal streamgages near, the Chesapeake Bay watershed were chosen for analysis (fig. 2). This subset of streamgages in the bay watershed was selected because most of the streamgages have continuous daily mean discharge data extending for at least 80 years. The 30 streamgages selected for this analysis have watersheds that range in area from 303 to 62,419 km² (table 1). The Susquehanna River and its tributaries drain nearly half of the Chesapeake Bay watershed; slightly more than half of the streamgages analyzed in this report are located in the Susquehanna River Basin (table 1). Within the dataset are several streamgages that lie upstream from other streamgages used in the analysis. Thus, a degree of redundancy is present in some of the results, but the difference in drainage area between upstream and downstream sites warrants the inclusion of both. Unfortunately, streamgages located in the Coastal Plain part of the bay watershed, including the Eastern Shore, have records of insufficient length to be included in this analysis.

Methods

Data were analyzed by comparing the numerical results of calculated flow statistics for the period of record, 1930–2010, and by analyzing two subsets of the period of record, 1930–1969 and 1970–2010. Three annual streamflow statistics were analyzed in this report. They are measures of high flow, average flow, and low flow.

The high-flow statistic is the annual maximum 1-day streamflow for the water year (October 1–September 30). High flows are important because of flood-hazard conditions and the resulting contaminants that affect water quality. Sediment and phosphorus fluxes during the highest streamflow days can be a substantial part of the total annual flux, and thus changes in high streamflow conditions could be important to Chesapeake Bay water quality. From a high-flow perspective, the annual peak discharge (highest instantaneous discharge during

4 Spatial and Temporal Trends in Runoff at Long-Term Streamgages within and near the Chesapeake Bay Watershed



Geographic Coordinate System, North American Datum 1983

Figure 2. Locations of streamgages analyzed. Abbreviated names are listed in table 1.

Table 1. Attributes associated with streamgages and their location, Chesapeake Bay watershed.

[Watersheds are listed from north to south. ID, identification number; latitude and longitude given in decimal degrees; km², square kilometers; Br., branch; N.Y., New York; Pa., Pennsylvania; Md., Maryland; Va., Virginia]

Stream name and location	Abbreviated name	Streamgage ID	North latitude	West longitude	Watershed area, km ²	Major watershed
Black River near Boonville, N.Y.	BLACK	04252500	43.51174	75.30656	787	Lake Ontario
Chenango River near Chenango Forks, N.Y.	CHENA	01512500	42.21813	75.84825	3,841	Susquehanna
Susquehanna River at Conklin, N.Y.	SCONK	01503000	42.03535	75.80297	5,781	Susquehanna
Chemung River at Chemung, N.Y.	CHEMU	01531000	42.00230	76.63467	6,491	Susquehanna
Susquehanna River at Towanda, Pa.	STOWA	01531500	41.76535	76.44077	20,194	Susquehanna
Towanda Creek near Monroeton, Pa.	TOWAN	01532000	41.70702	76.48467	557	Susquehanna
Tunkhannock Creek near Tunkhannock, Pa.	TUNKH	01534000	41.55841	75.89464	992	Susquehanna
Lycoming Creek near Trout Run, Pa.	LYCOM	01550000	41.41841	77.03275	448	Susquehanna
Driftwood Branch Sinnemahoning Creek at Sterling Run, Pa.	DRIFT	01543000	41.41340	78.19695	704	Susquehanna
West Branch Susquehanna River at Renovo, Pa.	SRENO	01545500	41.32451	77.75054	7,705	Susquehanna
Susquehanna River at Wilkes-Barre, Pa.	SWILK	01536500	41.25091	75.88075	25,796	Susquehanna
West Br. Susquehanna River at Williamsport, Pa.	SWILL	01551500	41.23619	76.99663	14,716	Susquehanna
Bush Kill at Shoemakers, Pa.	BUSHK	01439500	41.08815	75.03767	303	Delaware
Clearfield Creek at Dimeling, Pa.	CLEAR	01541500	40.97172	78.40585	961	Susquehanna
Susquehanna River at Danville, Pa.	SDANV	01540500	40.95814	76.61912	29,060	Susquehanna
West Branch Susquehanna River at Bower, Pa.	SBOWE	01541000	40.89701	78.67697	816	Susquehanna
Juniata River at Newport, Pa.	JUNIA	01567000	40.47842	77.12915	8,687	Susquehanna
Susquehanna River at Harrisburg, Pa.	SHARR	01570500	40.25481	76.88608	62,419	Susquehanna
Raystown Branch Juniata River at Saxton, Pa.	RAYST	01562000	40.21591	78.26529	1,958	Susquehanna
North Branch Potomac River at Luke, Md.*	PLUKE	01598500	39.47897	79.06378	1,052	Potomac
Potomac River at Point of Rocks, Md.	PPTRX	01638500	39.27358	77.54311	24,996	Potomac
Goose Creek near Leesburg, Va.	GOOSE	01644000	39.01955	77.57749	860	Potomac
Rappahannock River near Fredericksburg, Va.	RAPPA	01668000	38.30846	77.52915	4,131	Rappahannock
James River at Cartersville, Va.	JCART	02035000	37.67098	78.08583	16,193	James
James River at Buchanan, Va.	JBUCH	02019500	37.53069	79.67893	5,369	James
Roanoke River at Roanoke, Va.	ROANO	02055000	37.25847	79.93865	995	Albemarle Sound
New River at Radford, Va.*	NEWRI	03171000	37.14167	80.56944	7,167	Kanawha
Reed Creek at Grahams Forge, Va.	REEDC	03167000	36.93901	80.88730	668	Kanawha
North Fork Holston River near Saltville, Va.	HOLST	03488000	36.89678	81.74623	572	Tennessee
Banister River at Halifax, Va.	BANIS	02077000	36.77653	78.91584	1,417	Albemarle Sound

*Streamgage excluded from the 1930–2010 analyses.

the year) or the 1-day maximum streamflow can be used. For watersheds of the size considered in this study, the annual maximum 1-day streamflow is highly correlated with the annual peak discharge. Thus, selecting the annual maximum 1-day discharge as the variable to analyze allows the entire analysis to be based on the daily flow record, rather than some parts being based on peak flows and other parts on daily flows.

Daily mean streamflow is highly relevant to the water balance of the watershed, as mean streamflow integrates the effects of precipitation and evapotranspiration. Like the annual

maximum 1-day streamflow statistic, daily mean streamflow also is computed on a water-year basis.

The low-flow statistic used is the annual 7-day minimum discharge, calculated for the climate year (April 1 through March 31). The 7-day minimum is used because of its relevance to regulations regarding water withdrawals and wastewater discharges. In addition to this relevance to regulatory criteria, the 7-day minimum may be a more robust indicator of low flow than the 1-day minimum. One-day minimums are more likely to be strongly influenced by short-term fluctuations due to the operations of small reservoirs in the watershed

rather than the overall water balance in the watershed. The use of the climate year for low-flow statistics (rather than the water year) is a common practice in hydrology, because it minimizes the probability that individual drought events will span multiple years and thus be counted twice in the time series (Riggs, 1982, 1985; Gordon and others, 2004).

Seasonal trend analyses were performed on the full period of record. Seasons were defined as fall (September through November), winter (December through February), spring (March through May), and summer (June through August). The same three flow statistics that were calculated for the annual analysis were calculated for each season.

For the analysis of the spatial pattern of the trends, streamflow records for the 28 streamgages were analyzed for 1930 through 2010, including annual data and seasonal data. To test for temporal trends, the 80-year record was divided into two subsets. Records for 28 streamgages were analyzed for 1930 through 1969 and records for 30 streamgages were analyzed for 1970 through 2010.

Time-Series Graphs

The analysis of long-term variation in streamflow characteristics used in this study builds on time-series smoothing methods that were pioneered by Cleveland (1979) and Cleveland and Devlin (1988). For any given time series, the graphs included in the appendix of this report show a scatterplot of runoff (Q_i) as a function of time (T_i), for i from one to n , where Q_i is the i^{th} annual value of the streamflow statistic, expressed in millimeters per day, and T_i is the time value at the midpoint of the period over which the statistic is evaluated, expressed in years. For example, for a flow statistic computed for water year 1972, the T_i value is approximately 1972.25, which represents the decimal-year value of the half-way point in the 1972 water year.

In addition to showing the actual values of the annual or seasonal streamflow statistic, the graphs show a curve that represents a smoothed representation of the time series. The smoothing method used is based on locally weighted scatterplot smoothing (lowess) but with some particular features that are described below. The purpose of producing the smooth curves is an attempt to extract patterns of change that describe broad temporal-scale variations, at timespans of about a decade or more. Such curves are very resistant to the influence of 1 or 2 years with extremely high or low flows.

The term y_i is the log-transformed value of the flow statistic:

$$y_i = \ln(Q_i),$$

where

\ln is the natural logarithm function.

If the flow statistic is equal to zero, Q_i is replaced with a constant, set equal to 0.1 percent of the long-term daily mean discharge for the streamgage. The logarithm transformation was applied because streamflow data typically are highly skewed,

approximating a log-normal distribution in many cases. The logarithm transformation results in weighted regressions in which the residuals are more nearly normal, and thus individual extreme values do not exert a large amount of influence on the estimates. This results in a more robust smoothing process. It also means that the \hat{Q}_i values are more nearly an approximation of the median of the time series than they are an approximation of the mean. Helsel and Hirsch (1992, p. 254–260) provide additional discussion of transformation issues.

In log space, the smooth curve is defined by a series of n -weighted regressions on the dataset. The estimate, \hat{y}_i , of y_i is defined as:

$$\hat{y}_i = \beta_{0i} + \beta_{1i} \bullet T_i \quad \text{for } i=1, n, \quad (1)$$

where:

- β_{0i} is the estimated regression intercept for the regression model fitted for year i , and
- β_{1i} is the estimated regression slope for the regression model fitted for year i .

The two regression coefficients, β_{0i} and β_{1i} , were computed from a weighted regression, where the weights are equal to 1 for the observation for the year in which the estimate is being made, and decay to 0 at a time separation of 30 years between a given observation and the time of the estimate. The specific weights are computed with the Tukey tri-cubed weight function (Tukey, 1977). The weight for the i^{th} streamflow value in the computation of the smoothed value for the j^{th} year is:

$$w_{i,j} = \begin{cases} \left(1 - \left(|d_{i,j}|/30\right)^3\right)^3 & \text{if } |d_{i,j}| \leq 30 \\ 0 & \text{if } |d_{i,j}| \geq 30 \end{cases}, \quad (2)$$

where $d_{i,j} = T_i - T_j$.

The shape of the weight function is such that all of the observations between 0 and 15 years before or after the year for which the estimate is being made have weights that are at least 67 percent as large as the largest weight. The largest weight is for the observation that is in the year for which the estimate is being made. For observations that are 25 years before or after the year for which the estimate is being made, the weight is only 7 percent of the maximum weight. At 30 years, the weight is 0. The “half-window width,” in this case, 30 years, was selected by visual examination of graphics for many alternatives. The half-window width was selected to be as narrow as possible, such that individual year-to-year oscillations are fully damped out. The smoothing process takes place on the full discharge record, not just the record shown in the graphs. Therefore, data prior to 1930, if available, were used to calculate the lowess line.

The final step in producing the graphic of the smoothed annual values is the retransformation:

$$\hat{Q}_i = \exp(\hat{y}_i). \quad (3)$$

Graphs showing time series with lowess trends for the 7-day minimum, mean, and the 1-day maximum for annual and seasonal data for each streamgauge are included in the appendix.

Flow Statistics

A numerical basis for comparisons across various flow statistics, across various starting and ending years, and across the various streamgages used in the analysis is useful. To present the results in a manner that enhances comparability, changes are best expressed in terms of a percent change per year, such as percent change per decade for the indicated period. Because the watershed areas vary over three orders of magnitude (table 1), normalizing by watershed area is necessary so that depth of runoff at each streamgauge can be compared, rather than discharge, which is determined largely by the size of the watershed. The trend slopes (described below) were used to identify general patterns over the broad Chesapeake Bay watershed region. No statistical significance levels (p-values) were calculated for any one streamgauge, because the focus is on general patterns in the region, and trend significance can be overestimated if the data are serially correlated (Koutsoyiannis, 2003; Cohn and Lins, 2005), as is the case with the dataset. The units (the percent change per decade for the indicated period) reported for each streamgauge take into account the length of record and the watershed area. Thus, the units give the most appropriate value for comparing spatial and temporal trends in streamflow across a region.

USGS streamflow data, provided in units of cubic feet per second, were downloaded from the National Water Information System (<http://waterdata.usgs.gov/nwis>). For this analysis, streamflow data were converted to runoff by dividing cubic feet per second by the watershed area and multiplying by conversion factors to obtain millimeters per day. Values in millimeters per day were multiplied by 365.25 to obtain millimeters per year, which is the unit shown on the graphs in the appendix.

The trend slopes were computed as:

$$\frac{(\hat{Q}_{end} - \hat{Q}_{start}) \cdot 100}{\hat{Q}_{start} \cdot (T_{end} - T_{start})}, \quad (4)$$

where:

\hat{Q}_{end} is the selected year index value (identified by the lowess line, in millimeters per year) of the ending year,

T_{end} (2010) and \hat{Q}_{start} are the selected year index value of the starting year, and

T_{start} (1930) is the comparison being made (1930–2010).

The difference multiplied by 100 yields the percent change in daily mean runoff over the selected period, which is divided by the number of decades between the start and end years, yielding a trend slope in percent change per decade. A positive trend slope is defined as a value greater than 1-percent increase per decade; a near-zero trend slope is defined as a value from -1- to 1-percent change per decade; and a negative trend slope is defined as a value greater than 1-percent decrease per decade. For the temporal analysis, where the dataset was divided into two subsets, the values for T_{end} were 1969 and 2010, and the values for T_{start} were 1930 and 1970, and the divisor was four for each subset.

Spatial Trends In Runoff

In this report, the period of record is defined as extending from 1930 through 2010. During this period, spatial trends in flow statistics were analyzed for 28 streamgages. The results indicate that the trend slopes tend to be of opposite signs in the northern part of the watershed compared to the southern part, or if of the same sign, of larger magnitude in the north relative to the south. Accordingly, the latitude 40.25 degrees (°) north was selected to differentiate between “north” and “south” for this study. A total of 18 streamgages are located north of 40.25°, and 10 streamgages are located south of 40.25°.

Annual Flow Statistics

The focus of this section of the report is on the flow statistics that were calculated from the annual data at each of the streamgages, including the annual 7-day minimum runoff, the annual mean runoff, and the annual 1-day maximum runoff, for the full period of record, 1930 through 2010. Two streamgages, North Branch Potomac River at Luke, Maryland (Md.), and New River at Radford, Virginia (Va.), were excluded from this analysis because of an insufficient length of data record. Values of the trend slopes, in percent change per decade, are shown in table 2.

Annual 7-Day Minimum Runoff

Data from 28 streamgages were included in the analysis of the annual 7-day minimum runoff. A total of 21 streamgages showed positive slopes, 2 streamgages showed near-zero slopes, and 5 streamgages showed negative slopes (fig. 3). The average slope was 3.8 (table 3). All 5 of the streamgages showing negative slopes are located south of 40.25° north latitude, whereas north of 40.25° north latitude, all 18 streamgages showed positive slopes (fig. 3; table 4).

8 Spatial and Temporal Trends in Runoff at Long-Term Streamgages within and near the Chesapeake Bay Watershed

Table 2. Results of annual and seasonal trend slopes for 1930–2010.

[ID, identification number; trend slope units in percent change per decade]

Abbreviated name of streamgage	Streamgage ID	7-day minimum	Mean	1-day maximum	Abbreviated name of streamgage	Streamgage ID	7-day minimum	Mean	1-day maximum
Annual									
BLACK	04252500	15.0	4.3	2.9	PPTRX	01638500	3.9	2.2	-1.7
CHENA	01512500	3.9	1.8	-0.5	GOOSE	01644000	27.9	21.1	27.3
SCONK	01503000	3.4	1.5	1.3	RAPPA	01668000	-5.5	0.7	3.2
CHEMU	01531000	9.0	1.7	-1.4	JCART	02035000	-2.2	1.4	4.9
STOWA	01531500	4.0	2.0	1.1	JBUCH	02019500	2.2	3.0	3.9
TOWAN	01532000	4.2	0.6	-0.1	ROANO	02055000	-3.5	-0.2	3.3
TUNKH	01534000	6.7	3.4	4.4	REEDC	03167000	-0.2	-0.4	-1.0
LYCOM	01550000	1.5	0.9	2.8	HOLST	03488000	-0.7	-0.5	-1.9
DRIFT	01543000	2.6	0.3	3.0	BANIS	02077000	2.3	4.0	16.8
SRENO	01545500	6.6	0.0	-2.2	Winter				
SWILK	01536500	5.7	2.6	1.5	BLACK	04252500	3.9	6.7	10.9
SWILL	01551500	3.9	-0.2	-0.9	CHENA	01512500	8.4	6.7	5.5
BUSHK	01439500	2.2	2.4	5.6	SCONK	01503000	7.9	5.8	8.1
CLEAR	01541500	12.4	0.0	-1.1	CHEMU	01531000	17.6	10.8	10.0
SDANV	01540500	3.8	2.2	1.3	STOWA	01531500	11.3	7.6	9.8
SBOWE	01541000	10.4	-0.8	-1.0	TOWAN	01532000	11.2	8.8	11.1
JUNIA	01567000	3.8	0.3	-2.3	TUNKH	01534000	16.0	10.0	9.3
SHARR	01570500	3.8	1.4	0.9	LYCOM	01550000	12.9	9.7	15.5
RAYST	01562000	-1.0	0.0	-0.3	DRIFT	01543000	7.0	4.8	12.0
PPTRX	01638500	3.1	0.3	-1.3	SRENO	01545500	10.5	4.5	5.7
GOOSE	01644000	15.0	4.4	6.7	SWILK	01536500	13.3	9.0	10.6
RAPPA	01668000	-7.7	-1.0	-1.2	SWILL	01551500	10.6	5.2	8.3
JCART	02035000	-3.3	-2.1	-2.9	BUSHK	01439500	8.8	7.1	11.2
JBUCH	02019500	2.4	-1.2	-2.4	CLEAR	01541500	14.5	3.0	3.1
ROANO	02055000	-3.7	-2.6	-3.1	SDANV	01540500	12.8	7.2	8.5
REEDC	03167000	0.7	-0.6	-2.0	SBOWE	01541000	12.8	1.5	3.8
HOLST	03488000	-0.6	-1.6	-0.3	JUNIA	01567000	8.7	3.4	0.9
BANIS	02077000	-2.1	-1.9	-3.3	SHARR	01570500	12.0	6.8	7.0
Fall					RAYST	01562000	4.2	1.4	-1.1
BLACK	04252500	8.9	10.2	9.4	PPTRX	01638500	3.0	0.7	-2.3
CHENA	01512500	3.5	6.1	5.3	GOOSE	01644000	18.7	6.9	3.5
SCONK	01503000	2.7	3.5	0.9	RAPPA	01668000	0.2	-1.1	-0.3
CHEMU	01531000	11.0	6.0	9.8	JCART	02035000	-0.5	-2.4	-1.9
STOWA	01531500	3.6	4.4	4.1	JBUCH	02019500	0.9	-2.9	-4.6
TOWAN	01532000	5.2	6.1	4.2	ROANO	02055000	1.5	-3.5	-5.4
TUNKH	01534000	7.3	7.4	3.8	REEDC	03167000	1.0	-0.3	-2.5
LYCOM	01550000	3.3	4.0	1.6	HOLST	03488000	-1.0	-2.9	-3.4
DRIFT	01543000	4.8	5.2	10.5	BANIS	02077000	2.7	1.5	4.2
SRENO	01545500	7.3	4.5	8.8	Spring				
SWILK	01536500	6.0	7.1	7.0	BLACK	04252500	4.5	0.3	1.7
SWILL	01551500	5.1	4.2	7.4	CHENA	01512500	0.6	-1.7	-1.7
BUSHK	01439500	4.1	12.3	7.6	SCONK	01503000	1.0	-1.4	0.4
CLEAR	01541500	11.5	2.5	4.5	CHEMU	01531000	2.9	-1.9	-1.3
SDANV	01540500	3.4	7.6	6.8	STOWA	01531500	1.8	-1.1	-0.1
SBOWE	01541000	8.5	2.3	3.4	TOWAN	01532000	2.6	-2.9	-2.8
JUNIA	01567000	4.4	3.3	5.8	TUNKH	01534000	2.7	-1.1	1.7
SHARR	01570500	5.1	5.3	4.8	LYCOM	01550000	3.4	-3.0	-1.8
RAYST	01562000	-1.1	1.0	4.0	DRIFT	01543000	0.4	-2.6	-0.9
					SRENO	01545500	1.1	-2.5	-3.3

Table 2. Results of annual and seasonal trend slopes for 1930–2010.—Continued

[ID, identification number; trend slope units in percent change per decade]

Abbreviated name of streamgage	Streamgage ID	7-day minimum	Mean	1-day maximum
SWILK	01536500	1.5	-1.3	-0.4
SWILL	01551500	0.7	-3.1	-2.9
BUSHK	01439500	-0.3	-1.6	1.5
CLEAR	01541500	3.5	-1.8	-4.5
SDANV	01540500	4.1	0.0	0.1
SBOWE	01541000	3.7	-2.2	-3.9
JUNIA	01567000	0.2	-1.3	-1.9
SHARR	01570500	1.6	-1.9	-1.2
RAYST	01562000	1.2	0.1	1.0
PPTRX	01638500	0.9	0.5	1.7
GOOSE	01644000	2.5	3.1	3.2
RAPPA	01668000	-2.3	-0.1	4.4
JCART	02035000	-3.0	-2.0	-3.1
JBUCH	02019500	-0.9	-0.9	-1.2
ROANO	02055000	-2.0	-2.3	-0.1
REEDC	03167000	0.6	-0.1	4.0
HOLST	03488000	-1.1	-1.0	3.5
BANIS	02077000	-1.2	-2.2	-3.8
Summer				
BLACK	04252500	14.7	11.0	14.5
CHENA	01512500	4.4	5.7	5.3
SCONK	01503000	4.4	4.9	5.8
CHEMU	01531000	7.4	4.1	3.0
STOWA	01531500	3.8	4.4	4.5
TOWAN	01532000	0.7	-1.4	-2.3
TUNKH	01534000	5.9	5.3	9.1
LYCOM	01550000	-0.1	-1.0	-2.8
DRIFT	01543000	3.2	0.2	-4.4
SRENO	01545500	5.1	-1.0	-4.4
SWILK	01536500	3.5	4.6	3.3
SWILL	01551500	1.9	-1.7	-5.2
BUSHK	01439500	-0.6	1.0	0.9
CLEAR	01541500	7.1	-0.2	-3.1
SDANV	01540500	2.7	3.7	2.3
SBOWE	01541000	9.2	-1.1	-5.6
JUNIA	01567000	1.8	-1.0	-0.8
SHARR	01570500	1.3	0.6	-1.6
RAYST	01562000	-1.7	-1.9	-2.7
PPTRX	01638500	-0.1	-1.2	-2.4
GOOSE	01644000	19.4	10.1	9.3
RAPPA	01668000	-7.8	-4.4	-2.2
JCART	02035000	-3.6	-4.5	-6.2
JBUCH	02019500	2.8	-0.9	-5.1
ROANO	02055000	-3.5	-3.0	-4.8
REEDC	03167000	0.4	-0.2	-0.3
HOLST	03488000	-0.7	-0.3	-1.9
BANIS	02077000	-4.1	-6.0	-6.5

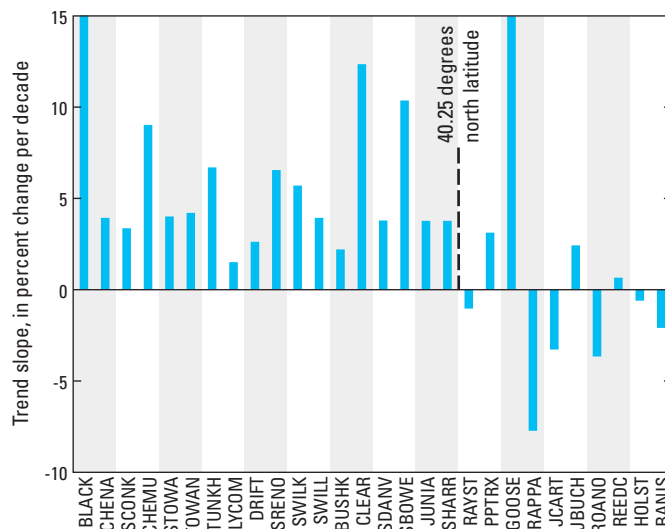


Figure 3. Spatial trend in annual 7-day minimum runoff, 1930–2010. Streamgages are listed in order from north (left side of graph) to south (right side of graph) with the dashed line indicating the position of 40.25 degrees north latitude that separates the 10 streamgages in the “south” subset from the 18 streamgages in the “north” subset.

Table 3. Summary of results of annual and seasonal trends in data for 1930–2010.

[n, number of streamgages; >, greater than; <, less than; trend slope units in percent change per decade]

Flow statistic	n, positive slope (> 1)	n, near-zero slope (-1 to 1)	n, negative slope (< -1)	Average slope
Annual				
7-day minimum	21	2	5	3.8
Mean	11	11	6	0.6
1-day maximum	10	6	12	0.2
Fall				
7-day minimum	22	2	4	4.6
Mean	24	4	0	4.8
1-day maximum	24	1	3	5.9
Winter				
7-day minimum	24	3	1	8.3
Mean	21	2	5	4.1
1-day maximum	19	2	7	4.9
Spring				
7-day minimum	15	8	5	1.1
Mean	1	7	20	-1.3
1-day maximum	9	6	13	-0.4
Summer				
7-day minimum	17	6	5	2.8
Mean	10	6	12	0.9
1-day maximum	9	3	16	-0.2

Table 4. Summary of results of annual and seasonal trends in data for 1930-2010 north and south of 40.25 degrees north latitude.

[n, number of streamgages; >, greater than; <, less than; trend slope units in percent change per decade; °, degrees]

Flow statistic	n, positive slope (> 1)	n, near-zero slope (-1 to 1)	n, negative slope (< -1)	Average slope
North of 40.25° north latitude, 18 streamgages				
Annual				
7-day minimum	18	0	0	5.7
Mean	10	8	0	1.4
1-day maximum	9	4	5	0.8
Fall				
7-day minimum	18	0	0	5.9
Mean	18	0	0	5.7
1-day maximum	17	1	0	5.9
Winter				
7-day minimum	18	0	0	11.1
Mean	18	0	0	6.6
1-day maximum	17	1	0	8.4
Spring				
7-day minimum	13	5	0	2.0
Mean	0	2	16	-1.7
1-day maximum	3	5	10	-1.2
Summer				
7-day minimum	15	3	0	4.2
Mean	9	3	6	2.1
1-day maximum	8	2	8	1.0
South of 40.25° north latitude, 10 streamgages				
Annual				
7-day minimum	3	2	5	0.3
Mean	1	3	6	-0.6
1-day maximum	1	2	7	-1.0
Fall				
7-day minimum	4	2	4	2.3
Mean	6	4	0	3.2
1-day maximum	7	0	3	5.9
Winter				
7-day minimum	6	3	1	3.1
Mean	3	2	5	-0.3
1-day maximum	2	1	7	-1.4
Spring				
7-day minimum	2	3	5	-0.5
Mean	1	5	4	-0.5
1-day maximum	6	1	3	1.0
Summer				
7-day minimum	2	3	5	0.1
Mean	1	3	6	-1.2
1-day maximum	1	1	8	-2.3

Annual Mean Runoff

Of the 28 streamgages that were analyzed for annual mean runoff, 11 showed positive slopes, 11 showed near-zero slopes, and 6 showed negative slopes (fig. 4). The average slope was 0.6 (table 3). South of 40.25° north latitude, 6 of the 10 streamgages showed negative slopes, and the majority located north of that latitude (10 out of 18) showed positive slopes (fig. 4; table 4).

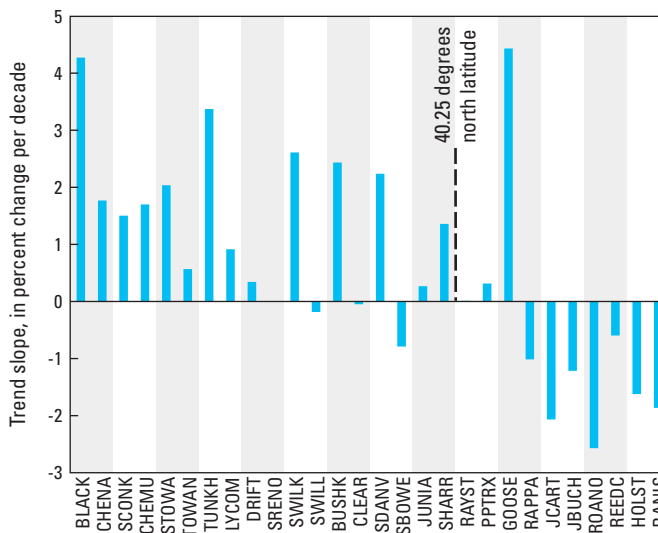


Figure 4. Spatial trend in annual mean runoff, 1930–2010. Streamgages are listed in order from north (left side of graph) to south (right side of graph) with the dashed line indicating the position of 40.25 degrees north latitude that separates the 10 streamgages in the “south” subset from the 18 streamgages in the “north” subset.

Annual 1-Day Maximum Runoff

Of the 28 streamgages that were analyzed for the annual 1-day maximum runoff, 10 showed positive slopes, 6 showed near-zero slopes, and 12 showed negative slopes (fig. 5). The average slope was 0.2 (table 3). South of 40.25° north latitude, 7 of 10 streamgages showed negative slopes (fig. 5; table 4). North of 40.25° north latitude, half of the streamgages showed positive slopes (fig. 5; table 4).

Seasonal Flow Statistics

The focus of this section of the report is on the flow statistics that were calculated from the seasonal data at each of the streamgages, including the 7-day minimum runoff, the mean runoff, and the 1-day maximum runoff for each season. Data were analyzed from 1930 through 2010. Two streamgages, North Branch Potomac River at Luke, Md., and New River at Radford, Va., were excluded from this analysis because of insufficient data. Values of the slopes, in percent change per decade, are shown in table 3.

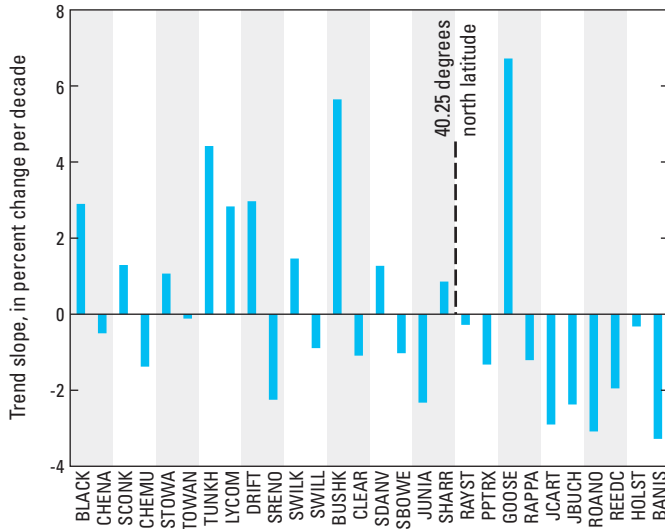


Figure 5. Spatial trend in annual 1-day maximum runoff, 1930–2010. Streamgages are listed in order from north (left side of graph) to south (right side of graph) with the dashed line indicating the position of 40.25 degrees north latitude that separates the 10 streamgages in the “south” subset from the 18 streamgages in the “north” subset.

The 7-Day Minimum Runoff

The 7-day minimum runoff for fall was analyzed for 28 streamgages. Results were mostly positive with 22 streamgages showing positive slopes, 2 with near-zero slopes, and 4 with negative slopes (fig. 6). The average slope was 4.6 (table 3). North of 40.25° north latitude, all

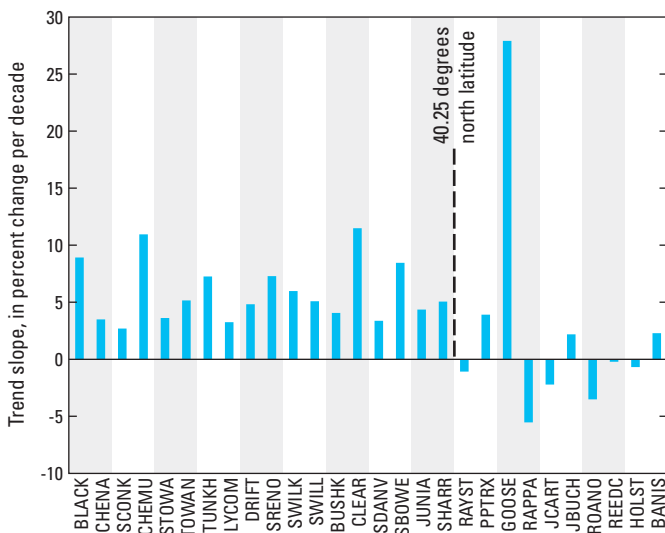


Figure 6. Spatial trend in fall 7-day minimum runoff, 1930–2010. Streamgages are listed in order from north (left side of graph) to south (right side of graph) with the dashed line indicating the position of 40.25 degrees north latitude that separates the 10 streamgages in the “south” subset from the 18 streamgages in the “north” subset.

18 streamgages showed positive slopes (fig. 6; table 4). The 4 streamgages showing negative slopes are located south of 40.25° north latitude (fig. 6; table 4).

The 7-day minimum runoff for winter was analyzed for 28 streamgages. The record for Goose Creek near Leesburg, Va., however, is missing data for the full 3 months of the winter of 1929 through 1930. Results were overall positive with 24 streamgages showing positive slopes, 3 streamgages with near-zero slopes, and 1 streamgage with a negative slope (fig. 7). The average slope was 8.3 (table 3). The 1 streamgage with a negative slope is located south of 40.25° north latitude (fig. 7; table 4).

The 7-day minimum runoff for spring was analyzed for 28 streamgages. Results were mostly positive with 15 streamgages showing positive slopes, 8 streamgages with near-zero slopes, and 5 with negative slopes (fig. 8). The average slope was 1.1 (table 3). All 5 of the streamgages with negative slopes are located south of 40.25° north latitude (fig. 8; table 4).

The 7-day minimum runoff for summer was analyzed for 28 streamgages. Results were mostly positive with 17 streamgages showing positive slopes, 6 streamgages with near-zero slopes, and 5 with negative slopes (fig. 9). The average slope was 2.8 (table 3). All 5 of the streamgages with negative slopes are located south of 40.25° north latitude (fig. 9; table 4).

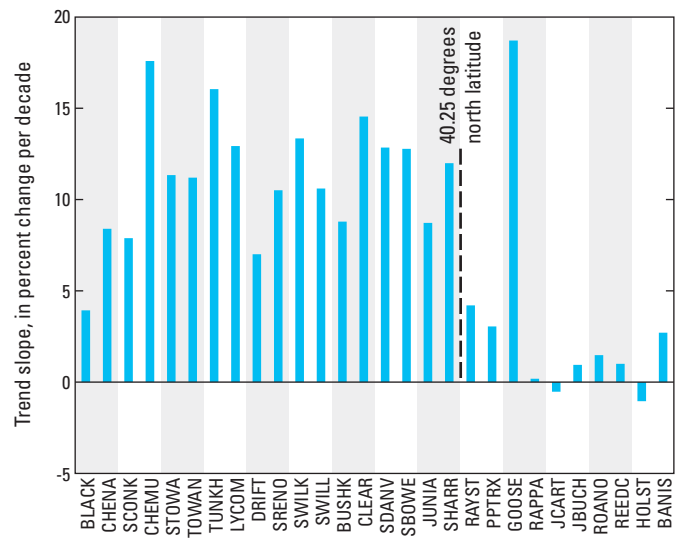


Figure 7. Spatial trend in winter 7-day minimum runoff, 1930–2010. Streamgages are listed in order from north (left side of graph) to south (right side of graph) with the dashed line indicating the position of 40.25 degrees north latitude that separates the 10 streamgages in the “south” subset from the 18 streamgages in the “north” subset.

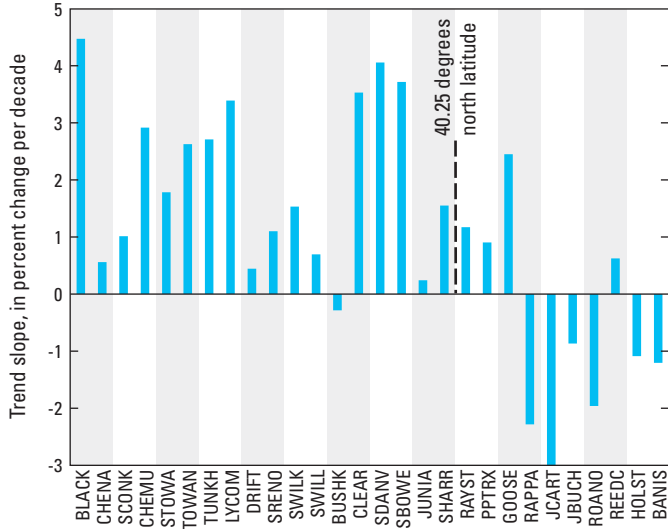


Figure 8. Spatial trend in spring 7-day minimum runoff, 1930–2010. Streamgages are listed in order from north (left side of graph) to south (right side of graph) with the dashed line indicating the position of 40.25 degrees north latitude that separates the 10 streamgages in the “south” subset from the 18 streamgages in the “north” subset.

Mean Runoff

Fall mean runoff was analyzed at 28 streamgages. Results were overall positive with 24 streamgages showing positive slopes and 4 with near-zero slopes; no negative slopes were observed (fig. 10). The average slope was 4.8 (table 3). The 4 streamgages with near-zero slopes are located south of 40.25° north latitude (fig. 10; table 4).

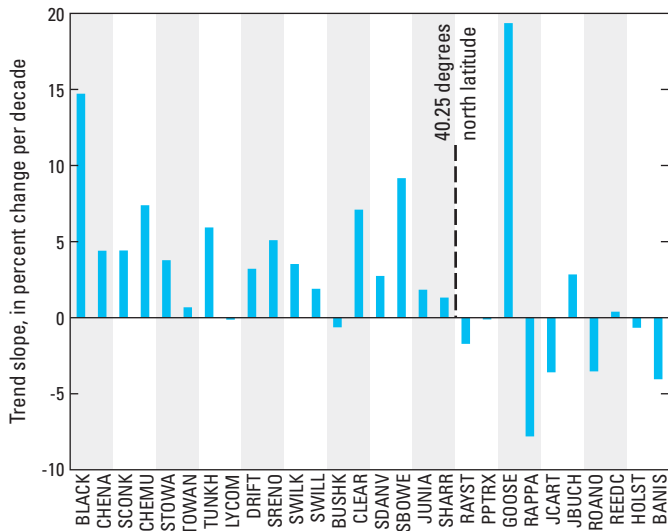


Figure 9. Spatial trend in summer 7-day minimum runoff, 1930–2010. Streamgages are listed in order from north (left side of graph) to south (right side of graph) with the dashed line indicating the position of 40.25 degrees north latitude that separates the 10 streamgages in the “south” subset from the 18 streamgages in the “north” subset.

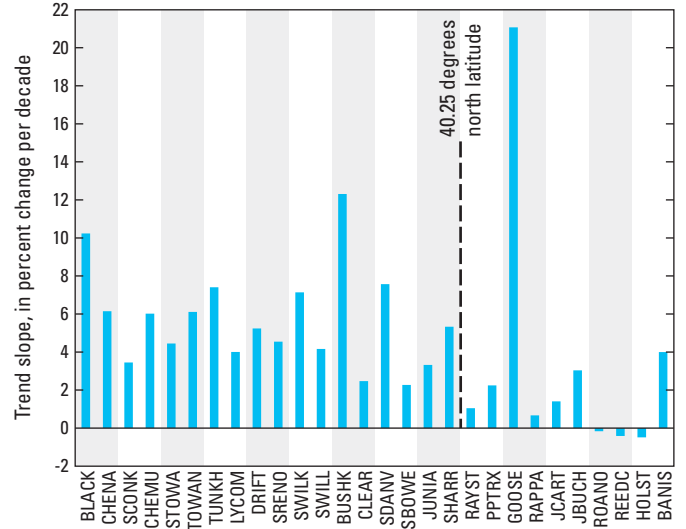


Figure 10. Spatial trend in fall mean runoff, 1930–2010. Streamgages are listed in order from north (left side of graph) to south (right side of graph) with the dashed line indicating the position of 40.25 degrees north latitude that separates the 10 streamgages in the “south” subset from the 18 streamgages in the “north” subset.

Results for 28 streamgages for winter mean runoff were mostly positive, with 21 positive slopes, 2 with near-zero slopes, and 5 with negative slopes (fig. 11). The average slope was 4.1 (table 3). The 5 streamgages with negative slopes are located south of 40.25° north latitude (fig. 11; table 4).

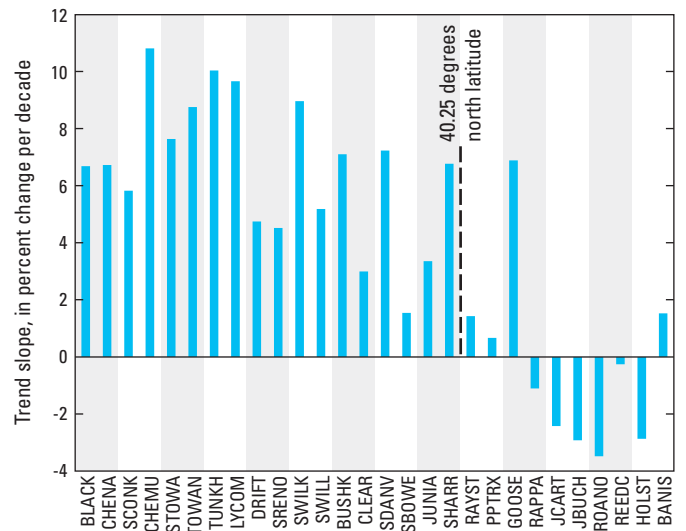


Figure 11. Spatial trend in winter mean runoff, 1930–2010. Streamgages are listed in order from north (left side of graph) to south (right side of graph) with the dashed line indicating the position of 40.25 degrees north latitude that separates the 10 streamgages in the “south” subset from the 18 streamgages in the “north” subset.

Results for 28 streamgages for spring mean runoff were mostly negative. Only 1 streamgage showed a positive slope, 7 had near-zero slopes, and 20 had negative slopes (fig. 12). The average slope was -1.3 (table 3). A total of 16 streamgages with negative slopes are located north of 40.25° north latitude (fig. 12; table 4).

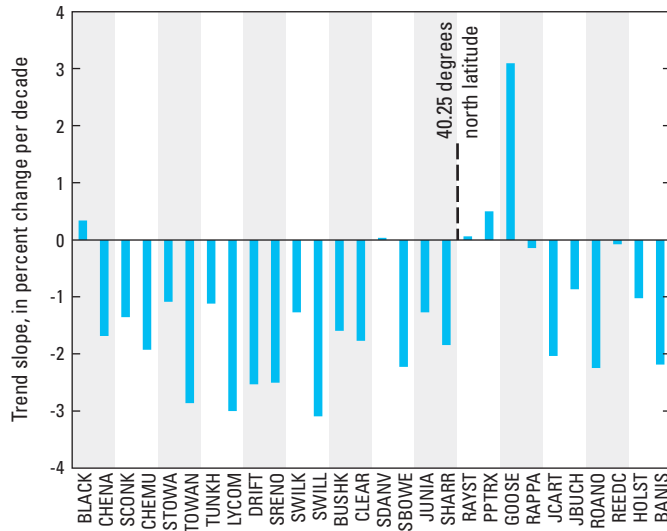


Figure 12. Spatial trend in spring mean runoff, 1930–2010. Streamgages are listed in order from north (left side of graph) to south (right side of graph) with the dashed line indicating the position of 40.25 degrees north latitude that separates the 10 streamgages in the “south” subset from the 18 streamgages in the “north” subset.

Summer mean runoff was analyzed at 28 streamgages. Results were mixed: 10 streamgages had positive slopes, 6 had a near-zero slope, and 12 streamgages had negative slopes (fig. 13). The average slope was 0.9 (table 3). A total of 6 of the 10 streamgages located south of 40.25° north latitude showed negative slopes; north of that latitude, 9 of the 18 streamgages showed positive slopes (fig. 13; table 4).

The 1-Day Maximum Runoff

The 1-day maximum runoff for fall was analyzed for 28 streamgages. Results were overall positive: 24 streamgages showed positive slopes, 1 had a near-zero slope, and 3 streamgages had negative slopes (fig. 14). The average slope was 5.9 (table 3). The 3 streamgages with negative slopes are located south of 40.25° north latitude (fig. 14; table 4).

The 1-day maximum runoff for winter was analyzed for 28 streamgages. A total of 19 of the 28 streamgages showed positive slopes, 2 had near-zero slopes, and 7 streamgages had negative slopes (fig. 15). The average slope was 4.9 (table 3). The 7 streamgages with negative slopes are located south of 40.25° north latitude (fig. 15; table 4).

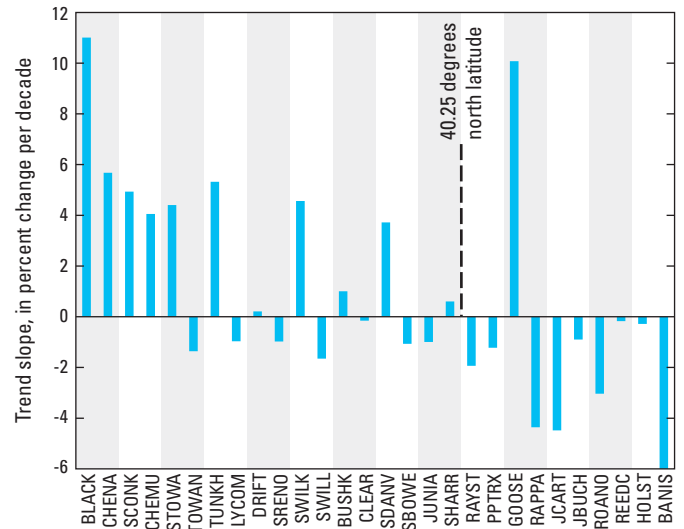


Figure 13. Spatial trend in summer mean runoff, 1930–2010. Streamgages are listed in order from north (left side of graph) to south (right side of graph) with the dashed line indicating the position of 40.25 degrees north latitude that separates the 10 streamgages in the “south” subset from the 18 streamgages in the “north” subset.

The 1-day maximum runoff for spring was analyzed for 28 streamgages. Results were mostly negative: 9 streamgages had positive slopes, 6 had near-zero slopes, and 13 streamgages had negative slopes (fig. 16). The average slope was -0.4 (table 3). A total of 10 of the 13 streamgages with negative slopes are located north of 40.25° north latitude (fig. 16; table 4).

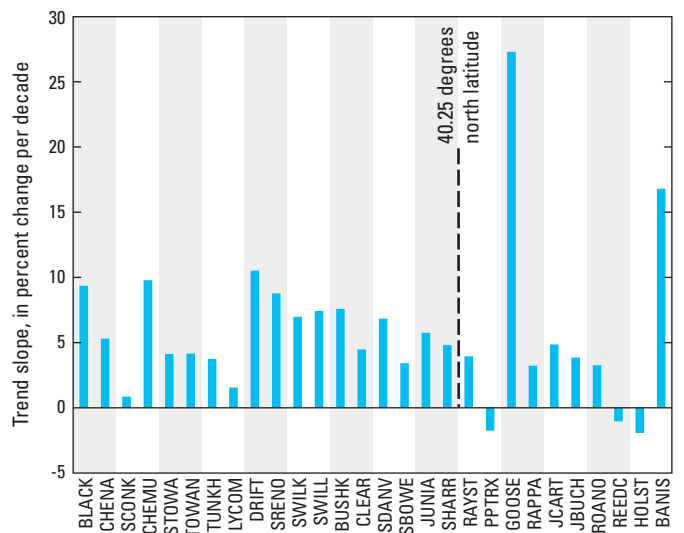


Figure 14. Spatial trend in fall 1-day maximum runoff, 1930–2010. Streamgages are listed in order from north (left side of graph) to south (right side of graph) with the dashed line indicating the position of 40.25 degrees north latitude that separates the 10 streamgages in the “south” subset from the 18 streamgages in the “north” subset.

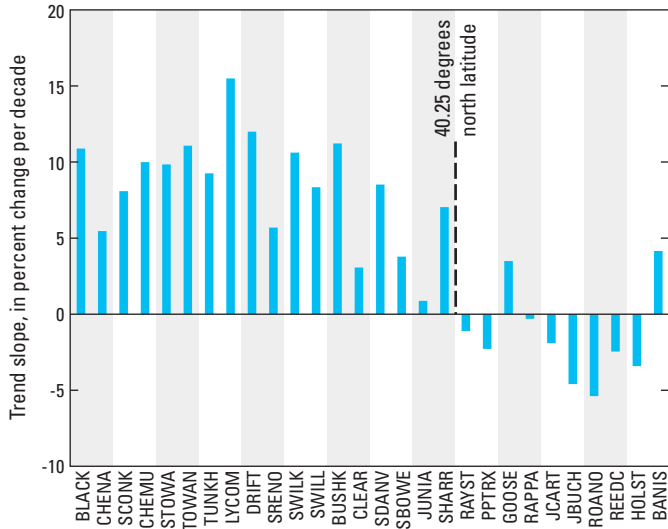


Figure 15. Spatial trend in winter 1-day maximum runoff, 1930–2010. Streamgages are listed in order from north (left side of graph) to south (right side of graph) with the dashed line indicating the position of 40.25 degrees north latitude that separates the 10 streamgages in the “south” subset from the 18 streamgages in the “north” subset.

The 1-day maximum runoff for summer was analyzed for 28 streamgages. Results were mostly negative: 9 streamgages had positive slopes, 3 had near-zero slopes, and 16 streamgages had negative slopes (fig. 17). The average slope was -0.2 (table 3). A total of 8 of the 9 streamgages with positive slopes are located north of 40.25° north latitude (fig. 17, table 4).

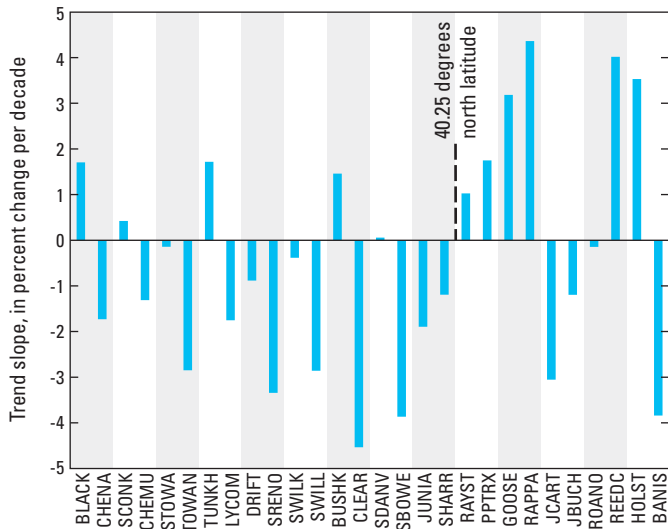


Figure 16. Spatial trend in spring 1-day maximum runoff, 1930–2010. Streamgages are listed in order from north (left side of graph) to south (right side of graph) with the dashed line indicating the position of 40.25 degrees north latitude that separates the 10 streamgages in the “south” subset from the 18 streamgages in the “north” subset.

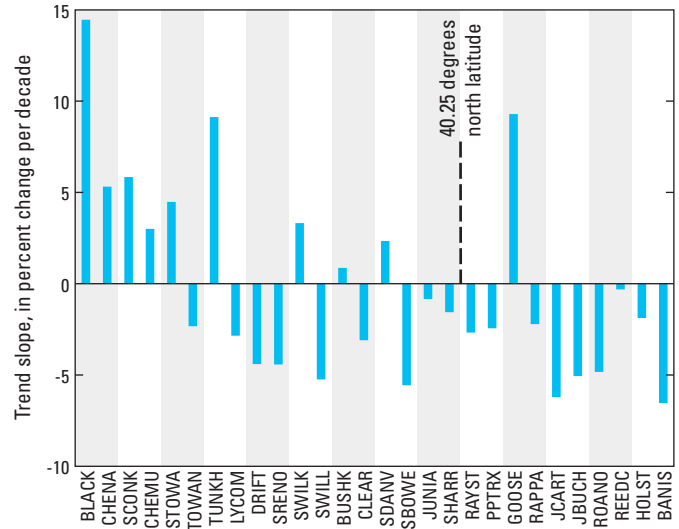


Figure 17. Spatial trend in summer 1-day maximum runoff, 1930–2010. Streamgages are listed in order from north (left side of graph) to south (right side of graph) with the dashed line indicating the position of 40.25 degrees north latitude that separates the 10 streamgages in the “south” subset from the 18 streamgages in the “north” subset.

Discussion Of Annual And Seasonal Flow Statistics

The flow statistics indicate that the 7-day minimum runoff, the mean runoff, and the 1-day maximum runoff generally have increased from 1930 through 2010. An accounting of the number of streamgages with positive, negative, and near-zero slopes shows that the majority of the slopes at the 28 streamgages were positive (table 3). In addition, the majority of the average slopes (12 out of 15) for each statistic were positive (table 3). These results of generally positive trends in streamflow in the Chesapeake Bay region are in accordance with previous assessments of streamflow trends in the U.S. (Lins and Slack, 1999; McCabe and Wolock, 2002) and in the New England States (Collins, 2009). Because the northeastern region of Karl and Knight (1998) does not include the southern part of the Chesapeake Bay study area, the documented increases in precipitation are not directly comparable to the runoff results presented here. Nevertheless, the general pattern of precipitation increase supports the general pattern of runoff increase, particularly in the northern part of the study area. Analysis of the effects of urbanization on streamflow lies beyond the scope of this report. Some sites, such as Goose Creek near Leesburg, Va., however, yielded anomalous results, suggesting that in some cases urbanization may be a more powerful influence on streamflow trends than is the climate.

In general, the average 7-day minimum and the average 1-day maximum slopes were greater than the average mean slopes (table 3). On an annual basis, the absolute difference between the average slopes of the 7-day minimum and the

mean was greater than the absolute difference between the average slopes of the mean and the 1-day maximum. This suggests that flows generally have become less variable; that is, the low flows have increased and moved closer to the mean flows, but the high flows have not moved an equal magnitude away from the mean flows. These results are in contrast to the modeling results of Hayhoe and others (2007), which predict that flow will become more variable throughout this century.

A notable difference is in the number of positive slopes among streamgages located in the north compared to streamgages located in the south (table 4). On an annual basis, in the north, there were 37 (out of 54) positive slopes (69 percent) and 5 (out of 54) negative slopes (9 percent), whereas in the south, there were 5 (out of 30) positive slopes (17 percent) and 18 (out of 30) negative slopes (60 percent). In addition, the magnitude of the average slopes in the north was greater than that of the average slopes in the south (table 4).

The absolute difference between the average slopes of the 7-day minimum and the mean was greater in the north than in the south (table 4). Likewise, the absolute difference between the average slopes of the mean and the 1-day maximum was slightly greater in the north than in the south. This suggests

that, on an annual basis, flows in the north have become less variable than flows in the south. The seasonal statistics suggest that in the north, the 1-day maximum flows were higher in the winter than in the other seasons, whereas in the south, the 1-day maximum flows were higher in the fall than in the other seasons. On a seasonal basis, the absolute difference between the average slopes of the 7-day minimum and the mean for streamgages in the north was greater than in the south for winter, spring, and summer; for fall, the absolute difference was slightly greater in the south. The absolute difference between the average slopes of the mean and the 1-day maximum was greater in the north for winter but was greater in the south for fall, spring, and summer.

Temporal Trends In Runoff

The analysis of data for the period 1930 through 2010 was further explored by dividing the period into two sub-periods: 1930 through 1969 and 1970 through 2010. The two subperiods were chosen because McCabe and Wolock (2002) identified a step increase in U.S. river flows in 1970, which

Table 5. Results of annual and seasonal trend slopes for 1930–1969 and 1970–2010.

[ID, identification number; trend slope units in percent change per decade; —, insufficient data]

Abbreviated name of streamgage	Streamgage ID	1930-1969			1970-2010		
		7-day minimum	Mean	1-day maximum	7-day minimum	Mean	1-day maximum
Annual							
BLACK	04252500	26.0	2.3	2.5	2.0	5.7	3.0
CHENA	01512500	-2.0	-1.1	-4.3	10.7	4.8	4.0
SCONK	01503000	-5.7	-1.0	-3.2	16.0	4.2	6.6
CHEMU	01531000	4.1	0.6	-2.6	12.0	2.7	-0.2
STOWA	01531500	-3.6	0.3	-0.4	13.6	3.7	2.5
TOWAN	01532000	-2.5	0.0	-0.6	12.2	1.2	0.4
TUNKH	01534000	0.3	0.4	2.8	13.0	6.2	5.4
LYCOM	01550000	-2.5	2.3	3.5	6.2	-0.4	1.9
DRIFT	01543000	-0.2	-0.8	-0.4	5.5	1.5	6.4
SRENO	01545500	9.5	1.6	-3.5	2.6	-1.5	-1.2
SWILK	01536500	-0.2	1.1	0.6	11.6	4.0	2.3
SWILL	01551500	8.6	1.1	-1.4	-0.6	-1.4	-0.4
BUSHK	01439500	-5.9	-0.7	4.0	13.5	5.7	6.3
CLEAR	01541500	16.8	1.2	-3.6	4.8	-1.2	1.7
SDANV	01540500	-0.4	0.2	-1.2	8.1	4.3	3.9
SBOWE	01541000	11.4	1.0	1.4	6.4	-2.4	-3.2
JUNIA	01567000	0.0	-0.2	-3.7	7.5	0.8	-1.2
SHARR	01570500	2.1	0.5	0.2	5.0	2.1	1.5
RAYST	01562000	-2.7	-0.1	-1.2	0.7	0.1	0.7
PLUKE	01598500	—	—	—	19.6	0.6	-7.3
PPTRX	01638500	2.0	1.0	-1.1	3.9	-0.3	-1.6
GOOSE	01644000	58.7	8.8	5.8	-8.0	0.5	5.9
RAPPA	01668000	-5.7	-1.0	1.3	-12.6	-1.1	-3.5

16 Spatial and Temporal Trends in Runoff at Long-Term Streamgages within and near the Chesapeake Bay Watershed

Table 5. Results of annual and seasonal trend slopes for 1930–1969 and 1970–2010.—Continued

[ID, identification number; trend slope units in percent change per decade; —, insufficient data]

Abbreviated name of streamgage	Streamgage ID	1930-1969			1970-2010		
		7-day minimum	Mean	1-day maximum	7-day minimum	Mean	1-day maximum
JCART	02035000	-2.2	-0.4	2.0	-4.8	-3.8	-7.2
JBUCH	02019500	-2.6	0.2	3.9	8.3	-2.7	-7.5
ROANO	02055000	-3.9	-0.9	0.3	-4.1	-4.4	-6.4
NEWRI	03171000	—	—	—	-4.4	-4.2	-7.1
REEDC	03167000	3.3	4.3	4.3	-1.8	-4.7	-7.0
HOLST	03488000	-1.4	0.5	7.8	0.2	-3.7	-6.4
BANIS	02077000	15.7	-0.9	-8.0	-12.2	-3.3	1.2
Fall							
BLACK	04252500	24.6	7.8	4.6	-3.4	9.7	11.9
CHENA	01512500	-3.2	-3.5	-4.5	11.8	18.4	18.5
SCONK	01503000	-7.1	-5.2	-5.0	17.6	15.4	8.4
CHEMU	01531000	2.4	1.0	2.5	17.8	10.6	15.6
STOWA	01531500	-5.0	-3.7	-3.2	15.3	14.7	13.1
TOWAN	01532000	-2.6	-2.0	-2.9	14.5	15.5	12.6
TUNKH	01534000	-1.6	-4.4	-5.5	17.2	23.3	16.6
LYCOM	01550000	0.7	4.6	5.5	5.6	2.8	-2.0
DRIFT	01543000	1.1	1.3	1.2	8.2	8.7	18.8
SRENO	01545500	9.1	5.5	7.7	4.0	2.9	7.5
SWILK	01536500	-1.4	-1.3	-1.1	14.2	16.4	15.7
SWILL	01551500	7.7	5.3	8.6	1.9	2.5	4.7
BUSHK	01439500	-5.9	-1.8	-3.1	18.5	28.4	21.0
CLEAR	01541500	15.3	4.5	-0.2	4.8	0.4	9.3
SDANV	01540500	-1.5	-1.7	-2.4	8.7	18.1	17.8
SBOWE	01541000	10.0	2.4	-0.9	4.9	1.9	8.0
JUNIA	01567000	-1.0	-0.9	-0.1	10.1	7.8	11.6
SHARR	01570500	1.3	-0.1	0.8	8.4	10.8	8.5
RAYST	01562000	-2.9	-0.6	0.0	0.8	2.7	7.9
PLUKE	01598500	—	—	—	14.5	5.6	-5.4
PPTRX	01638500	1.8	0.4	-1.2	5.6	4.0	-2.4
GOOSE	01644000	51.6	26.8	28.4	-0.4	5.4	8.9
RAPPA	01668000	-6.1	-0.9	-1.0	-6.6	2.3	7.8
JCART	02035000	-2.3	0.7	-1.2	-2.3	2.1	11.4
JBUCH	02019500	-2.4	0.6	-0.7	7.5	5.4	8.6
ROANO	02055000	-4.9	0.0	-0.1	-2.7	-0.3	6.7
NEWRI	03171000	—	—	—	-2.5	-2.1	5.8
REEDC	03167000	0.9	-1.3	-2.7	-1.3	0.5	0.7
HOLST	03488000	-1.9	-0.2	0.5	0.6	-0.8	-4.2
BANIS	02077000	13.7	4.4	3.6	-5.9	3.0	26.2
Winter							
BLACK	04252500	4.7	1.6	2.2	2.6	11.1	17.9
CHENA	01512500	3.0	3.3	2.7	12.3	8.9	7.4
SCONK	01503000	1.6	3.8	5.5	13.3	6.9	8.8
CHEMU	01531000	9.8	7.0	6.7	18.2	11.4	10.5
STOWA	01531500	5.3	5.3	7.2	14.4	8.2	9.7
TOWAN	01532000	5.3	4.8	7.8	14.1	10.6	10.9

Table 5. Results of annual and seasonal trend slopes for 1930–1969 and 1970–2010.—Continued

[ID, identification number; trend slope units in percent change per decade; —, insufficient data]

Abbreviated name of streamgage	Streamgage ID	1930-1969			1970-2010		
		7-day minimum	Mean	1-day maximum	7-day minimum	Mean	1-day maximum
TUNKH	01534000	6.3	4.0	7.8	20.6	13.9	8.2
LYCOM	01550000	5.1	7.2	13.3	17.3	9.4	11.6
DRIFT	01543000	3.8	0.5	3.8	8.9	8.8	17.5
SRENO	01545500	8.7	3.2	1.5	9.2	5.2	9.3
SWILK	01536500	6.4	5.9	8.0	16.2	9.8	10.1
SWILL	01551500	9.2	3.8	3.3	8.7	5.7	11.8
BUSHK	01439500	3.2	1.3	7.2	12.8	12.2	11.8
CLEAR	01541500	11.5	1.5	1.5	12.0	4.2	4.3
SDANV	01540500	7.1	4.6	4.8	14.5	8.3	10.3
SBOWE	01541000	9.8	0.6	2.0	11.3	2.4	5.1
JUNIA	01567000	4.2	1.7	0.5	11.3	4.7	1.2
SHARR	01570500	6.2	4.0	5.1	14.3	8.2	7.4
RAYST	01562000	2.7	0.7	1.3	5.1	2.1	-3.4
PLUKE	01598500	—	—	—	5.0	-0.9	-9.2
PPTRX	01638500	4.6	1.6	0.7	1.2	-0.2	-5.1
GOOSE	01644000	30.3	20.1	12.9	3.9	-3.1	-3.7
RAPPA	01668000	1.8	1.9	8.8	-1.4	-3.8	-6.9
JCART	02035000	1.1	0.4	3.9	-2.1	-5.1	-6.7
JBUCH	02019500	0.7	0.7	3.5	1.1	-6.3	-11.1
ROANO	02055000	1.0	0.5	2.9	1.9	-7.3	-12.2
NEWRI	03171000	—	—	—	-4.7	-4.7	-6.3
REEDC	03167000	5.0	10.4	18.4	-2.5	-7.7	-13.4
HOLST	03488000	0.4	1.6	4.4	-2.4	-6.9	-9.5
BANIS	02077000	6.9	7.0	8.7	-1.2	-3.1	-0.3
Spring							
BLACK	04252500	5.4	0.2	2.9	2.9	0.4	0.4
CHENA	01512500	-0.1	-1.5	-4.1	1.2	-2.1	0.8
SCONK	01503000	0.3	-0.6	-1.6	1.7	-2.1	2.6
CHEMU	01531000	2.2	-0.9	-1.6	3.4	-3.1	-1.1
STOWA	01531500	0.7	0.3	0.6	2.8	-2.5	-0.9
TOWAN	01532000	0.4	-0.1	0.0	4.7	-5.7	-5.7
TUNKH	01534000	3.9	0.5	5.2	1.3	-2.7	-1.4
LYCOM	01550000	-2.7	0.6	3.2	10.6	-6.5	-6.0
DRIFT	01543000	-0.3	-1.5	-2.7	1.2	-3.8	1.1
SRENO	01545500	0.3	0.6	-3.4	1.8	-5.5	-3.8
SWILK	01536500	1.5	0.5	1.1	1.5	-3.0	-1.8
SWILL	01551500	-0.1	-0.5	-2.0	1.5	-5.9	-4.0
BUSHK	01439500	-1.8	0.1	4.0	1.3	-3.3	-1.0
CLEAR	01541500	4.9	1.7	-3.3	1.8	-4.9	-6.6
SDANV	01540500	1.3	-0.5	-0.7	6.5	0.6	0.8
SBOWE	01541000	6.0	1.8	0.3	1.2	-5.8	-8.0
JUNIA	01567000	-0.3	-0.7	-3.4	0.8	-1.9	-0.4
SHARR	01570500	-0.6	-0.4	-0.7	3.8	-3.3	-1.8
RAYST	01562000	1.8	0.3	-1.2	0.5	-0.2	3.5
PLUKE	01598500	—	—	—	5.3	-1.0	-3.9

18 Spatial and Temporal Trends in Runoff at Long-Term Streamgages within and near the Chesapeake Bay Watershed

Table 5. Results of annual and seasonal trend slopes for 1930–1969 and 1970–2010.—Continued

[ID, identification number; trend slope units in percent change per decade; —, insufficient data]

Abbreviated name of streamgage	Streamgage ID	1930-1969			1970-2010		
		7-day minimum	Mean	1-day maximum	7-day minimum	Mean	1-day maximum
PPTRX	01638500	2.2	1.8	-0.7	-0.4	-0.7	4.3
GOOSE	01644000	9.9	4.4	-1.6	-3.6	1.5	8.5
RAPPA	01668000	0.0	-0.1	1.0	-4.6	-0.2	7.4
JCART	02035000	0.0	1.4	4.1	-6.0	-5.2	-8.8
JBUCH	02019500	0.2	2.8	8.0	-1.9	-4.1	-7.9
ROANO	02055000	0.9	3.6	14.7	-4.7	-7.1	-9.4
NEWRI	03171000	—	—	—	-3.9	-6.0	-6.3
REEDC	03167000	8.6	8.8	16.0	-5.4	-6.6	-4.8
HOLST	03488000	0.6	4.4	16.2	-2.7	-5.5	-5.6
BANIS	02077000	2.5	-0.1	-7.1	-4.5	-4.3	-0.8
Summer							
BLACK	04252500	21.5	9.0	6.6	4.2	9.6	17.6
CHENA	01512500	-2.0	-3.2	-6.7	11.8	16.7	23.7
SCONK	01503000	-5.8	-4.5	-6.6	19.1	17.4	24.8
CHEMU	01531000	1.4	-0.5	-0.3	12.7	8.8	6.4
STOWA	01531500	-3.8	-3.1	-3.8	13.4	13.6	15.1
TOWAN	01532000	-2.2	-2.5	-5.9	3.9	-0.2	1.6
TUNKH	01534000	-1.4	-2.0	-1.9	13.9	13.7	21.8
LYCOM	01550000	-2.2	0.9	-1.9	2.2	-2.7	-4.1
DRIFT	01543000	1.7	-0.9	-4.7	4.4	1.3	-5.1
SRENO	01545500	8.9	2.8	-0.8	1.0	-4.3	-8.3
SWILK	01536500	-1.0	-1.1	-2.4	8.3	10.8	9.9
SWILL	01551500	6.9	2.5	-2.9	-2.4	-5.3	-8.6
BUSHK	01439500	-5.8	-4.9	-5.9	5.8	8.6	10.0
CLEAR	01541500	10.5	1.6	-3.1	2.6	-1.8	-3.6
SDANV	01540500	-1.6	-1.6	-2.6	7.5	9.7	8.0
SBOWE	01541000	12.0	1.6	-3.9	4.3	-3.5	-8.6
JUNIA	01567000	-0.7	-1.0	-3.9	4.5	-1.0	2.6
SHARR	01570500	0.3	-0.8	-2.6	2.3	2.1	-0.6
RAYST	01562000	-2.3	-1.6	-4.3	-1.3	-2.4	-1.3
PLUKE	01598500	—	—	—	22.9	11.0	9.5
PPTRX	01638500	0.5	-0.4	1.1	-0.7	-2.1	-5.8
GOOSE	01644000	75.9	26.4	26.8	-9.2	-3.1	-4.0
RAPPA	01668000	-6.0	-4.8	-0.3	-12.6	-4.8	-4.2
JCART	02035000	-3.7	-3.7	-1.7	-4.1	-6.1	-11.5
JBUCH	02019500	-2.6	-3.2	-3.4	9.3	1.6	-7.8
ROANO	02055000	-5.7	-6.2	-10.4	-1.8	0.1	1.2
NEWRI	03171000	—	—	—	-3.5	-3.9	-0.1
REEDC	03167000	2.2	0.5	-2.6	-1.3	-0.8	2.2
HOLST	03488000	-2.3	-3.7	-4.1	1.0	3.6	0.4
BANIS	02077000	5.5	-4.2	-6.3	-11.2	-9.5	-9.1

Table 6. Summary of results of annual and seasonal trends in data for 1930–1969 and 1970–2010 north and south of 40.25 degrees north latitude.

[n, number of streamgages; >, greater than; <, less than; trend slope units in percent change per decade; °, degrees]

Flow statistic	1930-1969				1970-2010			
	n, positive slope (> 1)	n, near-zero slope (-1 to 1)	n, negative slope (< -1)	Average slope	n, positive slope (> 1)	n, near-zero slope (-1 to 1)	n, negative slope (< -1)	Average slope
North of 40.25° north latitude, 18 streamgages								
Annual								
7-day minimum	7	5	6	3.1	17	1	0	8.3
Mean	7	9	2	0.5	12	2	4	2.2
1-day maximum	5	5	8	-0.5	12	3	3	2.2
Fall								
7-day minimum	8	1	9	2.4	17	0	1	10.0
Mean	4	2	8	0.4	17	1	0	11.6
1-day maximum	6	4	8	0.1	17	0	1	12.1
Winter								
7-day minimum	18	0	0	6.2	18	0	0	12.9
Mean	16	2	0	3.6	18	0	0	8.3
1-day maximum	17	1	0	5.1	18	0	0	9.7
Spring								
7-day minimum	7	9	2	1.2	17	1	0	2.8
Mean	2	14	2	0.0	0	2	16	-3.4
1-day maximum	5	5	8	-0.3	2	5	11	-2.0
Summer								
7-day minimum	7	2	9	2.0	17	0	1	6.6
Mean	5	4	9	-0.4	11	1	6	5.2
1-day maximum	1	2	15	-3.0	11	1	6	5.7
South of 40.25° north latitude, 10 streamgages								
Annual								
7-day minimum	4	0	6	6.1	3	2	7	-1.3
Mean	3	6	1	1.1	0	4	8	-2.2
1-day maximum	6	1	3	1.5	2	1	9	-3.9
Fall								
7-day minimum	3	6	2	4.8	3	3	6	0.6
Mean	2	7	1	3.0	8	3	1	2.3
1-day maximum	2	4	4	2.6	8	1	3	6.0
Winter								
7-day minimum	8	2	0	5.5	6	0	6	0.3
Mean	6	4	0	4.5	1	2	9	-3.9
1-day maximum	9	1	0	6.5	0	1	11	-7.3
Spring								
7-day minimum	5	5	0	2.7	1	2	9	-2.7
Mean	7	3	0	2.7	1	3	8	-3.3
1-day maximum	6	1	3	4.9	4	1	7	-2.0
Summer								
7-day minimum	3	1	6	6.2	3	1	8	-1.0
Mean	1	2	7	-0.1	3	2	7	-1.4
1-day maximum	2	1	7	-0.5	3	2	7	-2.5

was confirmed for discharge in the New England States by Collins (2009). Comparison of the results of statistics for the two subperiods is shown in table 5, and a summary of the statistics north and south of latitude 40.25° north is shown in table 6.

The data in tables 5 and 6 suggest a discontinuity between the runoff values for 1930 through 1969 compared to those for 1970 through 2010. Because a large number of streamgages in the north are located on tributaries to the Susquehanna River, the sites were thinned to decrease spatial correlation and avoid extensive double counting of flows as these records were aggregated. As a result of the thinning, sites SRNEO, SWILK, and SDANV in the north and site JBUCH in the south were excluded from the analysis. To compare the data from the two subperiods, the mean of the runoff data for each site in the north (15 sites) for each year and the mean for each site in the south (11 sites) for each year were calculated. The mean of the data for all sites for each year was plotted for each of the six statistics of interest: the 7-day minimum runoff in the north and south (fig. 18); the mean runoff in the north and south (fig. 19); and the 1-day maximum runoff in the north and south (fig. 20).

Multiple regression models were developed and tested to define the nature of the change between the two subperiods. The general form of the multiple regression model is:

$$Q = \beta_0 + \beta_1 \cdot T + \beta_2 \cdot D + \beta_3 \cdot D \cdot T + \varepsilon \quad (5)$$

where:

- Q is the mean runoff for the region;
- T is time defined as water year minus 1970, so that the T variable ranges from -40 to +40;
- D is a dummy variable, defined as 0 for the years 1930 through 1969, and 1 for 1970 through 2010;
- ε is the random error; and

$\beta_0, \beta_1, \beta_2,$ and β_3 are regression coefficients.

Using analysis of covariance (ANCOVA; Helsel and Hirsch, 2002), models that are subsets of these explanatory variables were compared, and the regression coefficients were tested for statistical significance.

The six time series (figs. 18–20) were tested for differences in runoff for 1930 through 1969 and 1970 through 2010. Five regression models were considered as a description of each of the time series.

Model 0: $Q = \beta_0 + \varepsilon$. Model 0 is a stationary random process with no linear or step trend and is considered the null hypothesis.

Model 1: $Q = \beta_0 + \beta_1 \cdot T + \varepsilon$. Model 1 is a stationary random process with a single linear trend.

Model 2: $Q = \beta_0 + \beta_2 \cdot D + \varepsilon$. Model 2 is a stationary random process with a step trend after 1969.

Model 3: $Q = \beta_0 + \beta_1 \cdot T + \beta_2 \cdot D + \varepsilon$. Model 3 is a stationary random process with a single linear trend with a step trend added to it after 1969.

Model 4: $Q = \beta_0 + \beta_1 \cdot T + \beta_2 \cdot D + \beta_3 \cdot D \cdot T + \varepsilon$.

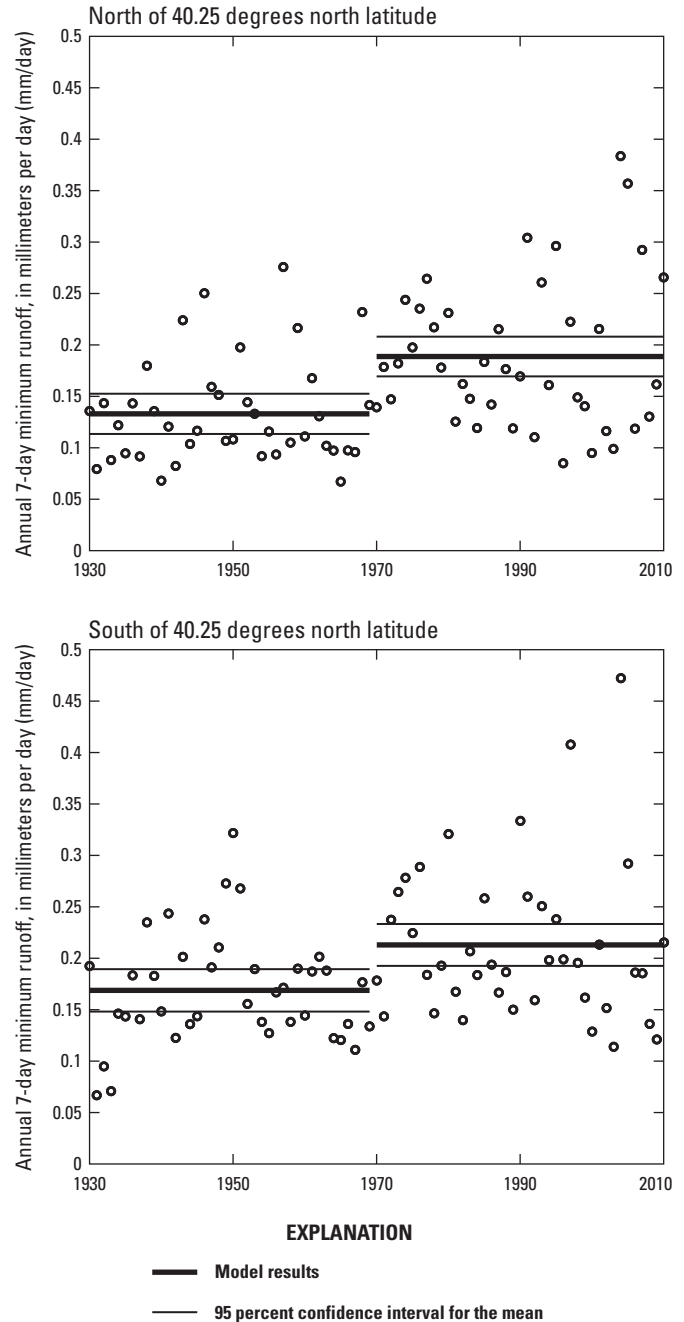
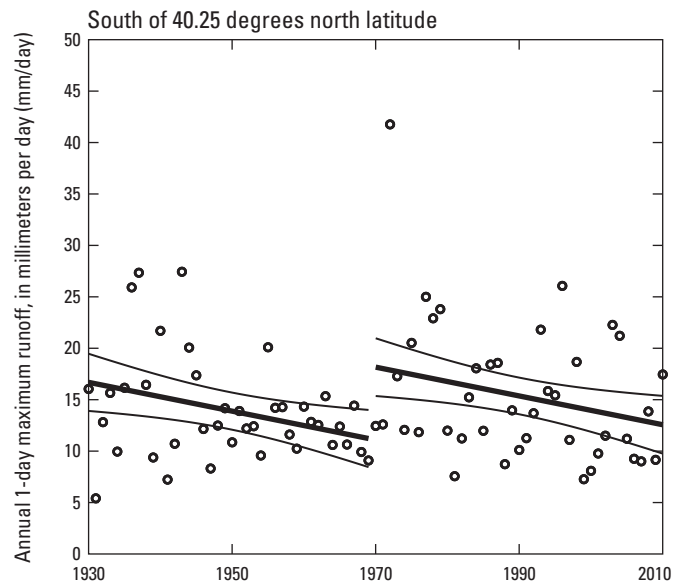
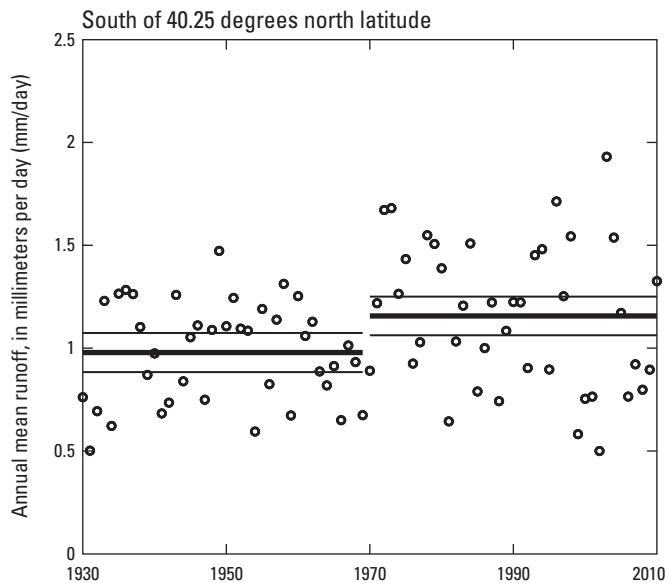
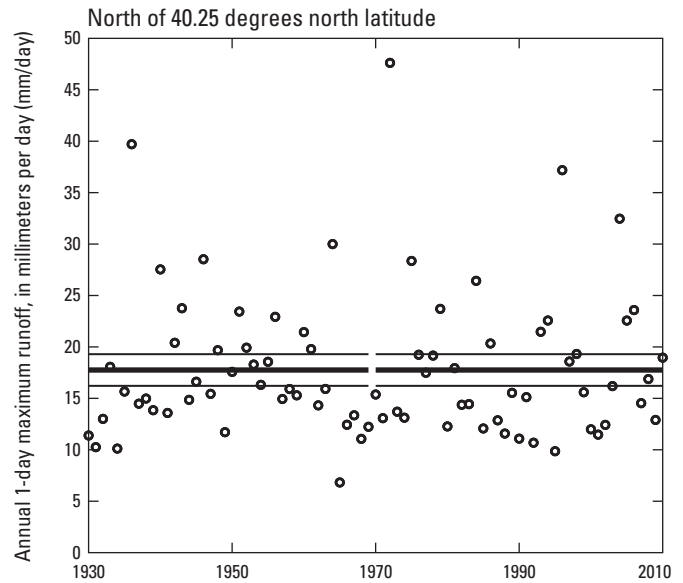
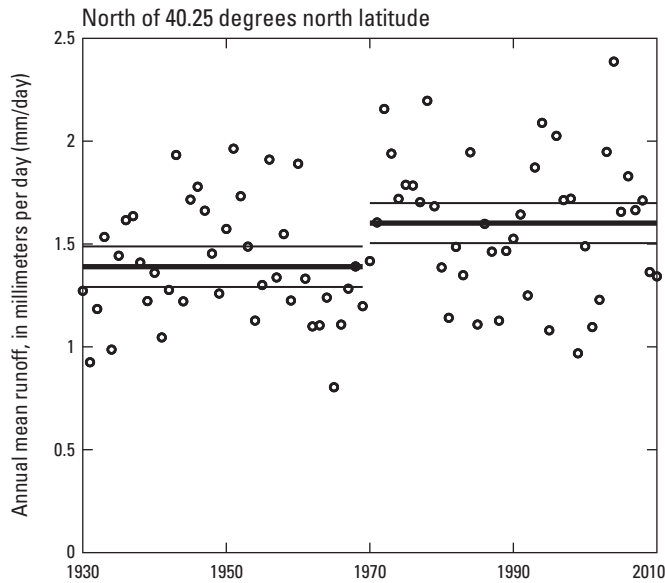


Figure 18. Selected regression model for means of the 7-day minimum runoff for sites north of 40.25 degrees north latitude and south of 40.25 degrees north latitude.

Model 4 is a stationary random process with two separate linear trends, one for 1930 through 1969 and one for 1970 through 2010.

The first step in selecting the optimal model for the time series was to fit all five of the models to each of the six time series. Model 1 and model 2, the two models with an identical number of coefficients, were compared; the model with the lowest sum of squared errors (SSE) was retained for further testing. The remaining models, model 0, model 3, and model 4,



EXPLANATION

- Model results
- 95 percent confidence interval for the mean

EXPLANATION

- Model results
- 95 percent confidence interval for the mean

Figure 19. Selected regression model for means of the mean runoff for sites north of 40.25 degrees north latitude and south of 40.25 degrees north latitude.

Figure 20. Selected regression model for means of the 1-day maximum runoff for sites north of 40.25 degrees north latitude and south of 40.25 degrees north latitude.

were compared to the retained model in a pairwise fashion from least complex (model 0) to most complex (model 4). For each comparison, an F test was performed to determine if the decrease in the SSE was sufficiently large to merit retaining the model. The choice of models was determined by the p-value (the attained significance level), that is, the probability that the decrease in SSE of this size or greater can be expected by chance alone. If the p-value was less than or equal to 0.05, the more complex model was accepted. If the p-value was

greater than 0.05, the simpler model was then compared to the next model. The decision to retain the next model was made on the basis of the p-value from the comparison with the next model. This procedure was repeated until all models had been tested.

The results of the model testing and model selection process for the six time series follow. RSS_i is the residual sum of squares for model i ; F is the test statistic; DF is the number of degrees of freedom; $=$ is equal to; and $<$ is less than.

Model selection for the 7-day minimum runoff in the north (fig. 18):

- Compare models 1 and 2, $RSS_1 = 0.309$, $RSS_2 = 0.305$, model 2 RSS is lower, therefore, proceed with model 2.
- Compare models 2 and 0, $F = 16.3$ on 1 and 79 DF, $p = 0.0001$, therefore, reject model 0 and proceed with model 2.
- Compare models 2 and 3, $F = 0.717$ on 1 and 78 DF, $p = 0.40$, do not reject model 2.
- Compare models 2 and 4, $F = 0.356$ on 2 and 77 DF, $p = 0.70$, do not reject model 2.
- Therefore, select model 2.

Model selection for the 7-day minimum runoff in the south (fig. 18):

- Compare models 1 and 2, $RSS_1 = 0.349$, $RSS_2 = 0.339$, model 2 RSS is lower, therefore, proceed with model 2.
- Compare models 2 and 0, $F = 9.2$ on 1 and 79 DF, $p = 0.003$, therefore, reject model 0 and proceed with model 2.
- Compare models 2 and 3, $F = 0.0024$ on 1 and 78 DF, $p = 0.96$, do not reject model 2.
- Compare models 2 and 4, $F = 0.042$ on 2 and 77 DF, $p = 0.964$, do not reject model 2.
- Therefore, select model 2.

Model selection for the mean runoff in the north (fig. 19):

- Compare models 1 and 2, $RSS_1 = 8.17$, $RSS_2 = 7.74$, model 2 RSS is lower, therefore, proceed with model 2.
- Compare models 2 and 0, $F = 9.28$ on 1 and 79 DF, $p = 0.003$, therefore, reject model 0 and proceed with model 2.
- Compare models 2 and 3, $F = 0.711$ on 1 and 78 DF, $p = 0.40$, do not reject model 2.
- Compare models 2 and 4, $F = 0.369$ on 2 and 77 DF, $p = 0.69$, do not reject model 2.
- Therefore, select model 2.

Model selection for the mean runoff in the south (fig. 19):

- Compare models 1 and 2, $RSS_1 = 7.58$, $RSS_2 = 7.22$, model 2 RSS is lower, therefore, proceed with model 2.
- Compare models 2 and 0, $F = 7.01$ on 1 and 79 DF, $p = 0.0097$, therefore, reject model 0 and proceed with model 2.

- Compare models 2 and 3, $F = 1.28$ on 1 and 78 DF, $p = 0.26$, do not reject model 2.
- Compare models 2 and 4, $F = 1.25$ on 2 and 77 DF, $p = 0.29$, do not reject model 2.
- Therefore, select model 2.

Model selection for the 1-day maximum runoff in the north (fig. 20):

- Compare models 1 and 2, $RSS_1 = 3877$, $RSS_2 = 3864$, model 2 RSS is lower, therefore, proceed with model 2.
- Compare models 2 and 0, $F = 0.26$ on 1 and 79 DF, $p = 0.61$, therefore, accept model 0 and reject model 2.
- Compare models 0 and 3, $F = 0.39$ on 2 and 78 DF, $p = 0.68$, do not reject model 0.
- Compare models 0 and 4, $F = 0.26$ on 3 and 77 DF, $p = 0.854$, do not reject model 0.
- Therefore, select model 0.

Model selection for the 1-day maximum runoff in the south (fig. 20):

- Compare models 1 and 2, $RSS_1 = 2814$, $RSS_2 = 2778$, model 2 RSS is lower, therefore, proceed with model 2.
- Compare models 2 and 0, $F = 1.42$ on 1 and 79 DF, $p = 0.29$, therefore, reject model 2 and proceed with model 0.
- Compare models 0 and 3, $F = 3.91$ on 2 and 78 DF, $p = 0.024$, therefore, reject model 0 and proceed with model 3.
- Compare models 3 and 4, $F = 0.17$ on 1 and 77 DF, $p = 0.68$, therefore, reject model 4.
- Therefore, select model 3.

A summary of the selected model for each of the time series is shown in table 7.

For the 7-day minimum runoff and the mean runoff in both the north and south, a clear distinction was noted, with the 1970 through 2010 subperiod having higher runoff values than the 1930 through 1969 subperiod. These differences range from as small as a 15-percent increase in the case of the mean runoff in the north, to as large as a 41-percent increase in the case of the 7-day minimum runoff in the north. For the 1-day maximum runoff in the north, there was no significant difference between the two subperiods. The situation for the 1-day maximum runoff in the south is more complicated. There was an upward step change between the two subperiods, but within each subperiod there was a decreasing trend with slopes that were not statistically significantly different from each other. The size of the upward step change was somewhat

Table 7. Model form, selected model and model coefficients, standard errors of the model coefficients, and R² values for the six time series tested.

Model form	Selected model	Standard errors of model coefficients	R ²
North 7-day minimum runoff			
Model 2	$Q = 0.133 + 0.0557 * D$	(0.0098) (0.014)	0.17
South 7-day minimum runoff			
Model 2	$Q = 0.169 + 0.0442 * D$	(0.010) (0.015)	0.10
North mean runoff			
Model 2	$Q = 1.39 + 0.212 * D$	(0.049) (0.070)	0.11
South mean runoff			
Model 2	$Q = 0.979 + 0.178 * D$	(0.048) (0.067)	0.08
North 1-day maximum runoff			
Model 0	$Q = 17.75$	(774)	0
South 1-day maximum runoff			
Model 3	$Q = 11.08 - 0.140 * T + 7.08 * D$	(1.44) (0.054) (2.5)	0.09

larger than the amount of decrease over each of the subperiods. If no linear trends were considered as possibilities, then a step trend characterization of these data would be that of a statistically insignificant slight increase over time.

The general conclusion that can be drawn from the analysis of the six time series is that the period from 1930 through 1969 was statistically significantly different from the period 1970 through 2010. Overall, the pattern is one of increasing runoff over time. No general pattern of hydrologic conditions becoming “more extreme” over time was identified, which would have been indicated by decreases in minimum flows and increases in maximum flows. The pattern of change in maximum discharge, however, is uncertain.

Summary

U.S. Geological Survey streamgages provide valuable information about streamflow for a variety of users and uses. In this report, long-term streamflow data were analyzed in an attempt to identify trends in streamflow within the Chesapeake Bay watershed and surrounding area. Data from 30 streamgages near and within the Chesapeake Bay watershed were selected for analysis because they have the longest period of record in common, 1930 through 2010. Stream discharge data from each streamgage were normalized by watershed area to obtain depth of runoff; annual runoff values were plotted as time series along with a lowess line that was determined by a robust smoothing process. The difference between the end points of the smoothed line was converted to percent change per decade for the period of interest, which was referred to as the trend slope. Trend slopes were categorized as positive, defined as a value greater than 1-percent increase per decade;

near-zero, defined as a value from -1- to 1-percent change per decade; or negative, defined as a value greater than 1-percent decrease per decade. Three runoff statistics were selected for analysis: the 7-day minimum; the mean; and the 1-day maximum.

Trend slopes in the runoff statistics were analyzed on an annual basis for the whole period of record as well as on a seasonal basis. The slopes also were analyzed both spatially and temporally. The overall pattern identified was one of increasing runoff through time, without becoming more variable. A distinct difference was observed in streamgages in the northern part of the watershed relative to those in the south. A latitude of 40.25 degrees north was identified as the line that generally separated the change of sign or magnitude of the trend slopes across the region.

The spatial results indicated that trend slopes in the north were generally greater than those in the south. In addition, runoff at streamgages in the north generally has become less variable over time than runoff in the south. This means that the low flows have increased so that they are closer to the mean flows and that the high flows have not increased as much as the low flows, remaining closer to the mean flows. In contrast, results in the south do not indicate a loss of variability as large as sites in the north. The seasonal statistics indicate that in the north, the 1-day maximum flows are higher in the winter than in the other seasons, whereas in the south, the 1-day maximum flows are higher in the fall than in the other seasons.

The temporal analysis was done by splitting the 80-year flow record into two subsets: 1930 through 1969 and 1970 through 2010. The mean of the data for all sites for each year were plotted so that the following datasets were analyzed: the 7-day minimum runoff for the north and south; the mean runoff for the north and south; and the 1-day maximum runoff for the north and south. Results indicated that the period 1930 through 1969 was statistically significantly different from the period 1970 through 2010. For the 7-day minimum runoff and the mean runoff, the latter period had significantly higher streamflow than did the earlier period, although within those two periods no significant linear trends were identified. For the 1-day maximum runoff, no step trend or linear trend could be shown to be statistically significant for the north, although the south showed a mixture of an upward step trend accompanied by linear downtrends within the periods. In no case was a change identified that indicated an increasing rate of change over time. No general pattern was identified of hydrologic conditions becoming “more extreme” over time, which would have been indicated by decreases in minimum flows and increases in maximum flows.

This analysis is the first to determine trends in runoff in the Chesapeake Bay watershed and surrounding area. The north-to-south extent of the study area spans two regions that generally are used for analysis of precipitation patterns, so previously published precipitation results and the runoff results presented here are not directly comparable. Nevertheless, the overall increase in runoff identified in this analysis generally is consistent with reported increases in precipitation in the

region over similar time periods. This report does not address future changes to streamflow, but the results should serve as a baseline by which future changes can be compared.

Acknowledgments

The authors wish to acknowledge the colleague reviews of the report provided by Samuel H. Austin, Hydrologist, USGS, Richmond, Virginia, and Karen R. Ryberg, Statistician, USGS, Bismarck, North Dakota.

References Cited

- Bricker, S.B., Clement, C.G., Pirhalla, D.E., Orlando, S.P., and Farrow, D.R.G., 1999, National estuarine eutrophication assessment—Effects of nutrient enrichment in the Nation’s estuaries: Silver Spring, Md., National Oceanic and Atmospheric Administration, National Ocean Service, Special Projects Office and National Centers for Coastal Ocean Science, 77 p.
- Bricker, S.B., Longstaff, B., Dennison, W., Jones, A., Boicourt, K., Wicks, C., and Woerner, J., 2007, Effects of nutrient enrichment in the Nation’s estuaries: A decade of change, National estuarine eutrophication assessment update: National Oceanic and Atmospheric Administration, National Centers for Coastal Ocean Science, Coastal Ocean Program Decision Analysis Series No. 26, 322 p.
- Cleveland, W.S., 1979, Robust locally weighted regression and smoothing scatterplots: *Journal of the American Statistical Association*, v. 74, p. 829–836.
- Cleveland, W.S., and Devlin, S.J., 1988, Locally weighted regression: An approach to regression analysis by local fitting: *Journal of the American Statistical Association*, v. 83, p. 596–610.
- Cohn, T.A., and Lins, H.F., 2005, Nature’s style: Naturally trendy: *Geophysical Research Letters*, 32, L23402, doi:10.1029/2005GL024476.
- Collins, M.J., 2009, Evidence for changing flood risk in New England since the late 20th century: *Journal of the American Water Resources Association*, v. 45, iss. 2, p. 279–290.
- Fenneman, N.M., and Johnson, D.W., 1946, Physical divisions of the United States: U.S. Geological Survey, 1 sheet, scale 1:7,000,000.
- Gordon, N.D., Finlayson, B.L., and McMahon, T.A., 2004, *Stream hydrology: An introduction for ecologists*: New York, John Wiley, 429 p.
- Hayhoe, Katharine, Wake, C.P., Huntington, T.G., Luo, Lifeng, Schwartz, M.D., Sheffield, Justin, Wood, Eric, Anderson, Bruce, Bradbury, James, DeGaetano, Art, Troy, T.J., and Wolfe, David, 2007, Past and future changes in climate and hydrological indicators in the US Northeast: *Climate Dynamics*, v. 28, p. 381–407.
- Helsel, D.R., and Hirsch, R.M., 1992, *Statistical methods in water resources*: New York, Elsevier, 522 p.
- Helsel, D.R., and Hirsch, R.M., 2002, *Statistical methods in water resources—Hydrologic analysis and interpretation: U.S. Geological Survey Techniques of Water Resources Investigations*, book 4, chap. A3, 510 p.
- Karl, T.R., and Knight, R.W., 1998, Secular trends of precipitation amount, frequency, and intensity in the United States: *Bulletin of the American Meteorological Society*, v. 79, no. 2, p. 231–241.
- Koutsoyiannis, Demetris, 2003, Climate change, the Hurst phenomenon and hydrological statistics: *Hydrological Sciences Journal*, v. 48, no. 1, p. 3–24.
- Lins, H.F., and Slack, J.R., 1999, Streamflow trends in the United States: *Geophysical Research Letters*, v. 26, p. 227–230.
- McCabe, G.J., and Wolock, D.M., 2002, A step increase in streamflow in the conterminous United States: *Geophysical Research Letters*, v. 29, p. 2185–2188.
- Najjar, R.G., Patterson, L., and Graham, Steve, 2009, Climate simulations of major estuarine watersheds in the mid-Atlantic region of the US: *Climatic Change*, v. 95, p. 139–168.
- Phillips, S.W., ed., 2007, *Synthesis of U.S. Geological Survey science for the Chesapeake Bay ecosystem and implications for environmental management: U.S. Geological Survey Circular 1316*, 63 p.
- Pyke, C.R., and Najjar, R.G., 2008, *Climate change and the Chesapeake Bay: State-of-the-science review and recommendations: Chesapeake Bay Program Science and Technical Advisory Committee*, 85 p.
- Riggs, H.C., 1982, *Low-flow investigations: U.S. Geological Survey Techniques of Water-Resources Investigations*, book 4, chap. B1, 18 p.
- Riggs, H.C., 1985, *Streamflow characteristics: Developments in water science 22*: New York, Elsevier, 249 p.
- Tukey, J.W., 1977, *Exploratory data analysis*: Reading, Mass., Addison-Wesley, 688 p.

Appendix

Black River near Boonville, N.Y.

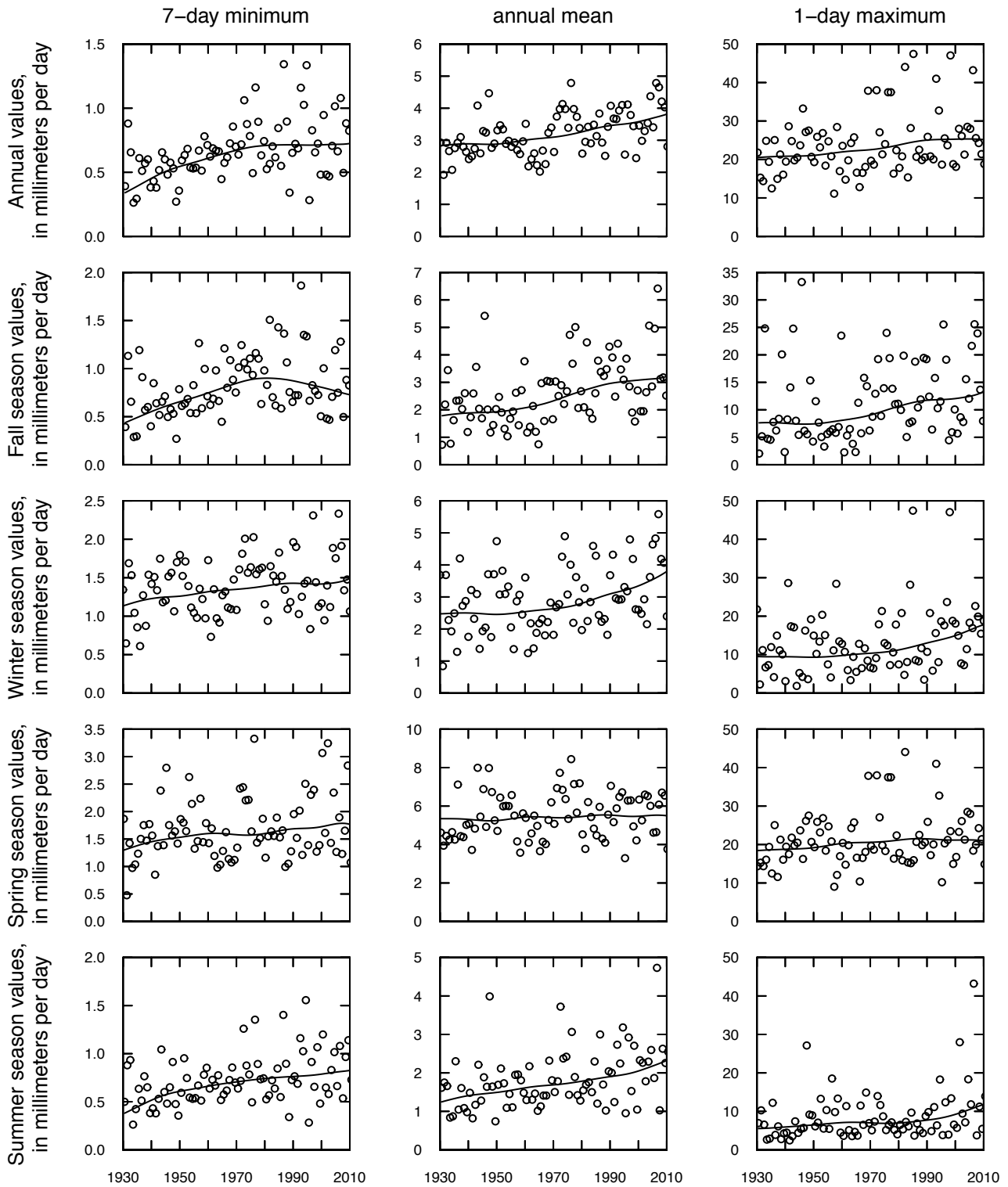


Figure 1-1. Streamflow statistics (circles) in units of millimeters per day, annual values and seasonal values; fall (September, October, and November), winter (December, January, and February), spring (March, April, and May), and summer (June, July, and August), and locally weighted scatterplot smooth (solid curve) for Black River near Boonville, N.Y., 1930–2010.

Chenango River near Chenango Forks, N.Y.

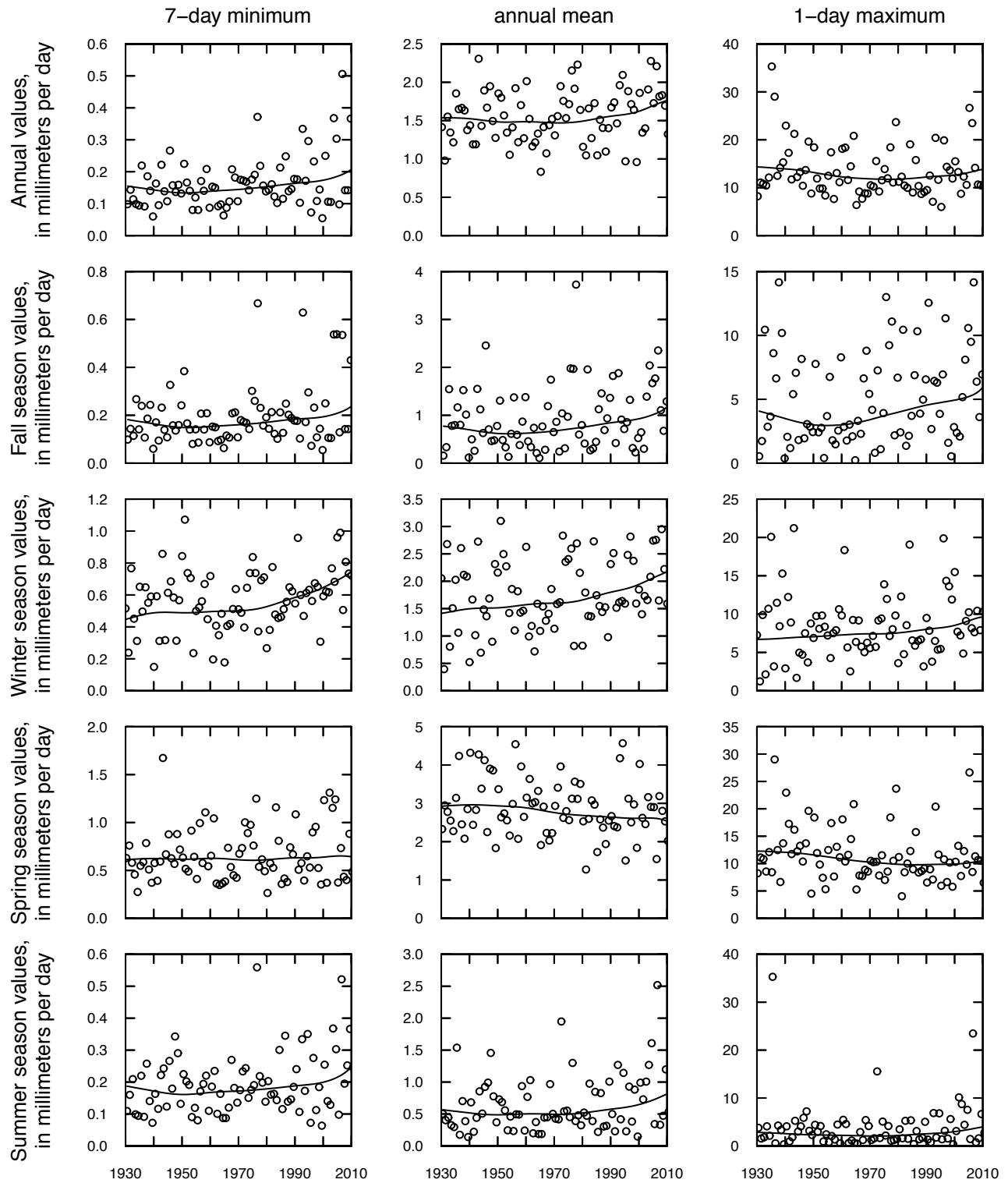


Figure 1-2. Streamflow statistics (circles) in units of millimeters per day, annual values and seasonal values; fall (September, October, and November), winter (December, January, and February), spring (March, April, and May), and summer (June, July, and August), and locally weighted scatterplot smooth (solid curve) for Chenango River near Chenango Forks, N.Y., 1930–2010.

Susquehanna River at Conklin, N.Y.

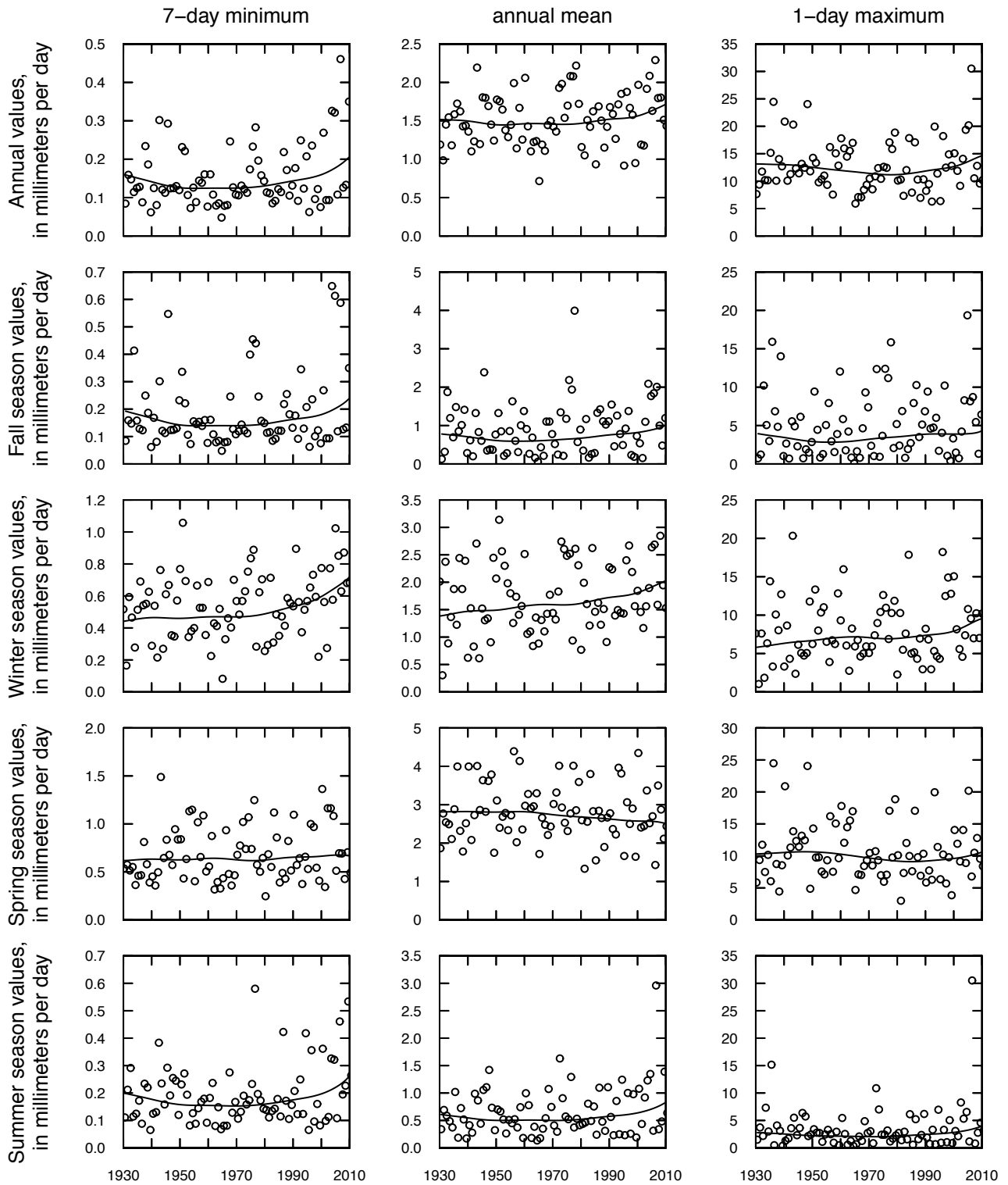


Figure 1-3. Streamflow statistics (circles) in units of millimeters per day, annual values and seasonal values; fall (September, October, and November), winter (December, January, and February), spring (March, April, and May), and summer (June, July, and August), and locally weighted scatterplot smooth (solid curve) for Susquehanna River at Conklin, N.Y., 1930–2010.

Chemung River at Chemung, N.Y.

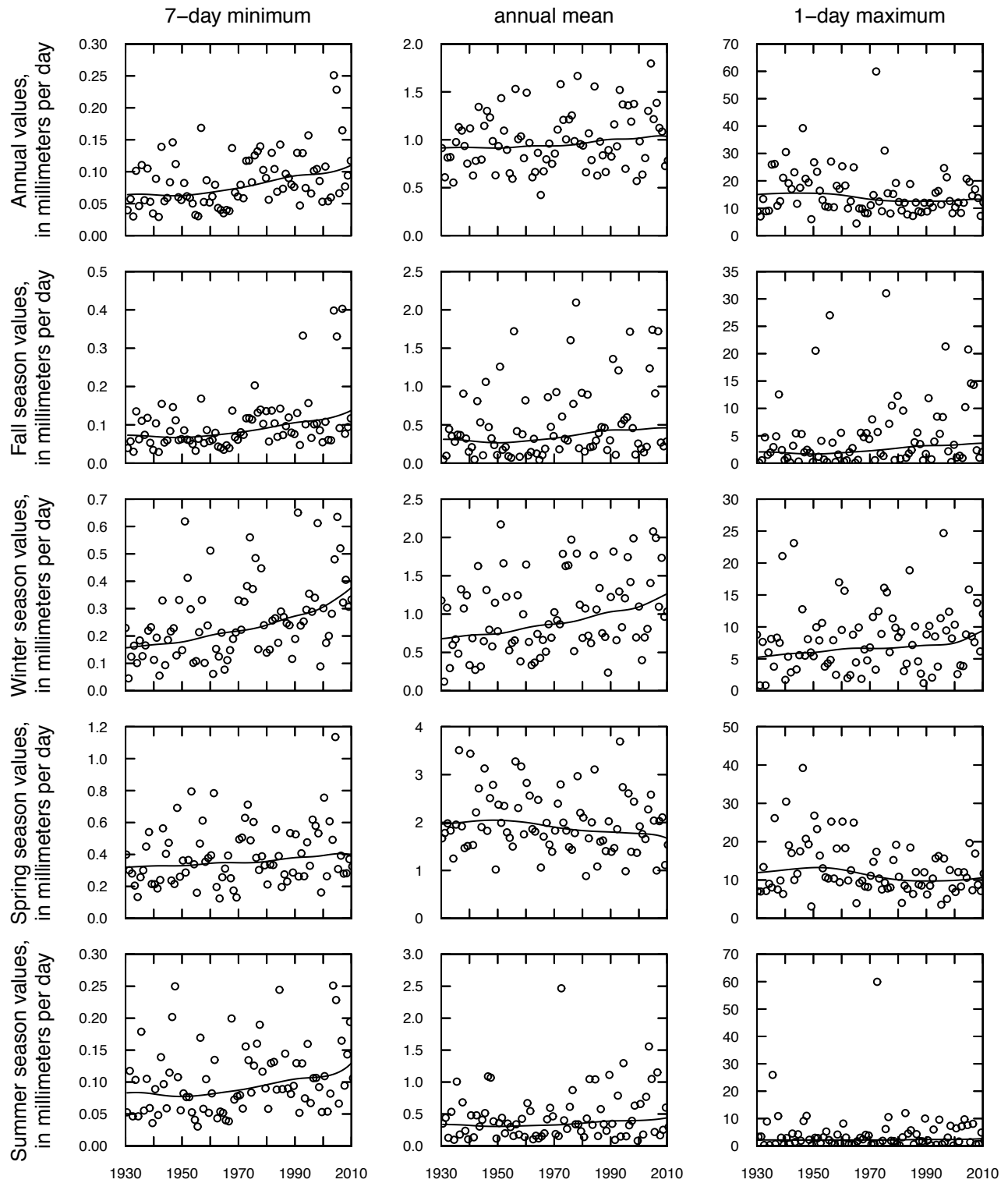


Figure 1-4. Streamflow statistics (circles) in units of millimeters per day, annual values and seasonal values; fall (September, October, and November), winter (December, January, and February), spring (March, April, and May), and summer (June, July, and August), and locally weighted scatterplot smooth (solid curve) for Chemung River at Chemung, N.Y., 1930–2010.

Susquehanna River at Towanda, Pa.

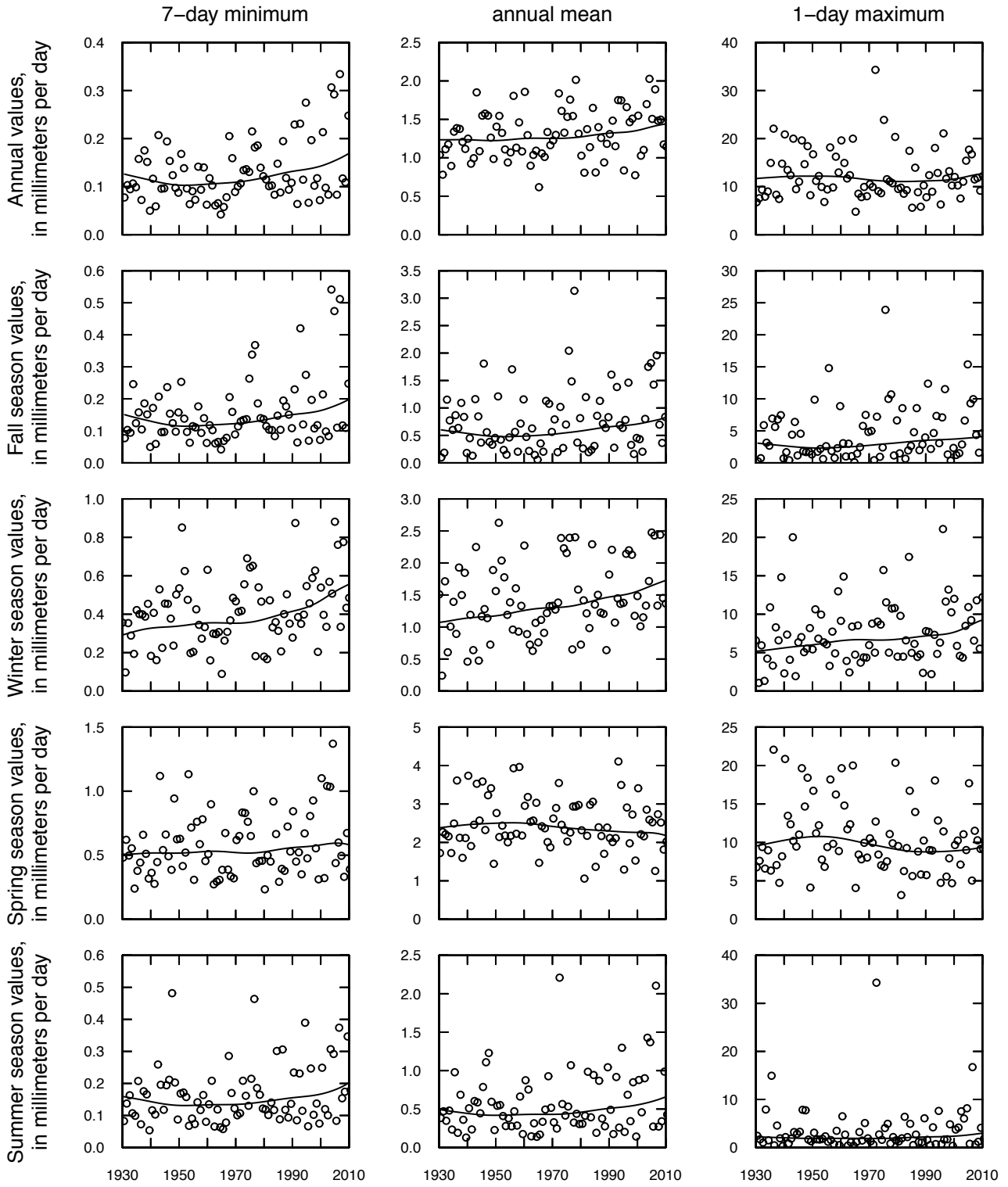


Figure 1-5. Streamflow statistics (circles) in units of millimeters per day, annual values and seasonal values; fall (September, October, and November), winter (December, January, and February), spring (March, April, and May), and summer (June, July, and August), and locally weighted scatterplot smooth (solid curve) for Susquehanna River at Towanda, Pa., 1930–2010.

Towanda Creek near Monroeton, Pa.

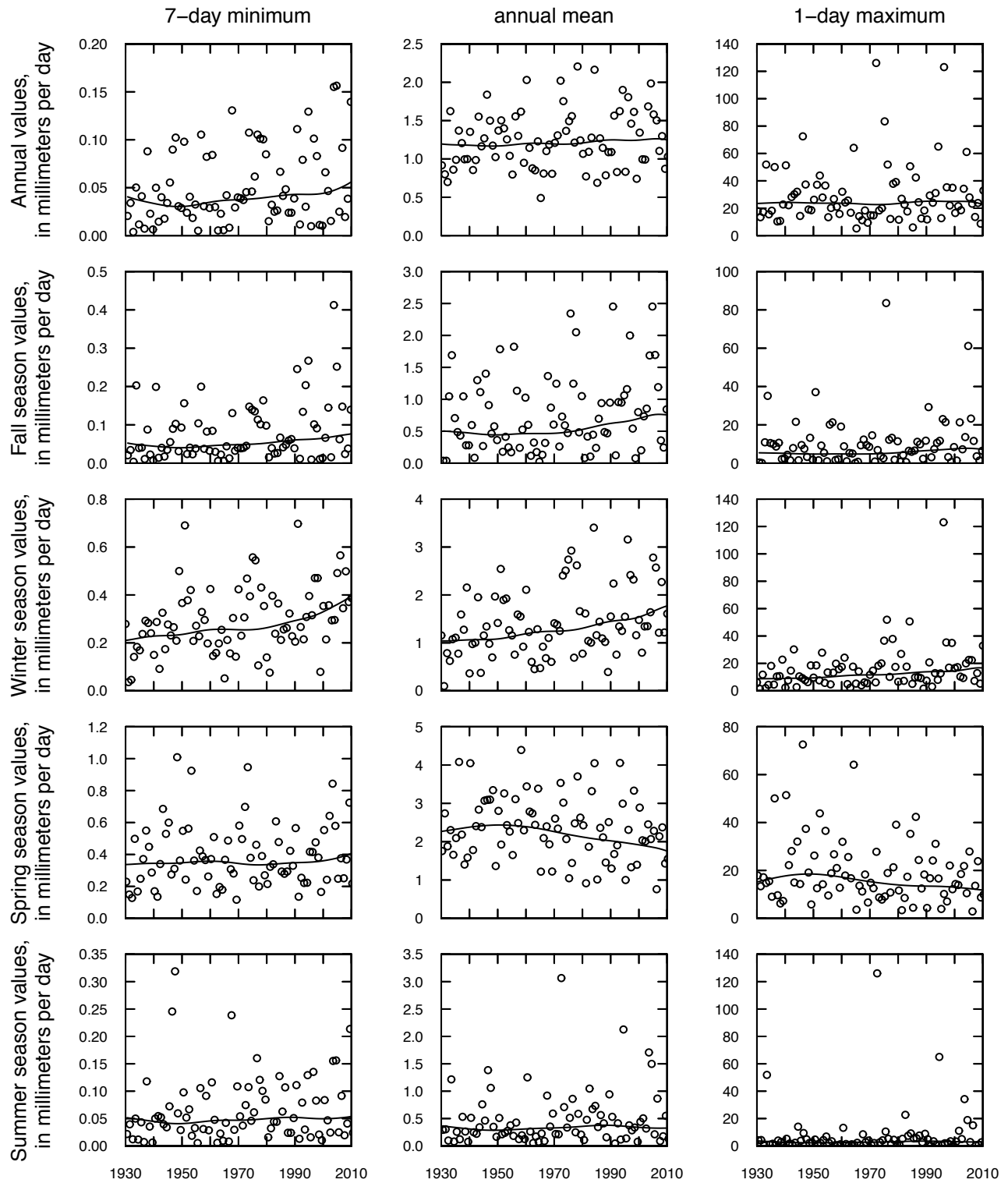


Figure 1-6. Streamflow statistics (circles) in units of millimeters per day, annual values and seasonal values; fall (September, October, and November), winter (December, January, and February), spring (March, April, and May), and summer (June, July, and August), and locally weighted scatterplot smooth (solid curve) for Towanda Creek near Monroeton, Pa., 1930-2010.

Tunkhannock Creek near Tunkhannock, Pa.

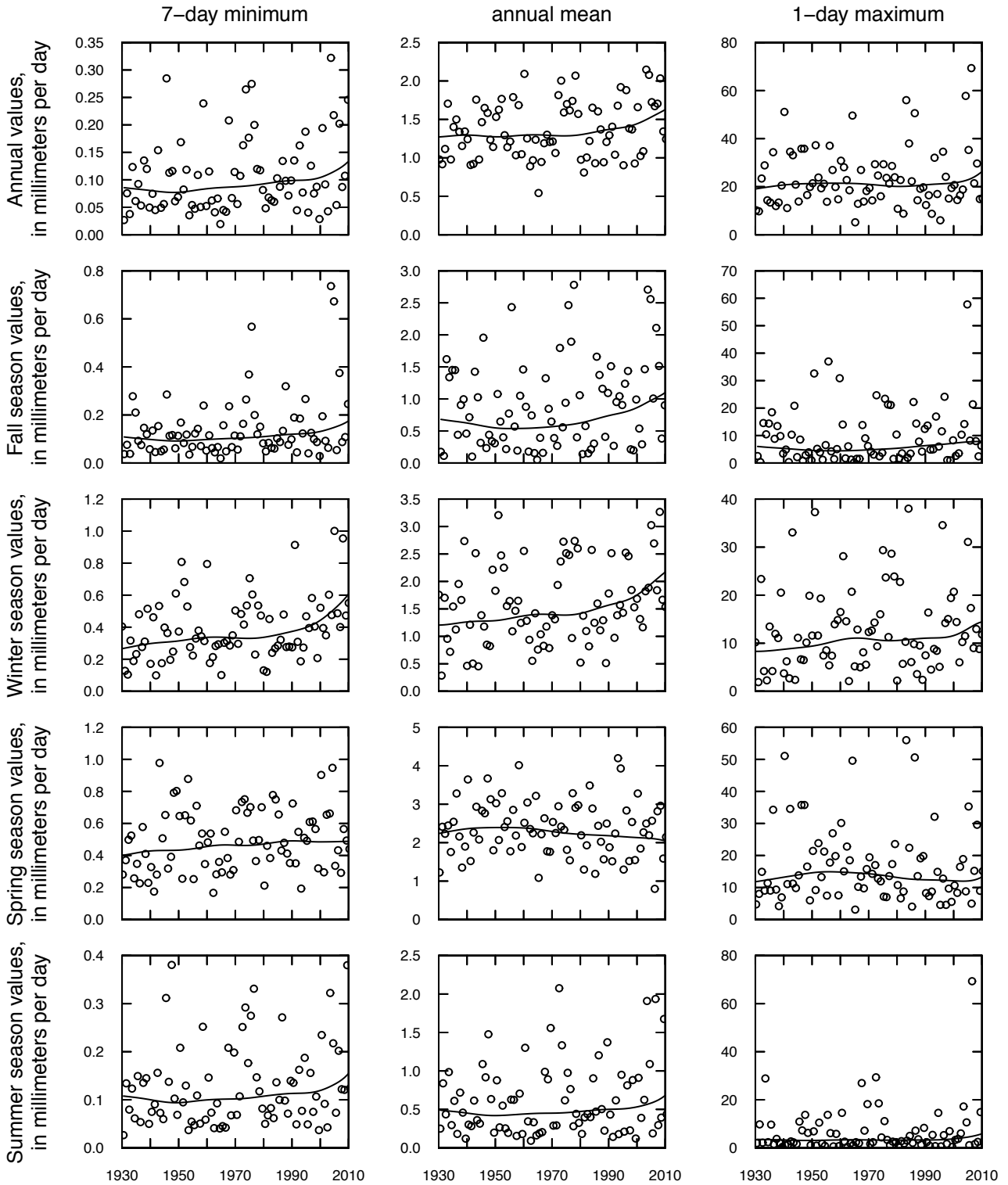


Figure 1-7. Streamflow statistics (circles) in units of millimeters per day, annual values and seasonal values; fall (September, October, and November), winter (December, January, and February), spring (March, April, and May), and summer (June, July, and August), and locally weighted scatterplot smooth (solid curve) for Tunkhannock Creek near Tunkhannock, Pa., 1930–2010.

Lycoming Creek near Trout Run, Pa.

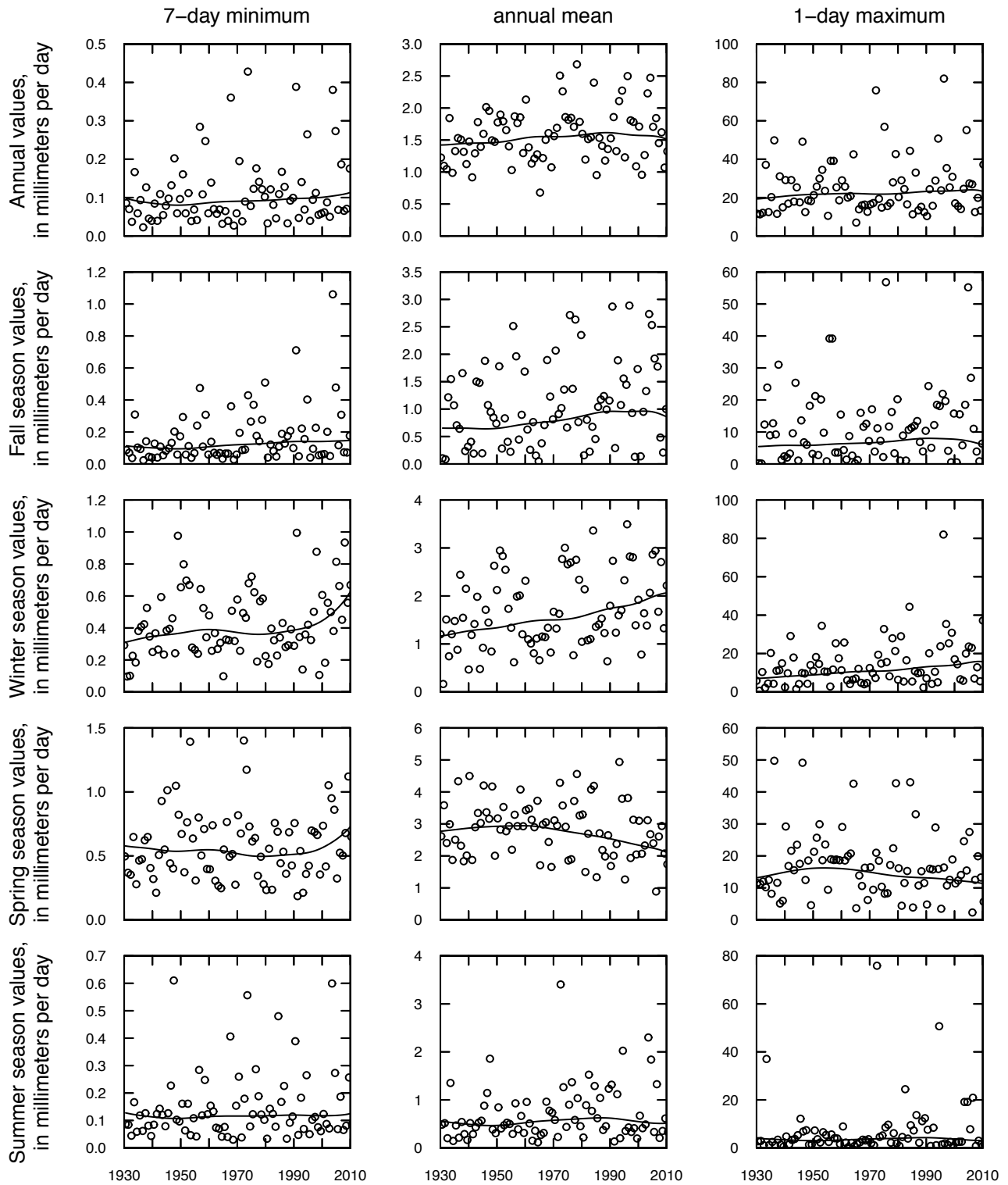


Figure 1-8. Streamflow statistics (circles) in units of millimeters per day, annual values and seasonal values; fall (September, October, and November), winter (December, January, and February), spring (March, April, and May), and summer (June, July, and August), and locally weighted scatterplot smooth (solid curve) for Lycoming Creek near Trout Run, Pa., 1930-2010.

Driftwood Branch Sinnemahoning Creek at Sterling Run, Pa.

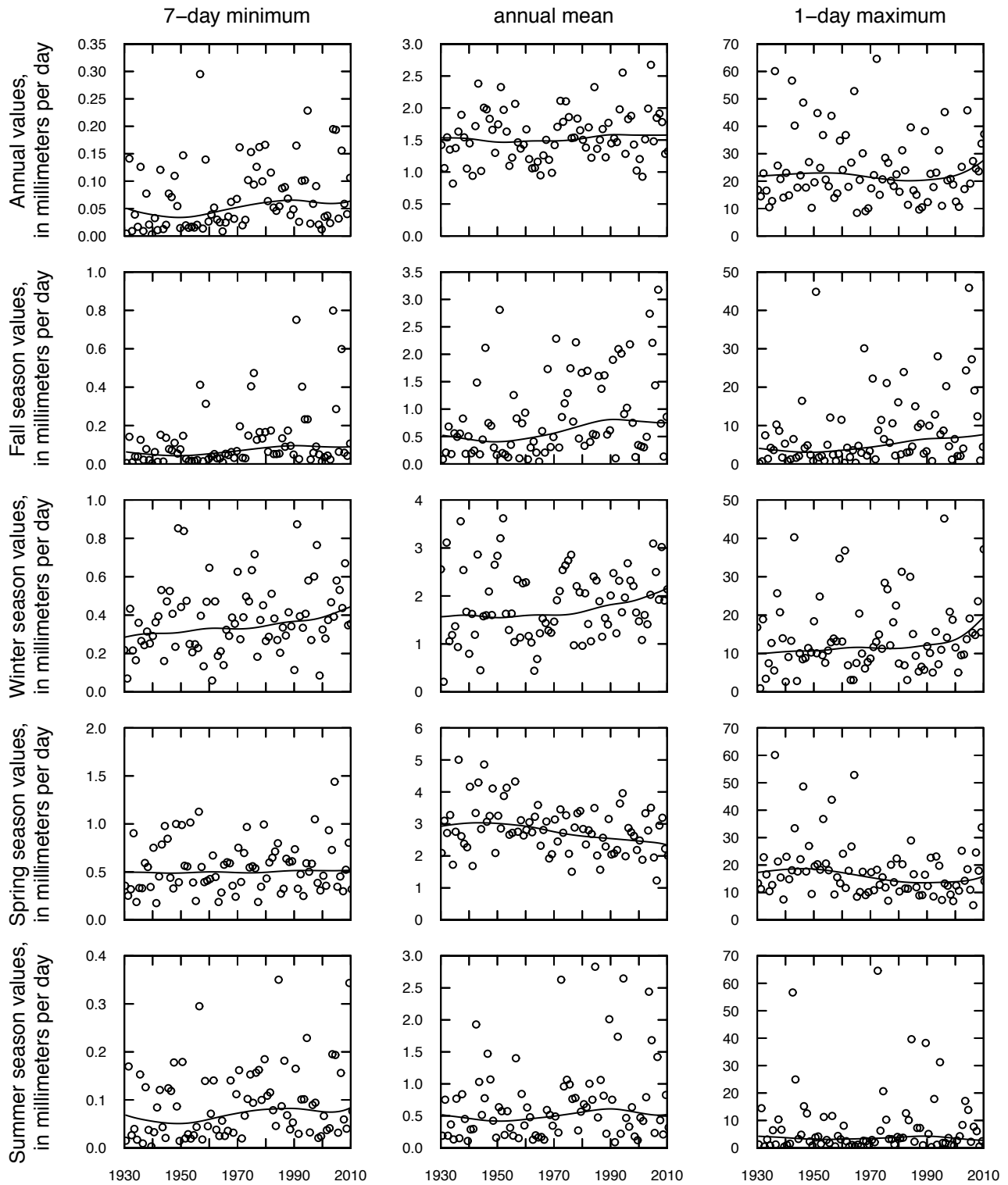


Figure 1-9. Streamflow statistics (circles) in units of millimeters per day, annual values and seasonal values; fall (September, October, and November), winter (December, January, and February), spring (March, April, and May), and summer (June, July, and August), and locally weighted scatterplot smooth (solid curve) for Driftwood Branch Sinnemahoning Creek at Sterling Run, Pa., 1930–2010.

West Branch Susquehanna River at Renovo, Pa.

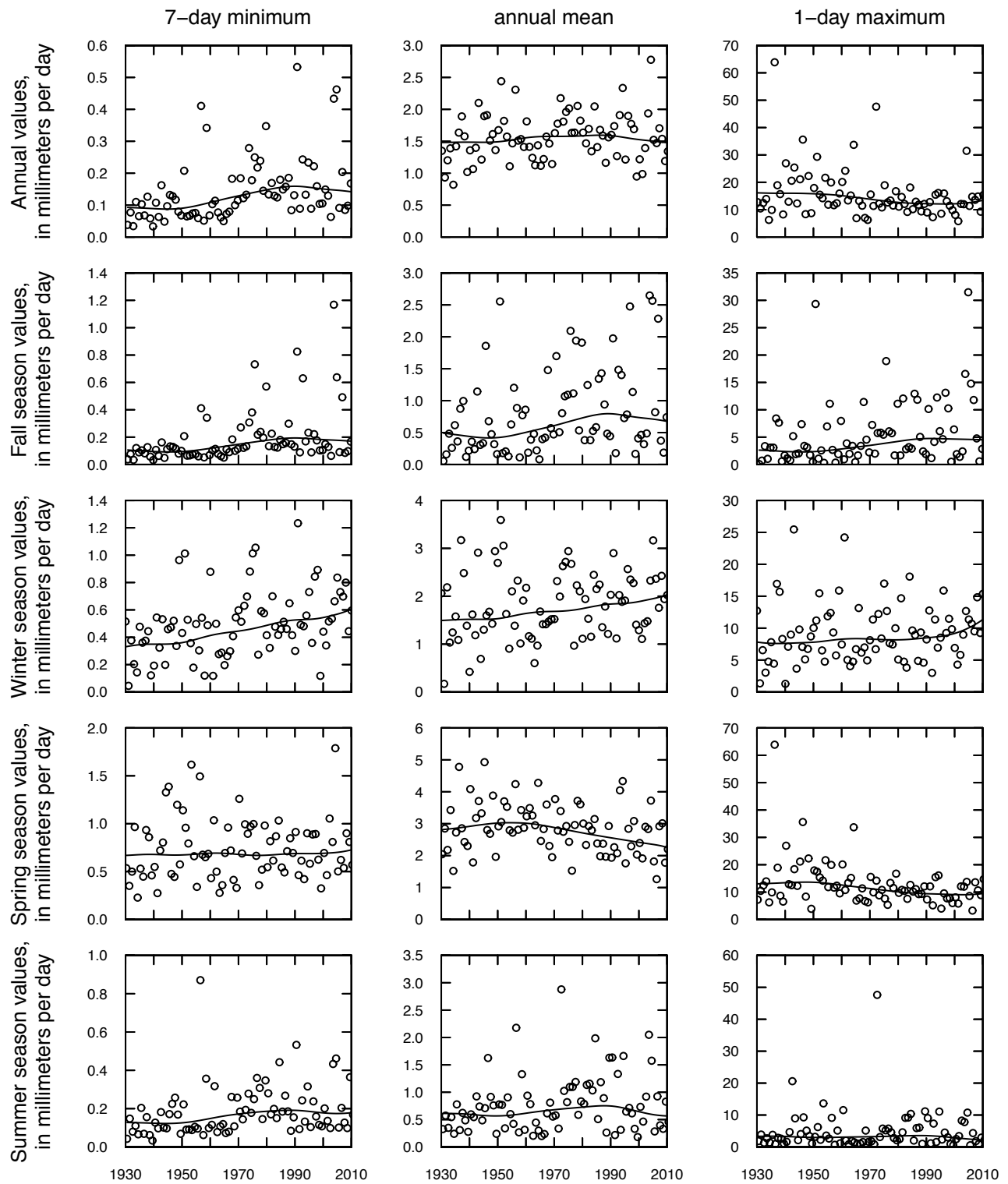


Figure 1-10. Streamflow statistics (circles) in units of millimeters per day, annual values and seasonal values; fall (September, October, and November), winter (December, January, and February), spring (March, April, and May), and summer (June, July, and August), and locally weighted scatterplot smooth (solid curve) for West Branch Susquehanna River at Renovo, Pa., 1930-2010.

Susquehanna River at Wilkes-Barre, Pa.

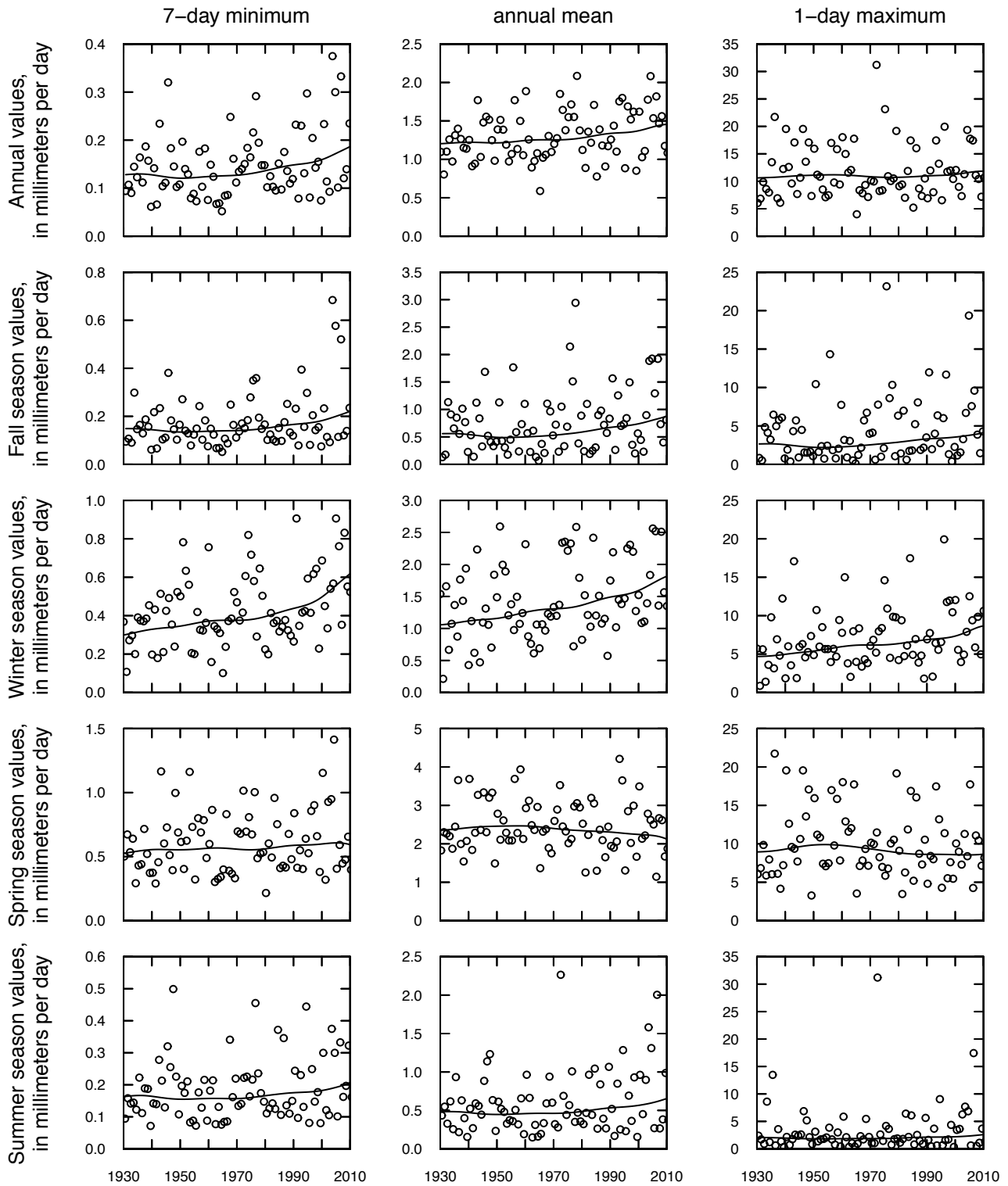


Figure 1-11. Streamflow statistics (circles) in units of millimeters per day, annual values and seasonal values; fall (September, October, and November), winter (December, January, and February), spring (March, April, and May), and summer (June, July, and August), and locally weighted scatterplot smooth (solid curve) for Susquehanna River at Wilkes-Barre, Pa., 1930–2010.

West Branch Susquehanna River at Williamsport, Pa.

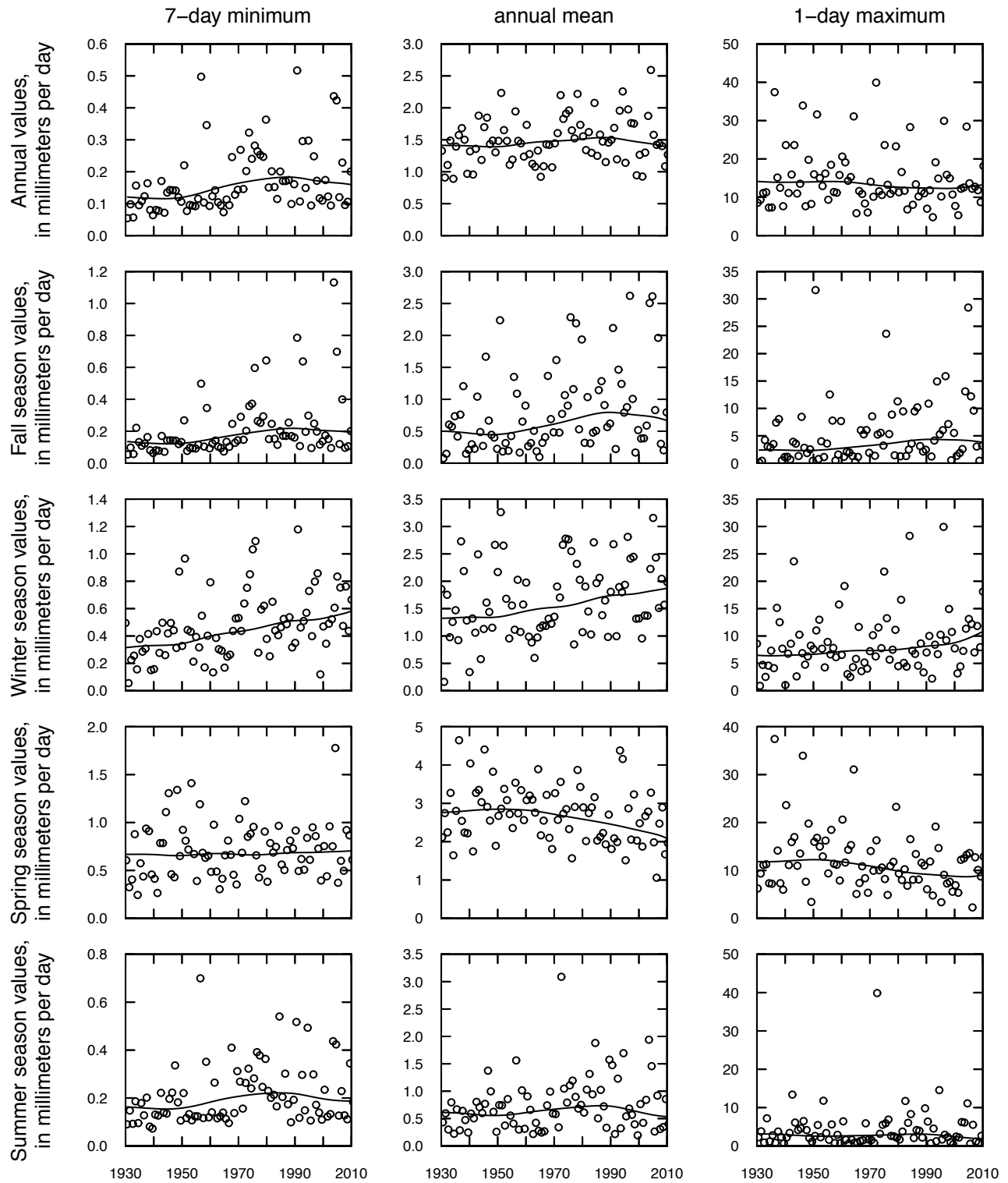


Figure 1-12. Streamflow statistics (circles) in units of millimeters per day, annual values and seasonal values; fall (September, October, and November), winter (December, January, and February), spring (March, April, and May), and summer (June, July, and August), and locally weighted scatterplot smooth (solid curve) for West Branch Susquehanna River at Williamsport, Pa., 1930–2010.

Bush Kill at Shoemakers, Pa.

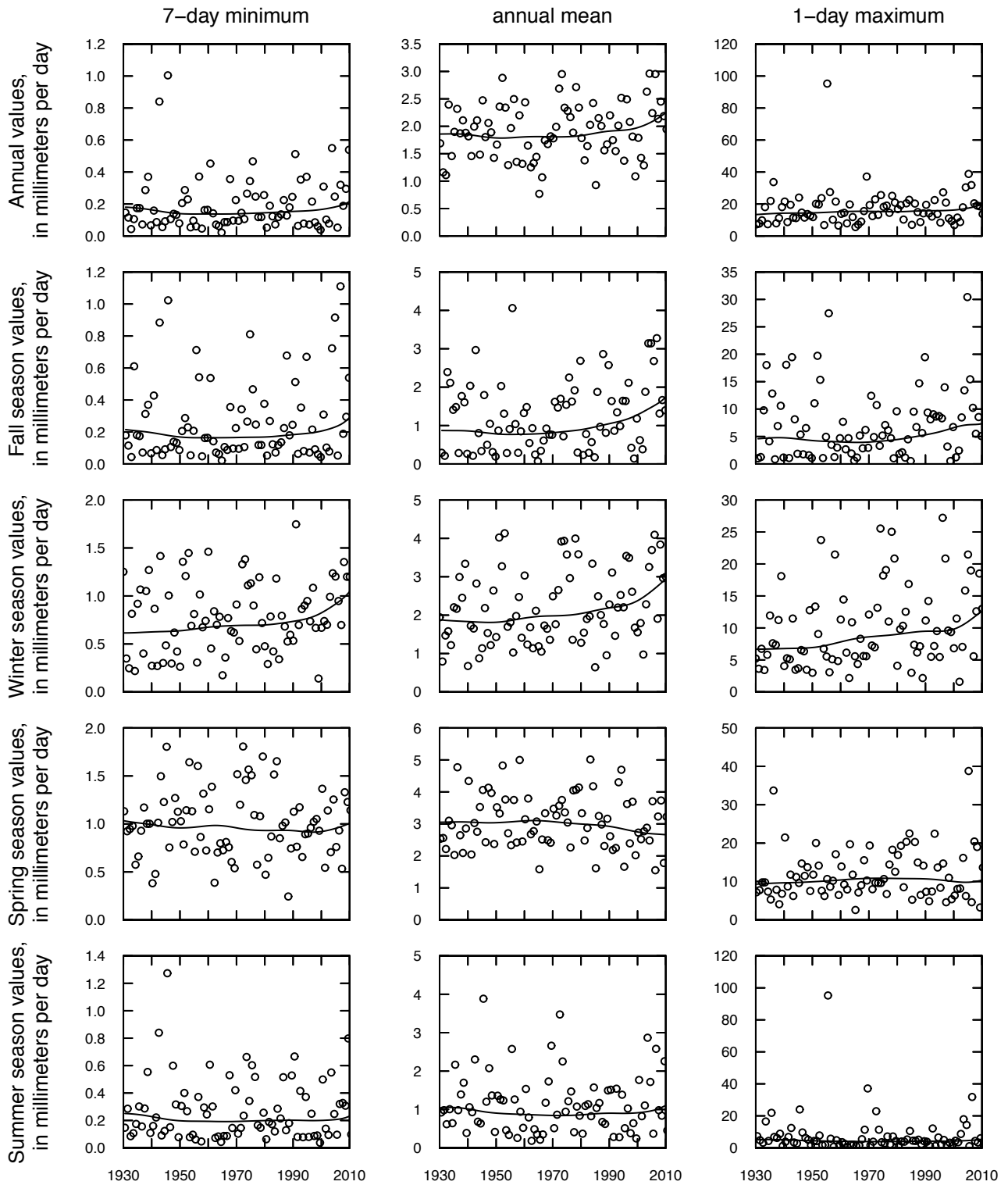


Figure 1-13. Streamflow statistics (circles) in units of millimeters per day, annual values and seasonal values; fall (September, October, and November), winter (December, January, and February), spring (March, April, and May), and summer (June, July, and August), and locally weighted scatterplot smooth (solid curve) for Bush Kill at Shoemakers, Pa., 1930–2010.

Clearfield Creek at Dimeling, Pa.

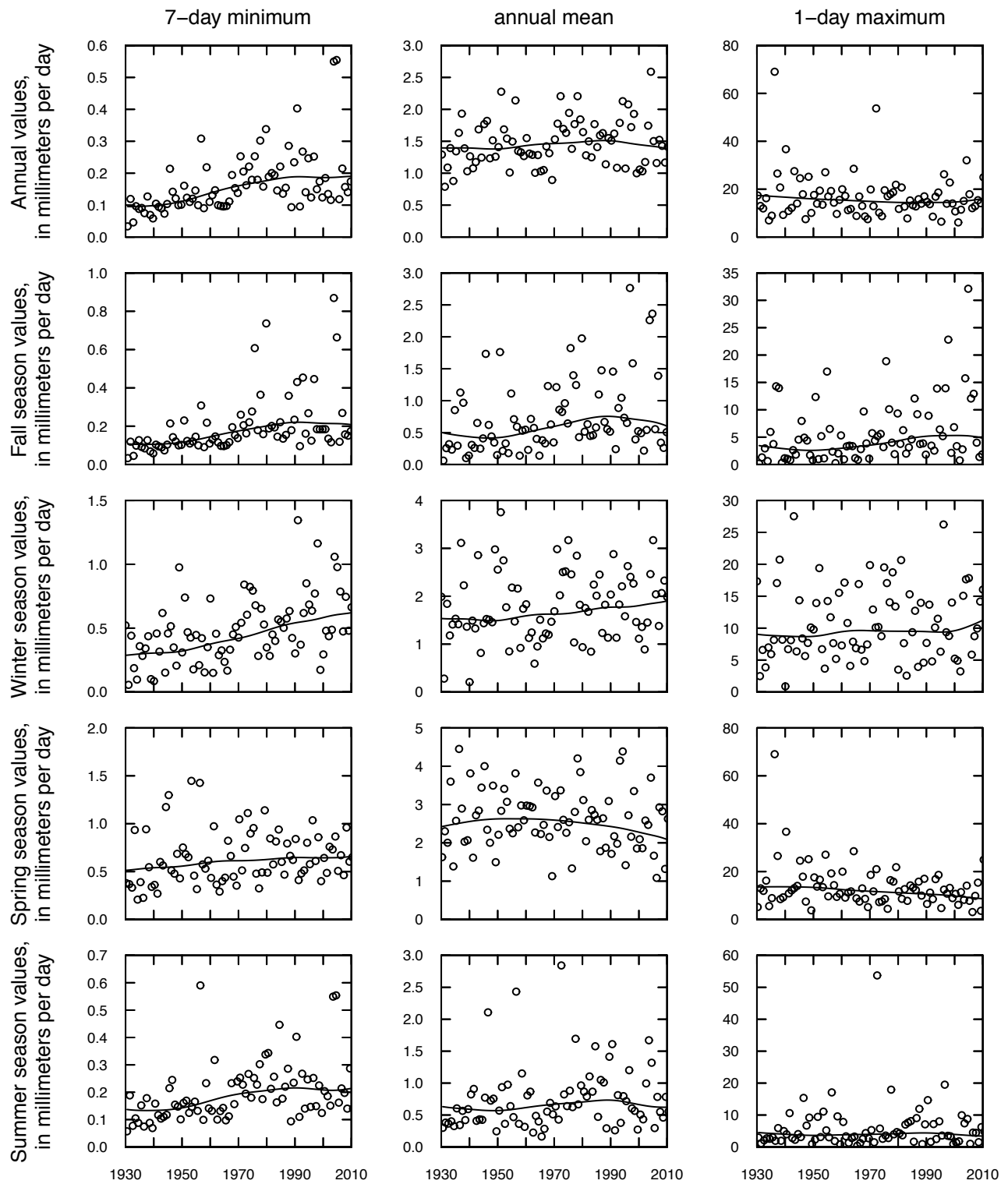


Figure 1-14. Streamflow statistics (circles) in units of millimeters per day, annual values and seasonal values; fall (September, October, and November), winter (December, January, and February), spring (March, April, and May), and summer (June, July, and August), and locally weighted scatterplot smooth (solid curve) for Clearfield Creek at Dimeling, Pa., 1930–2010.

Susquehanna River at Danville, Pa.

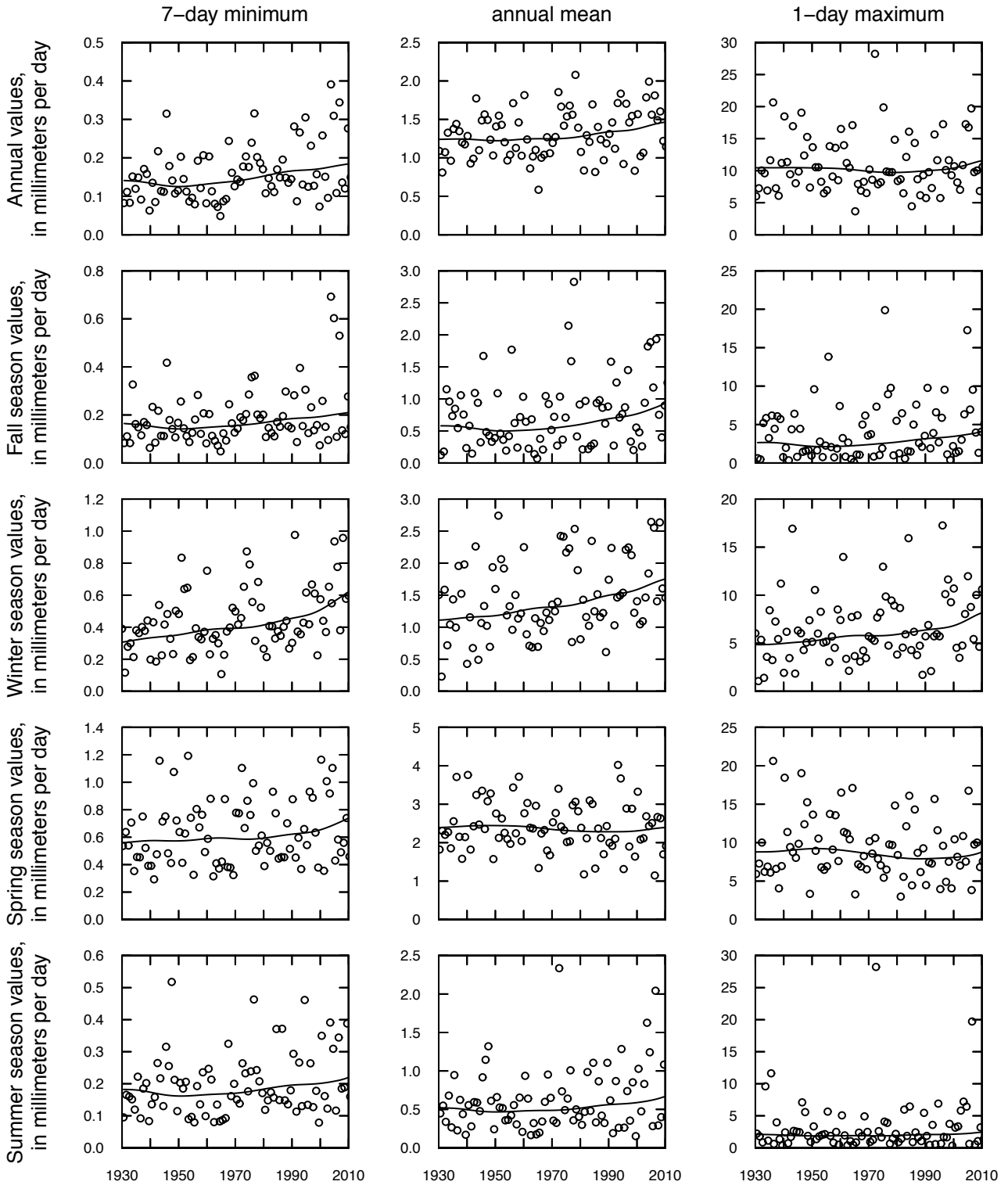


Figure 1-15. Streamflow statistics (circles) in units of millimeters per day, annual values and seasonal values; fall (September, October, and November), winter (December, January, and February), spring (March, April, and May), and summer (June, July, and August), and locally weighted scatterplot smooth (solid curve) for Susquehanna River at Danville, Pa., 1930–2010.

West Branch Susquehanna River at Bower, Pa.

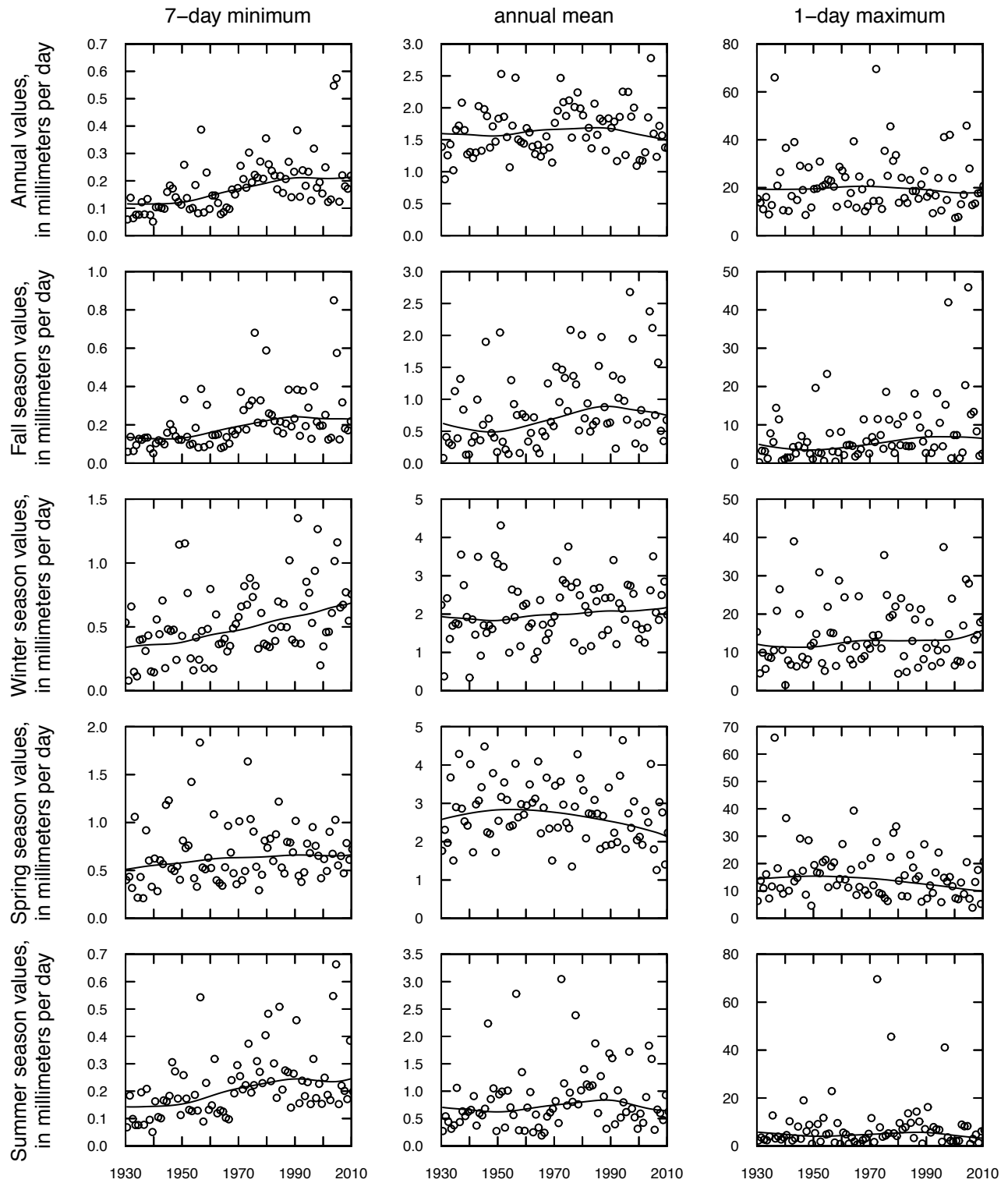


Figure 1-16. Streamflow statistics (circles) in units of millimeters per day, annual values and seasonal values; fall (September, October, and November), winter (December, January, and February), spring (March, April, and May), and summer (June, July, and August), and locally weighted scatterplot smooth (solid curve) for West Branch Susquehanna River at Bower, Pa., 1930–2010.

Juniata River at Newport, Pa.

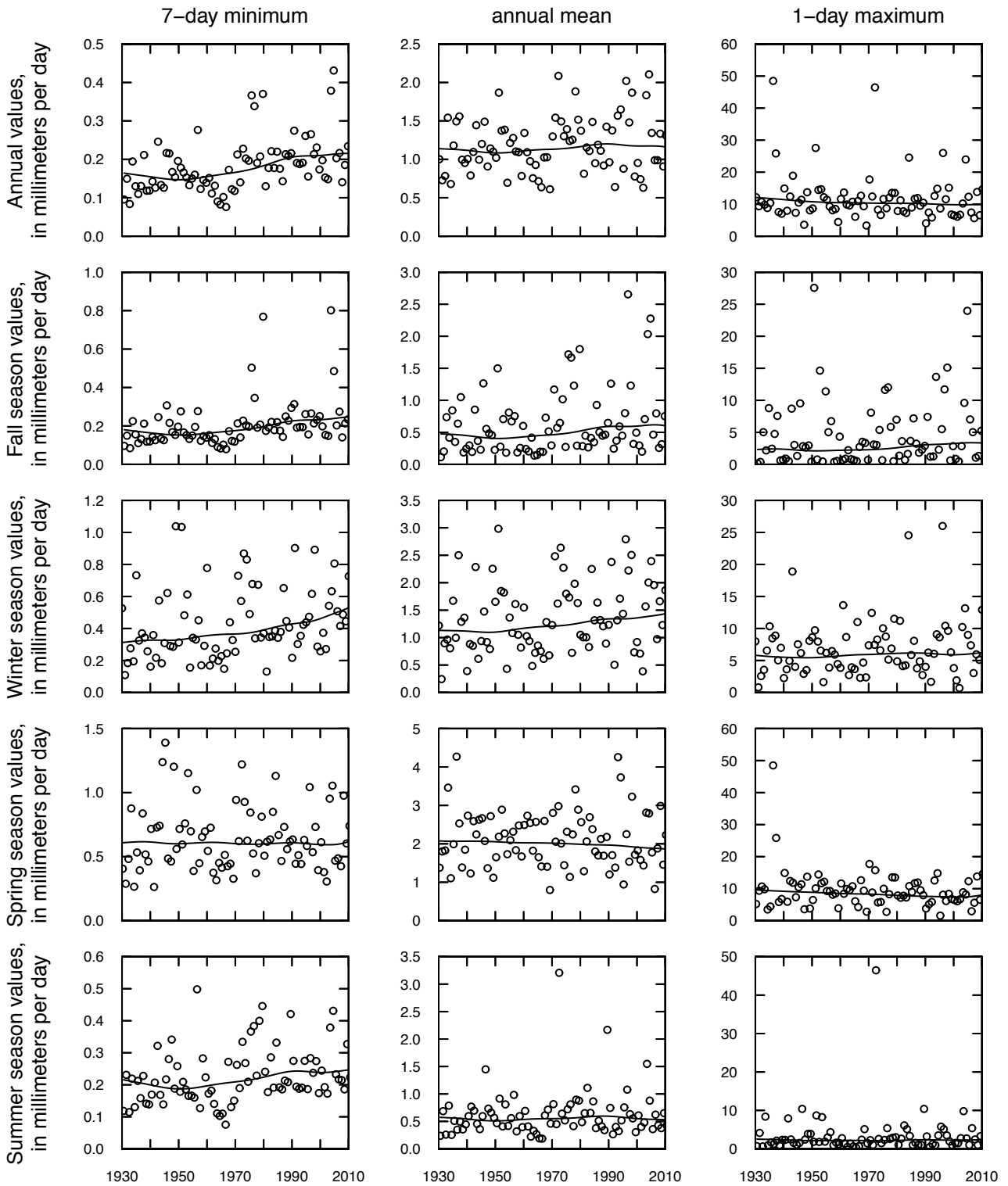


Figure 1-17. Streamflow statistics (circles) in units of millimeters per day, annual values and seasonal values; fall (September, October, and November), winter (December, January, and February), spring (March, April, and May), and summer (June, July, and August), and locally weighted scatterplot smooth (solid curve) for Juniata River at Newport, Pa., 1930–2010.

Susquehanna River at Harrisburg, Pa.

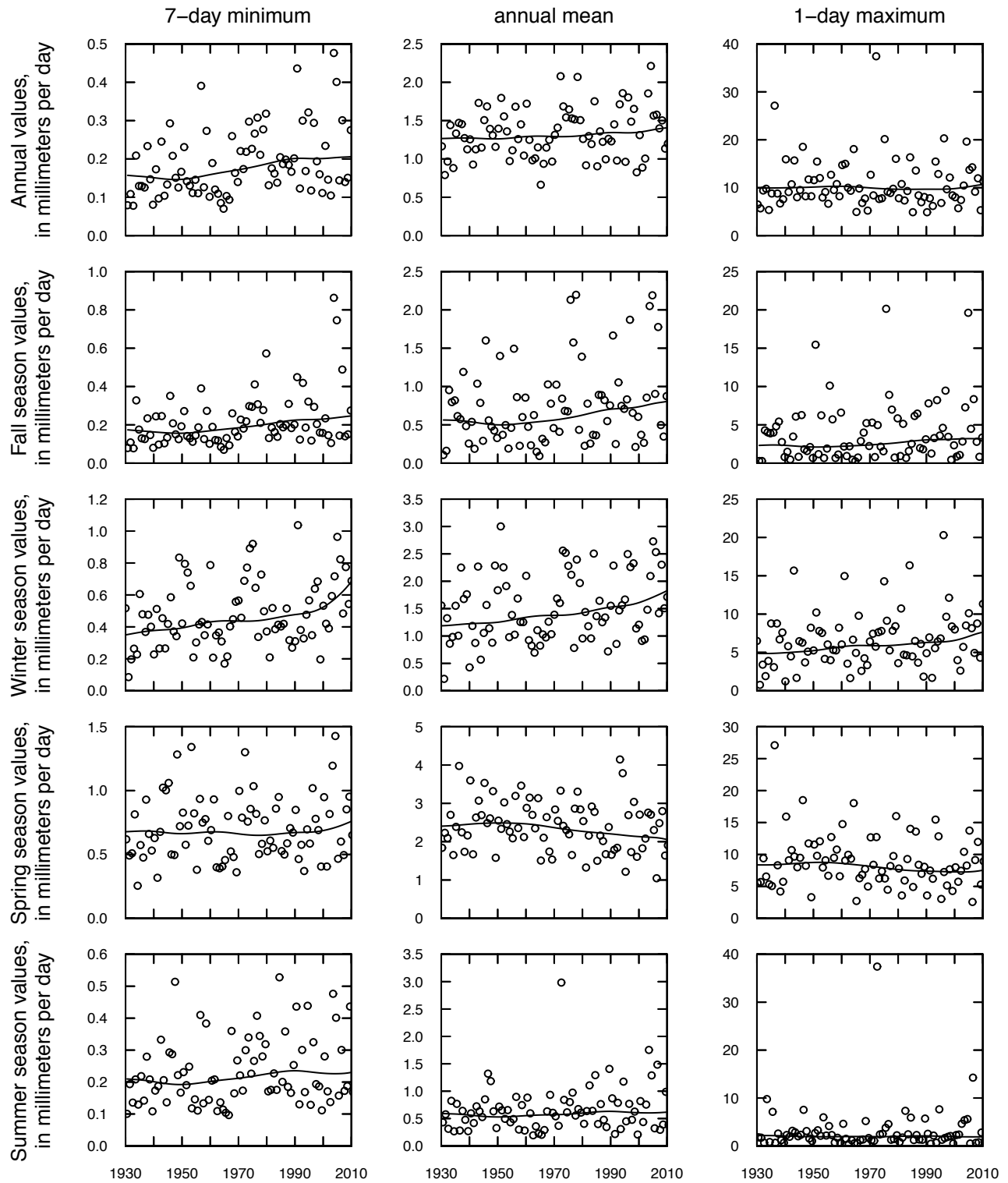


Figure 1-18. Streamflow statistics (circles) in units of millimeters per day, annual values and seasonal values; fall (September, October, and November), winter (December, January, and February), spring (March, April, and May), and summer (June, July, and August), and locally weighted scatterplot smooth (solid curve) for Susquehanna River at Harrisburg, Pa., 1930-2010.

Raystown Branch Juniata River at Saxton, Pa.

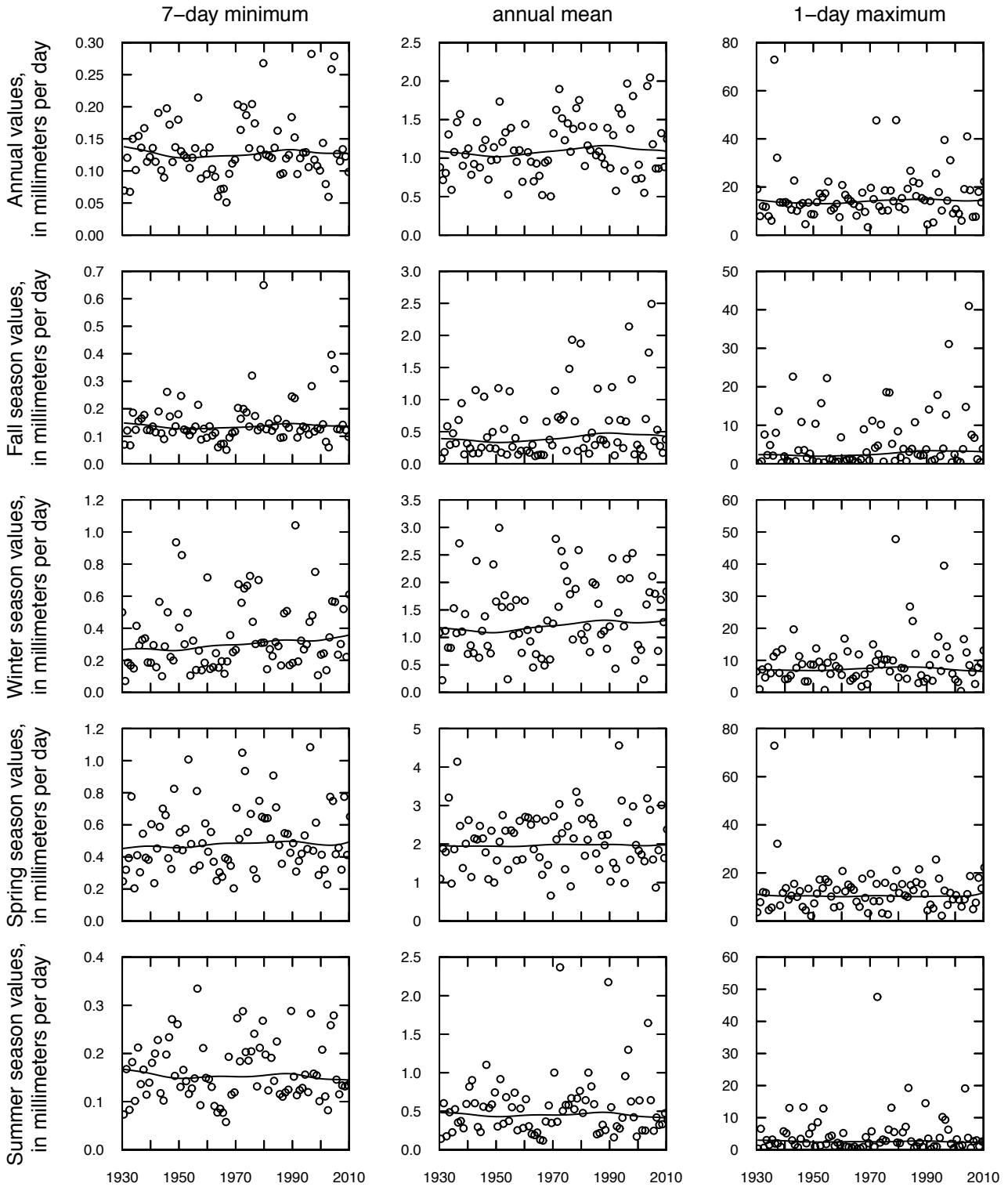


Figure 1-19. Streamflow statistics (circles) in units of millimeters per day, annual values and seasonal values; fall (September, October, and November), winter (December, January, and February), spring (March, April, and May), and summer (June, July, and August), and locally weighted scatterplot smooth (solid curve) for Raystown Branch Juniata River at Saxton, Pa., 1930–2010.

North Branch Potomac River at Luke, Md.

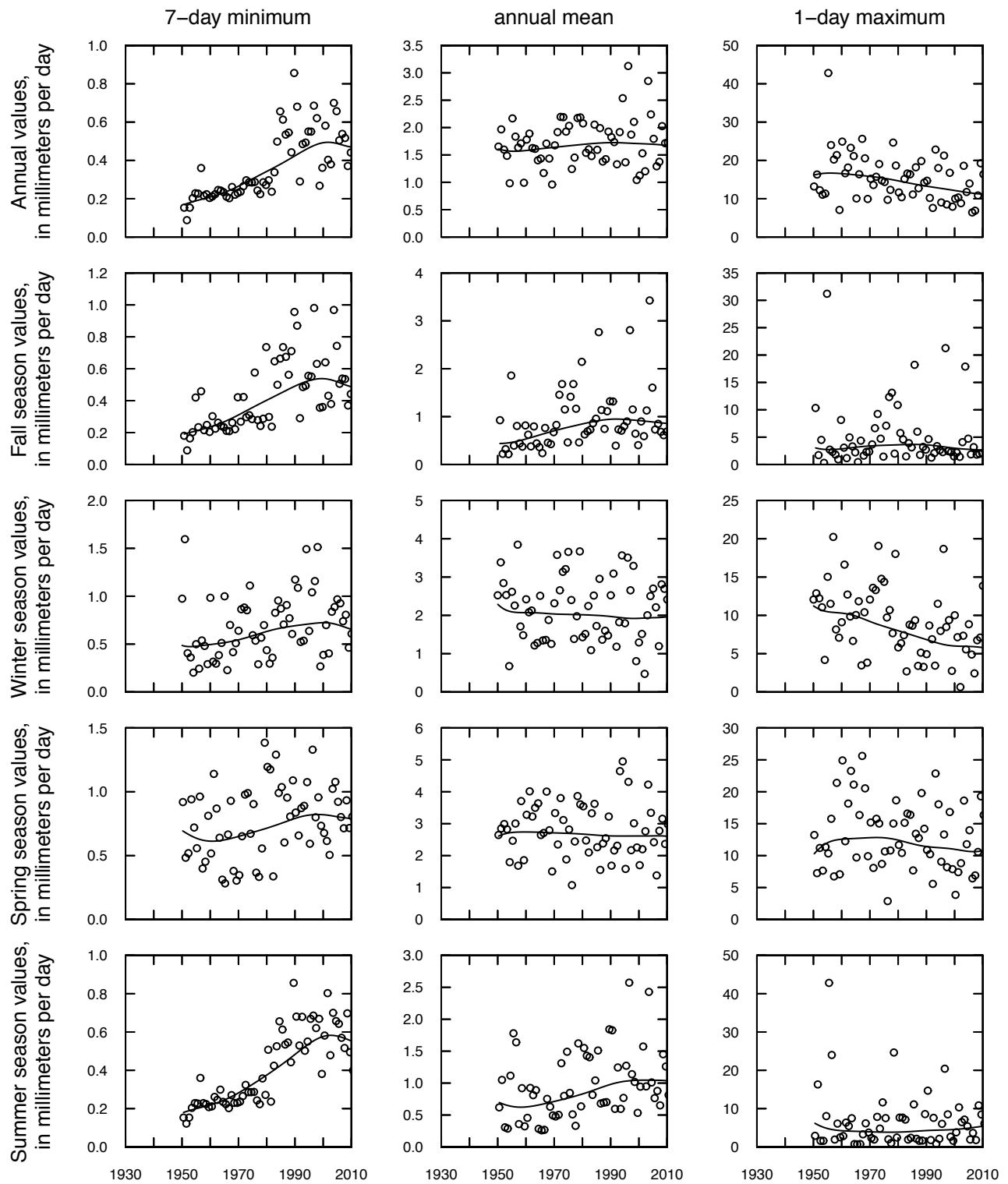


Figure 1-20. Streamflow statistics (circles) in units of millimeters per day, annual values and seasonal values; fall (September, October, and November), winter (December, January, and February), spring (March, April, and May), and summer (June, July, and August), and locally weighted scatterplot smooth (solid curve) for North Branch Potomac River at Luke, Md., 1930–2010.

Potomac River at Point of Rocks, Md.

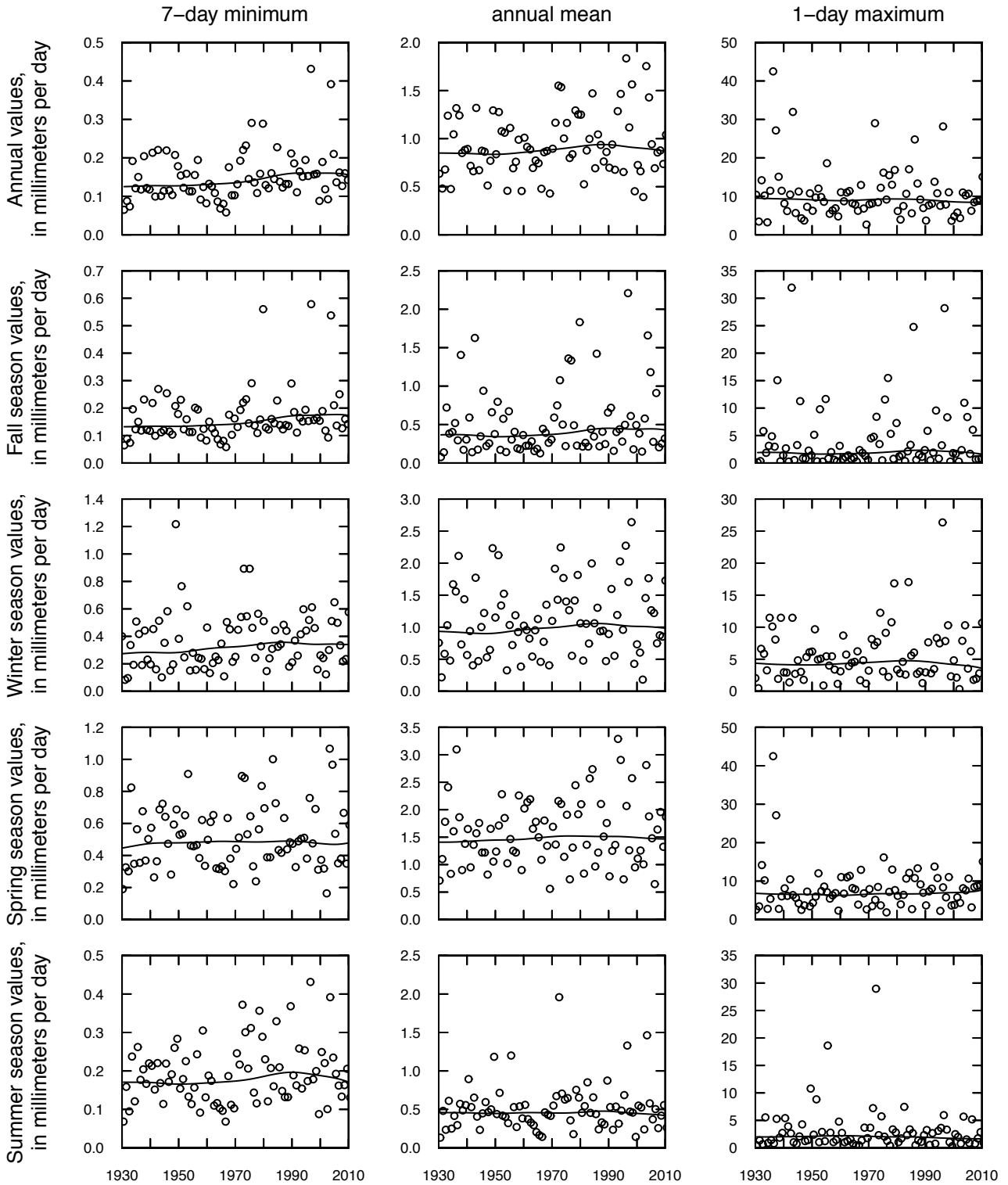


Figure 1-21. Streamflow statistics (circles) in units of millimeters per day, annual values and seasonal values; fall (September, October, and November), winter (December, January, and February), spring (March, April, and May), and summer (June, July, and August), and locally weighted scatterplot smooth (solid curve) for Potomac River at Point of Rocks, Md., 1930–2010.

Goose Creek near Leesburg, Va.

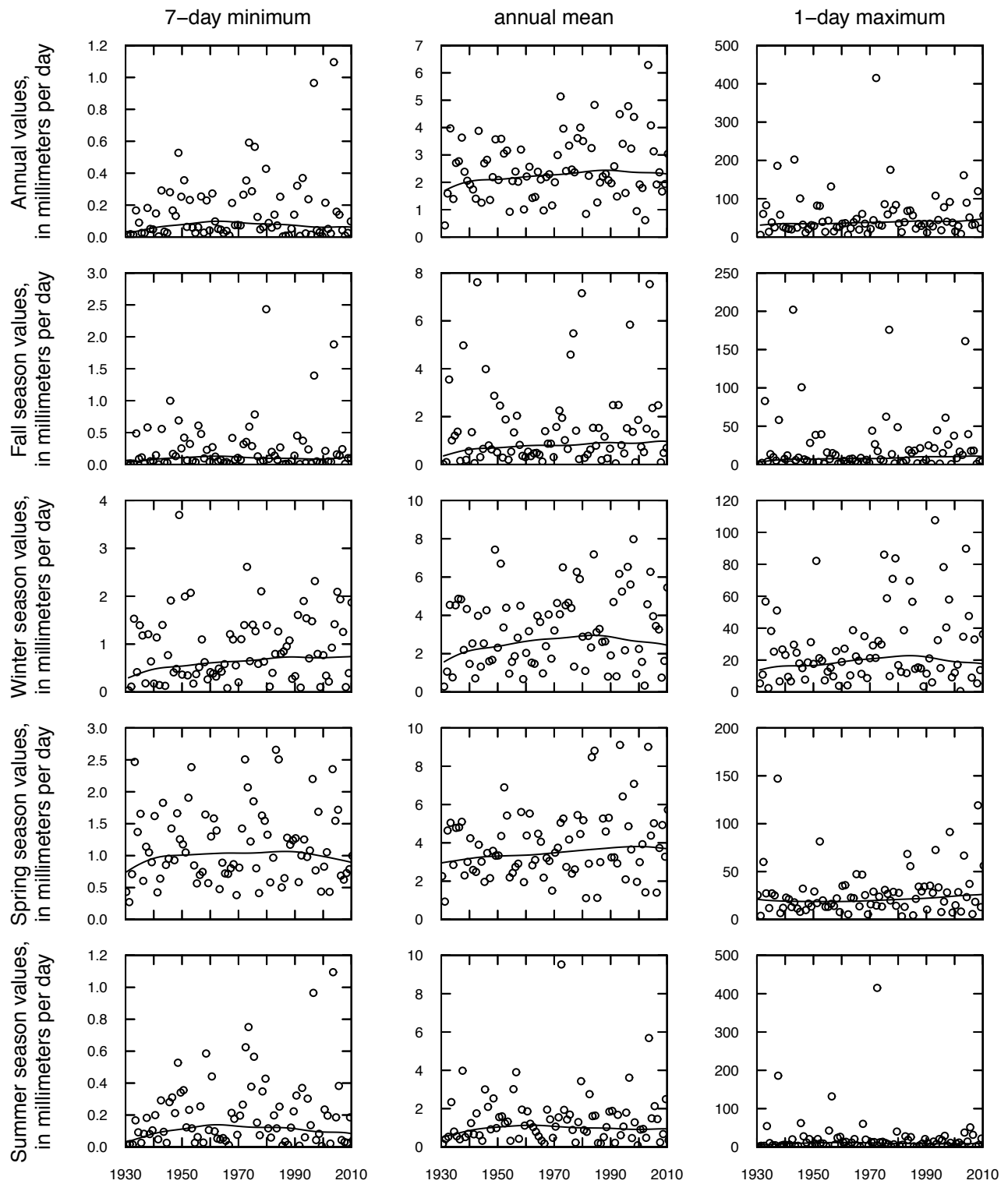


Figure 1-22. Streamflow statistics (circles) in units of millimeters per day, annual values and seasonal values; fall (September, October, and November), winter (December, January, and February), spring (March, April, and May), and summer (June, July, and August), and locally weighted scatterplot smooth (solid curve) for Goose Creek near Leesburg, Va., 1930–2010.

Rappahannock River near Fredericksburg, Va.

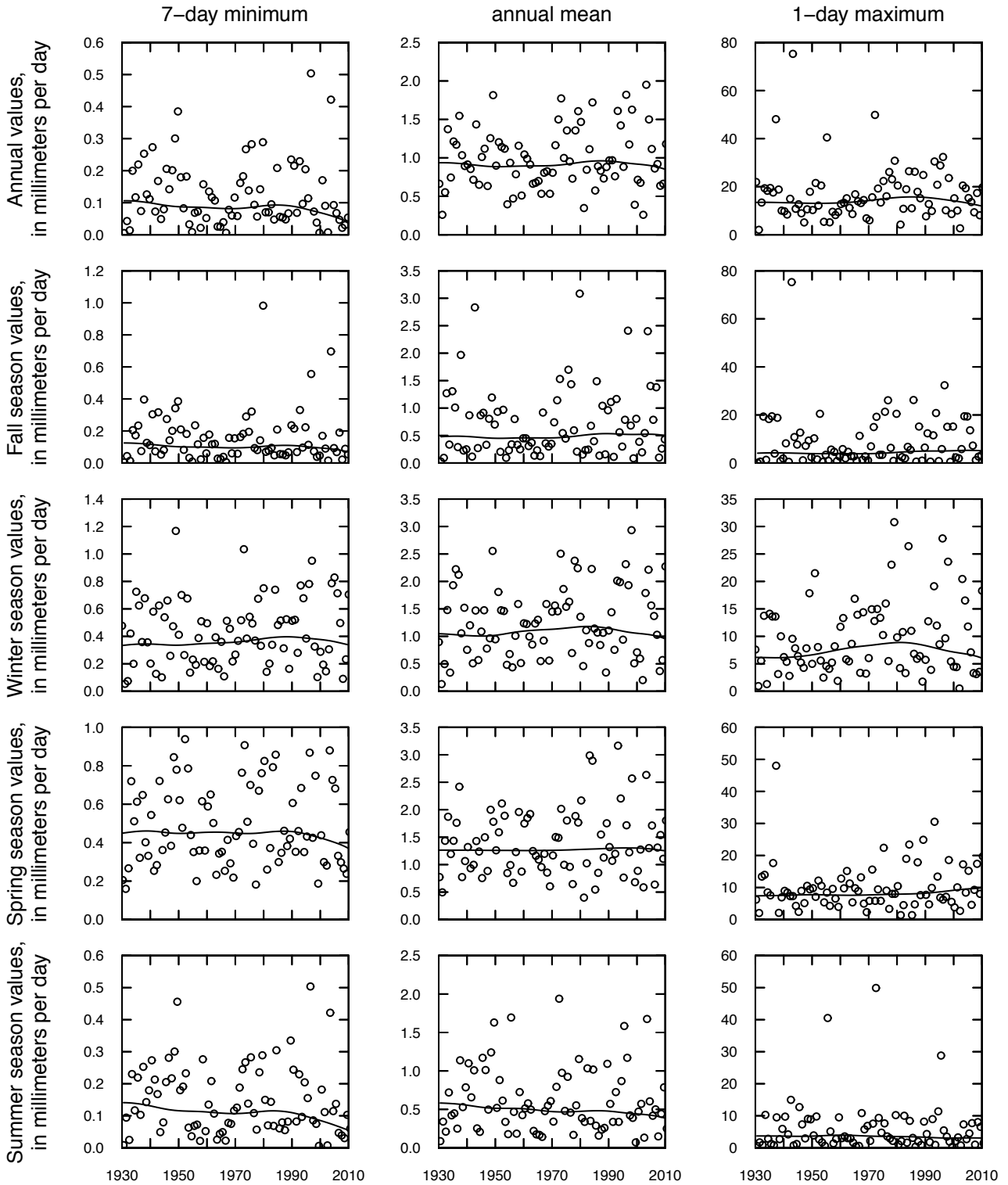


Figure 1-23. Streamflow statistics (circles) in units of millimeters per day, annual values and seasonal values; fall (September, October, and November), winter (December, January, and February), spring (March, April, and May), and summer (June, July, and August), and locally weighted scatterplot smooth (solid curve) for Rappahannock River near Fredericksburg, Va., 1930–2010.

James River at Cartersville, Va.

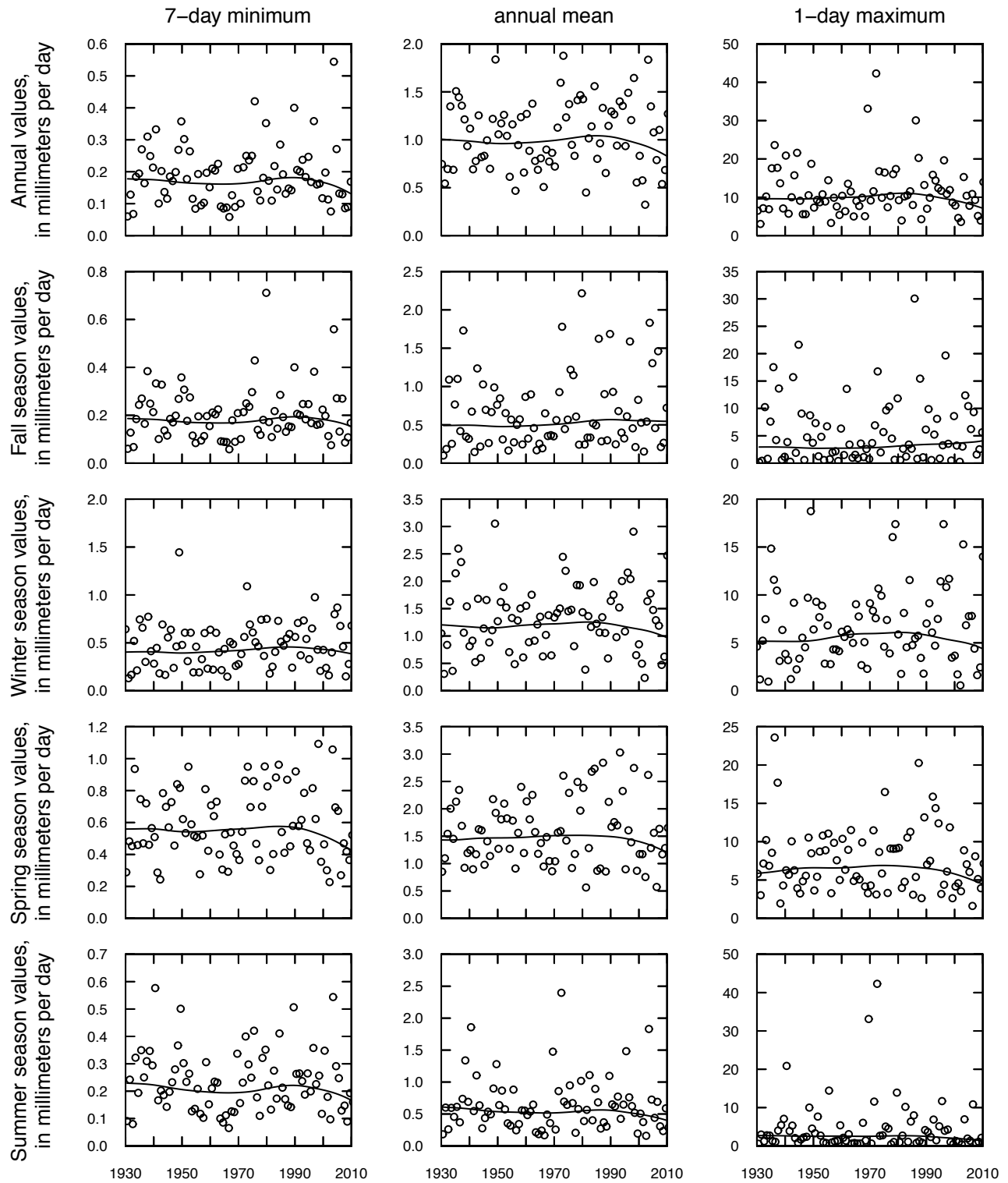


Figure 1-24. Streamflow statistics (circles) in units of millimeters per day, annual values and seasonal values; fall (September, October, and November), winter (December, January, and February), spring (March, April, and May), and summer (June, July, and August), and locally weighted scatterplot smooth (solid curve) for James River at Cartersville, Va., 1930–2010.

James River at Buchanan, Va.

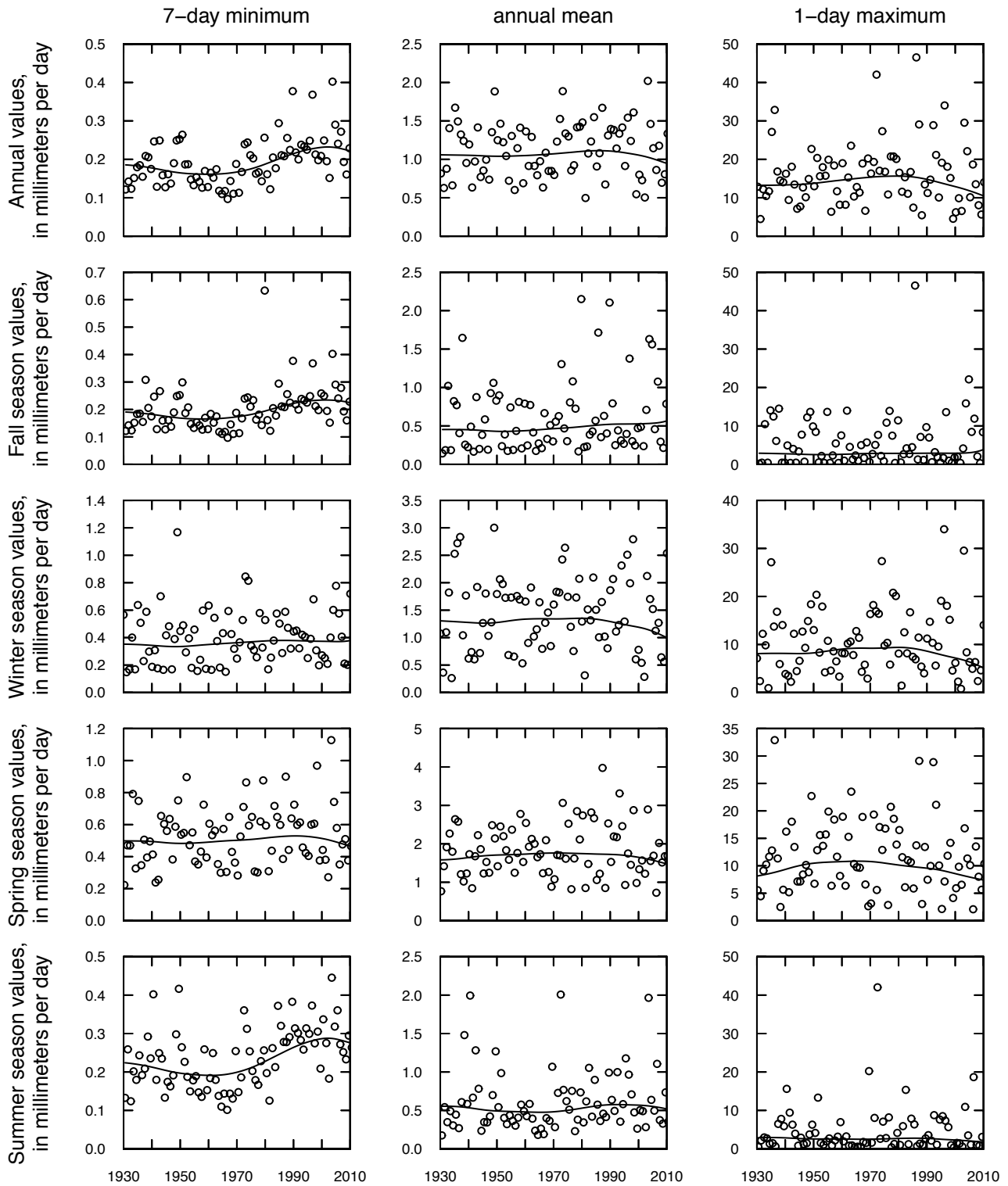


Figure 1-25. Streamflow statistics (circles) in units of millimeters per day, annual values and seasonal values; fall (September, October, and November), winter (December, January, and February), spring (March, April, and May), and summer (June, July, and August), and locally weighted scatterplot smooth (solid curve) for James River at Buchanan, Va., 1930–2010.

Roanoke River at Roanoke, Va.

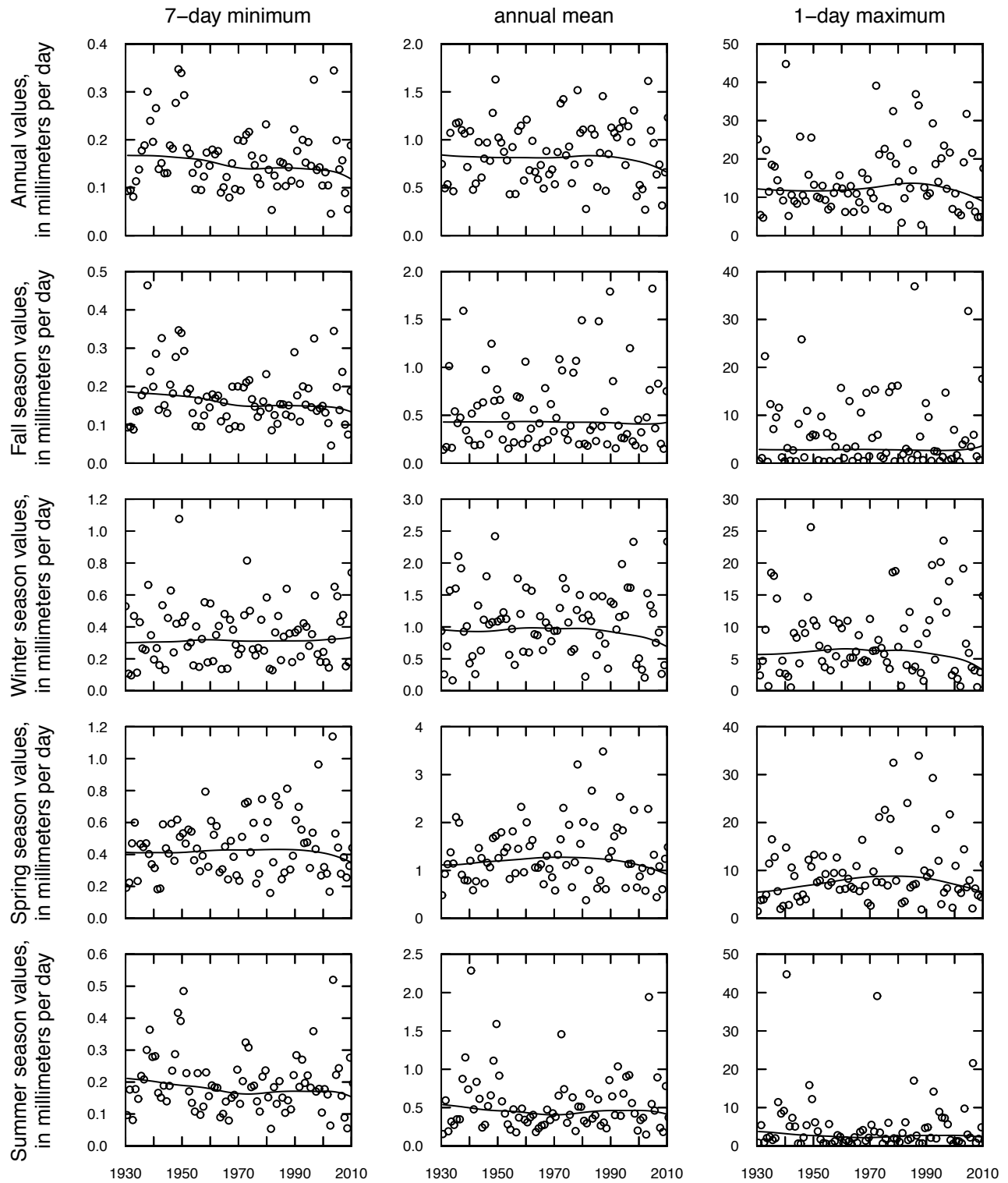


Figure 1-26. Streamflow statistics (circles) in units of millimeters per day, annual values and seasonal values; fall (September, October, and November), winter (December, January, and February), spring (March, April, and May), and summer (June, July, and August), and locally weighted scatterplot smooth (solid curve) for Roanoke River at Roanoke, Va., 1930–2010.

New River at Radford, Va.

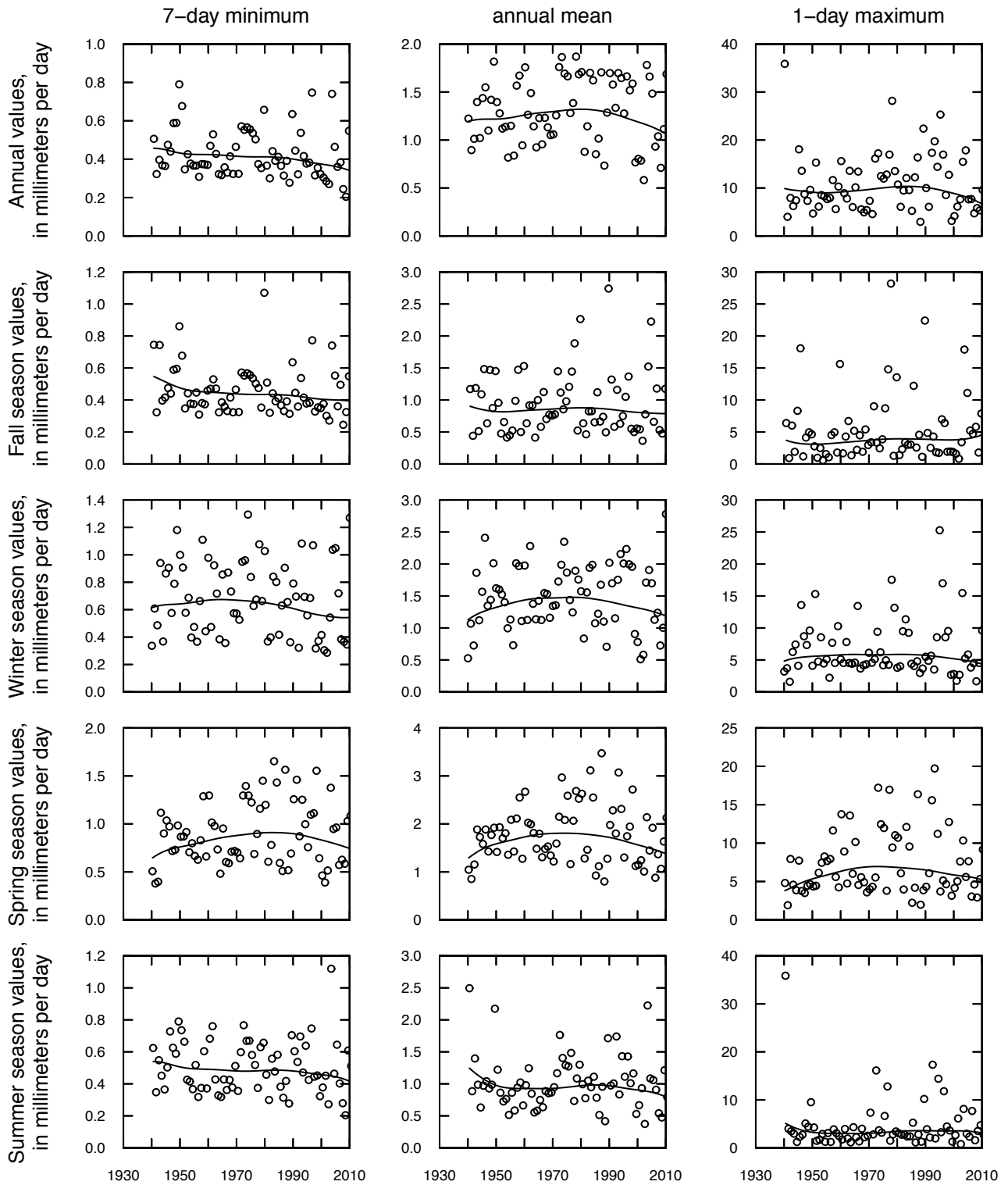


Figure 1-27. Streamflow statistics (circles) in units of millimeters per day, annual values and seasonal values; fall (September, October, and November), winter (December, January, and February), spring (March, April, and May), and summer (June, July, and August), and locally weighted scatterplot smooth (solid curve) for New River at Radford, Va., 1930–2010.

Reed Creek at Grahams Forge, Va.

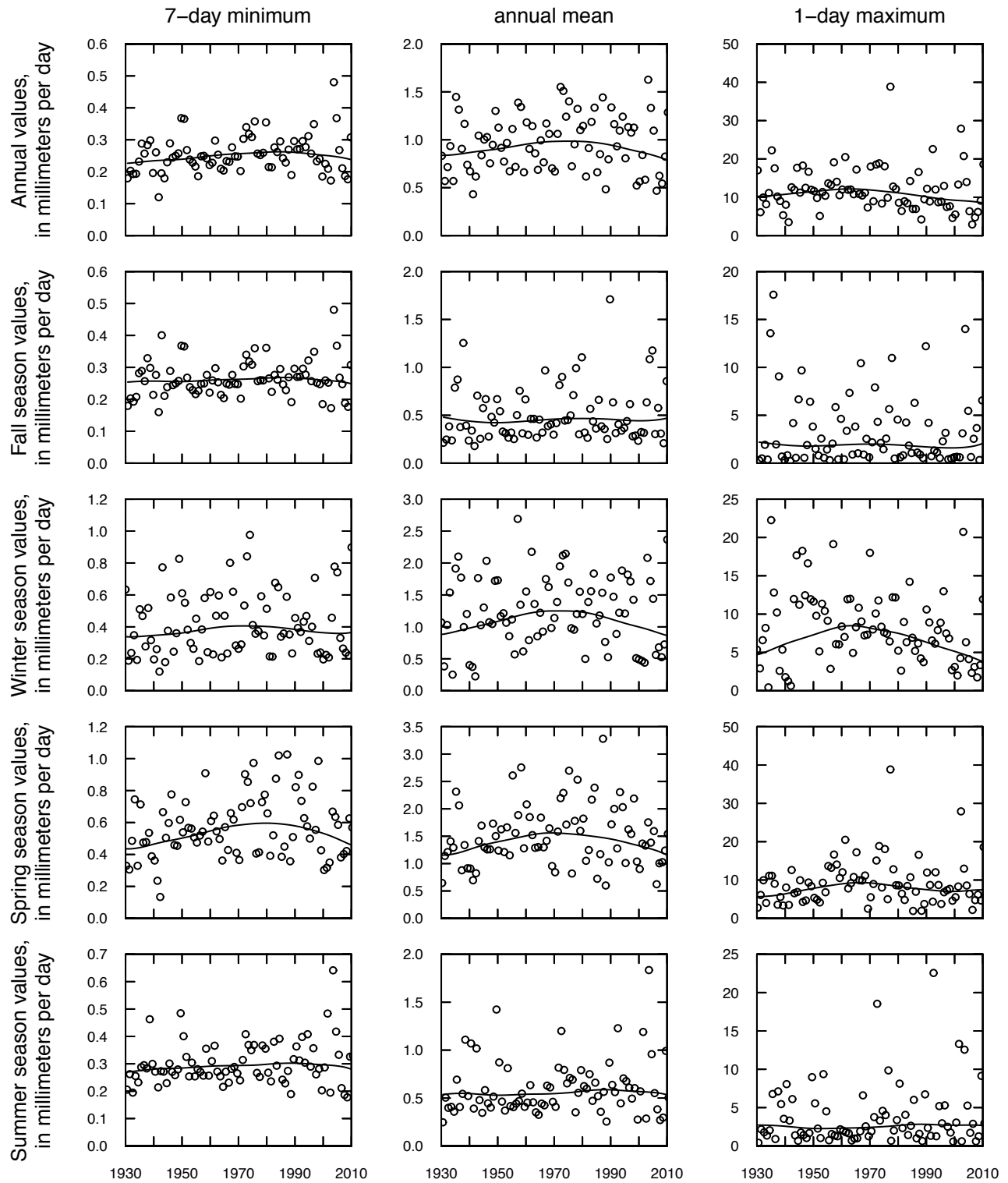


Figure 1-28. Streamflow statistics (circles) in units of millimeters per day, annual values and seasonal values; fall (September, October, and November), winter (December, January, and February), spring (March, April, and May), and summer (June, July, and August), and locally weighted scatterplot smooth (solid curve) for Reed Creek at Grahams Forge, Va., 1930-2010.

North Fork Holston River near Saltville, Va.

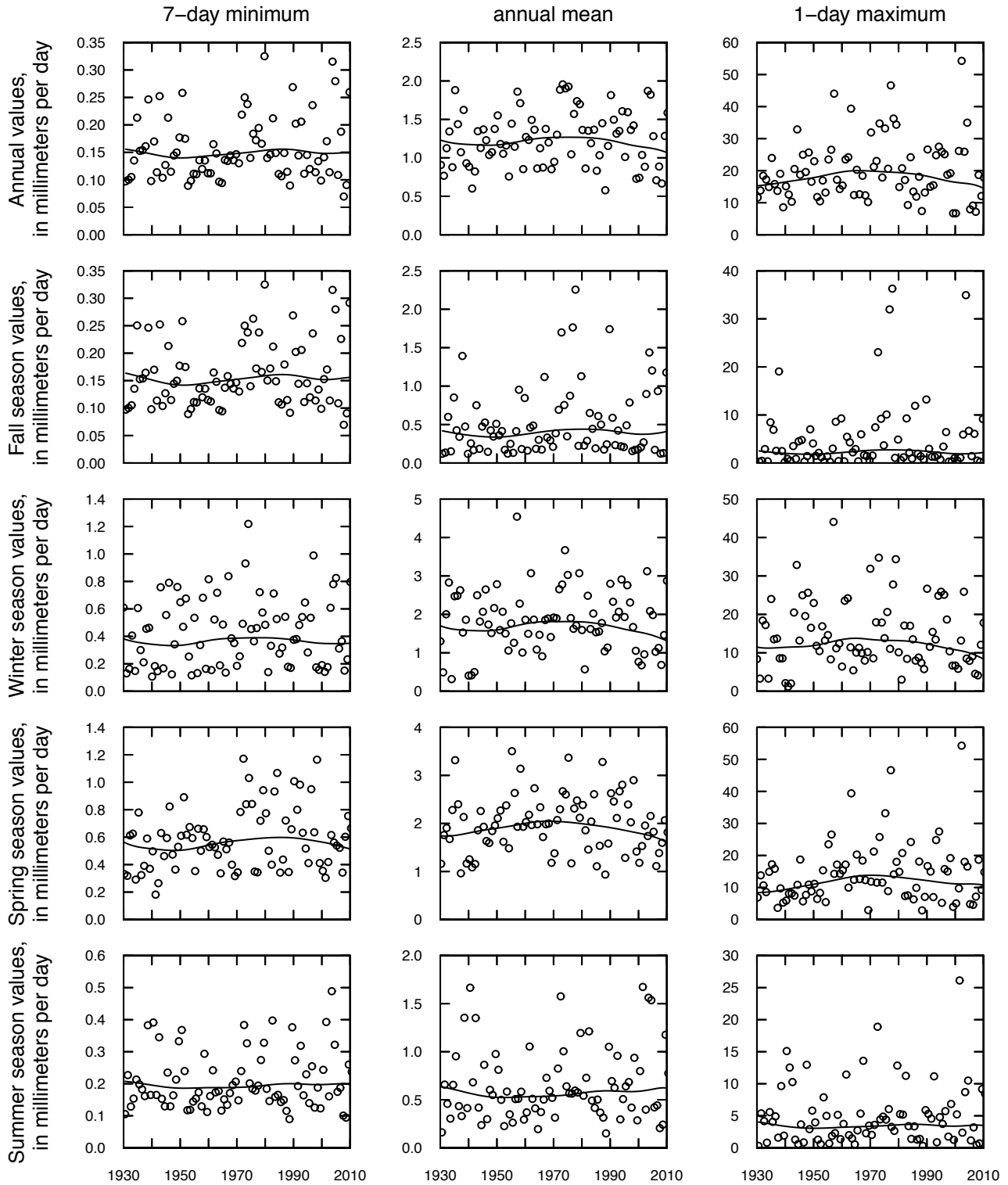


Figure 1-29. Streamflow statistics (circles) in units of millimeters per day, annual values and seasonal values; fall (September, October, and November), winter (December, January, and February), spring (March, April, and May), and summer (June, July, and August), and locally weighted scatterplot smooth (solid curve) for North Fork Holston River near Saltville, Va., 1930–2010.

Banister River at Halifax, Va.

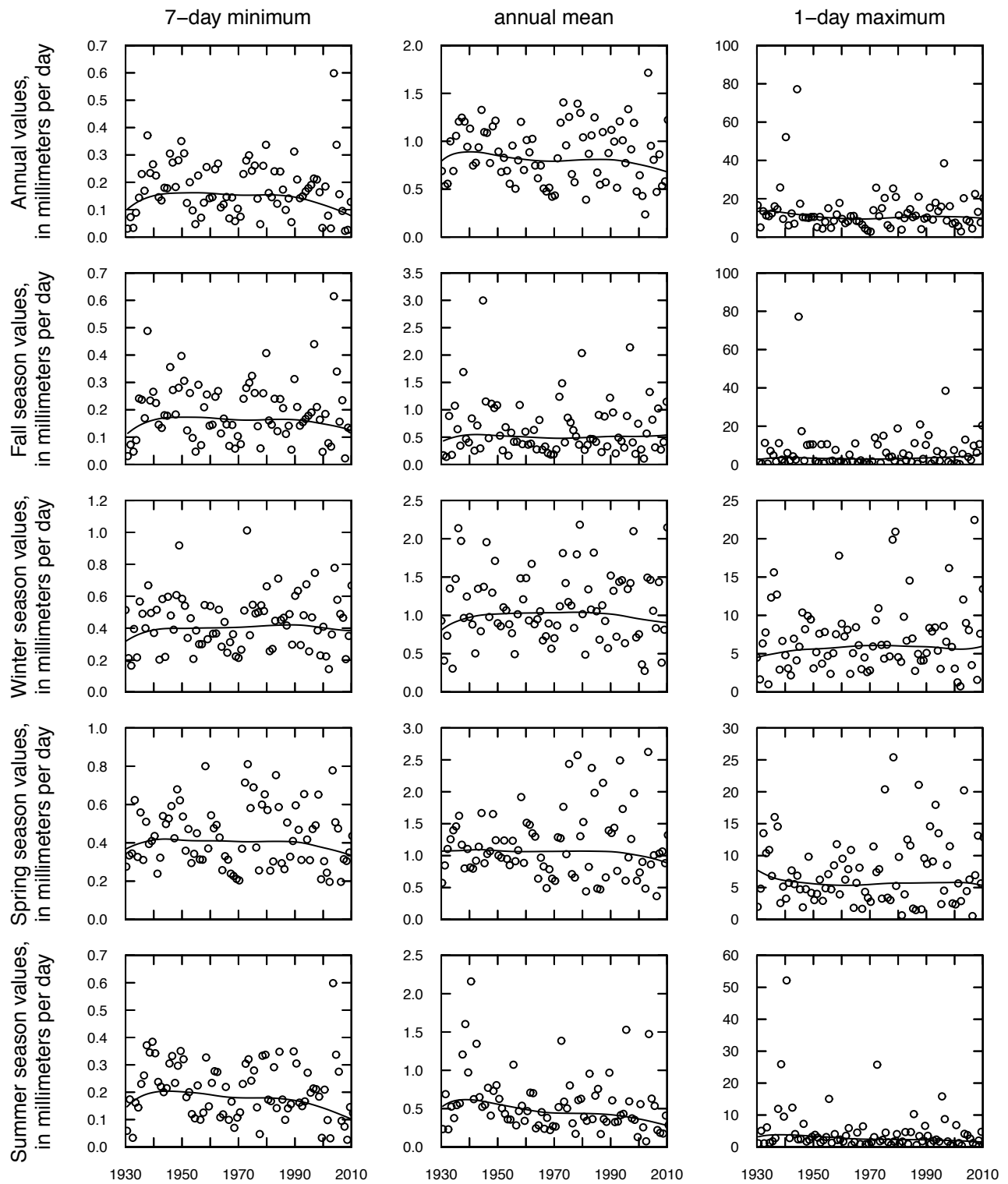


Figure 1-30. Streamflow statistics (circles) in units of millimeters per day, annual values and seasonal values; fall (September, October, and November), winter (December, January, and February), spring (March, April, and May), and summer (June, July, and August), and locally weighted scatterplot smooth (solid curve) for Banister River at Halifax, Va., 1930–2010.

Prepared by:

USGS Science Publishing Network
Raleigh Publishing Service Center
3916 Sunset Ridge Road
Raleigh, NC 27607

USGS Publishing Service Center staff:

Edited by Twila Darden Wilson
Layout and illustrations by James A. Tomberlin,
figure 1 by Timothy W. Auer

For additional information regarding this publication, contact:

Director
USGS Virginia Water Science Center
1730 East Parham Road
Richmond, VA 23228
(804) 261-2600
email: dc_va@usgs.gov

Or visit the USGS Virginia Water Science Center Web site at:

<http://va.water.usgs.gov>

By K.C. Rice and R.M. Hirsch—**Spatial and Temporal Trends in Runoff at Long-Term Streamgages within and near the Chesapeake Bay Watershed**—Scientific Investigations Report 2012–5151

ISBN 978-1-4113-3456-4

